RADC-TR-89-224
Final Technical Report
November 1989

PROGRAM TO STUDY THE PROCESS PARAMETERS OF OMVPE AND THEIR RELATIONSHIP TO THE PROPERTIES OF $Ga_{(0.47)}In_{(0.53)}As$ ON InP SUBSTRATES

Devcom Incorporated

I. Ahmed

ROME AIR DEVELOPMENT CENTER
Air Force Systems Command
Griffiss Air Force Base, NY 13441-5700

This report has been reviewed by the RADC Public Affairs Division (PA) and is releasable to the National Technical Information Service (NTIS). At NTIS it will be releasable to the general public, including foreign nations.

RADC-TR-89-224 has been reviewed and is approved for publication.

APPROVED: Kenneth P. Quinlan

KENNETH P. QUINLAN
Project Engineer

APPROVED: Harold Roth

HAROLD ROTH
Director of Solid State Sciences

FOR THE COMMANDER: James W. Hyde III

JAMES W. HYDE III
Directorate of Plans & Programs

If your address has changed or if you wish to be removed from the RADC mailing list, or if the addressee is no longer employed by your organization, please notify RADC (ESME) Hanscom AFB MA 01731-5000. This will assist us in maintaining a current mailing list.

Do not return copies of this report unless contractual obligations or notices on a specific document require that it be returned.

UNCLASSIFIED
SECURITY CLASSIFICATION OF THIS PAGE

REPORT DOCUMENTATION PAGE

Form Approved OMB No. 0704-0188

1a. REPORT SECURITY CLASSIFICATION UNCLASSIFIED	1b. RESTRICTIVE MARKINGS N/A
2a. SECURITY CLASSIFICATION AUTHORITY N/A	3. DISTRIBUTION/AVAILABILITY OF REPORT Approved for public release; distribution unlimited.
2b. DECLASSIFICATION/DOWNGRADING SCHEDULE N/A	
4. PERFORMING ORGANIZATION REPORT NUMBER(S) N/A	5. MONITORING ORGANIZATION REPORT NUMBER(S) RADC-TR-89-224
6a. NAME OF PERFORMING ORGANIZATION Devcom Incorporated 6b. OFFICE SYMBOL (If applicable)	7a. NAME OF MONITORING ORGANIZATION Rome Air Development Center (ESME)
6c. ADDRESS (City, State, and ZIP Code) 31 Bradford Road Framingham MA 01701	7b. ADDRESS (City, State, and ZIP Code) Hanscom AFB MA 01731-5000
8a. NAME OF FUNDING/SPONSORING ORGANIZATION Rome Air Development Center 8b. OFFICE SYMBOL (If applicable) ESME	9 PROCUREMENT INSTRUMENT IDENTIFICATION NUMBER F19628-84-C-0066
8c. ADDRESS (City, State, and ZIP Code) Hanscom AFB MA 01731-5000	10. SOURCE OF FUNDING NUMBERS PROGRAM ELEMENT NO: 62702F; PROJECT NO: 4600; TASK NO: 17; WORK UNIT ACCESSION NO: 57

11. TITLE (Include Security Classification)
PROGRAM TO STUDY THE PROCESS PARAMETERS OF OMVPE AND THEIR RELATIONSHIP TO THE PROPERTIES OF $Ga_{(0.47)}In_{(0.53)}As$ ON InP SUBSTRATES

12. PERSONAL AUTHOR(S)
I. Ahmed

13a. TYPE OF REPORT	13b. TIME COVERED	14. DATE OF REPORT (Year, Month, Day)	15. PAGE COUNT
Final	FROM Jun 84 TO Mar 88	November 1989	182

16. SUPPLEMENTARY NOTATION
N/A

17. COSATI CODES			18. SUBJECT TERMS (Continue on reverse if necessary and identify by block number)
FIELD	GROUP	SUB-GROUP	
07	02		Metalorganic Chemical Vapor Deposition, MOCVD
20	12		III-V Semiconductors

19. ABSTRACT (Continue on reverse if necessary and identify by block number)

The purpose of the work was a study of the process parameters of the organometallic vapor phase epitaxy technique and their relationship to the properties of gallium indium arsenide lattice matched to indium phosphide. The study was an extension of an earlier study at atmospheric to low pressure conditions and shows that the effects of parasitic reactions can be essentially eliminated by low pressures. The work has established ranges of operation (temperature and pressures) for high quality material with a high degree of compositional uniformity over the substrate. Some problem areas have been designated which can be encountered in the growth of the lattice matched composition. Methods for their resolution have been presented. Specific criteria for scale-up have been identified and methods for their implementation presented.

An understanding of the growth kinetics was obtained from a study using a double pumped mass spectrometer. The results of this study shed light (Continued on Reverse)

20 DISTRIBUTION/AVAILABILITY OF ABSTRACT ☒ UNCLASSIFIED/UNLIMITED ☐ SAME AS RPT ☐ DTIC USERS	21 ABSTRACT SECURITY CLASSIFICATION UNCLASSIFIED
22a. NAME OF RESPONSIBLE INDIVIDUAL Kenneth P. Quinlan	22b. TELEPHONE (Include Area Code) (617) 377-4045 22c. OFFICE SYMBOL RADC (ESME)

DD Form 1473, JUN 86 *Previous editions are obsolete.*

SECURITY CLASSIFICATION OF THIS PAGE
UNCLASSIFIED

Block 19 Continued:

on the growth of gallium indium arsenide and gallium arsenide. Empirical results on the retardation of the triethylindium-arsine reaction by the pre-mixing of trimethyl gallium have been explained. The extend of retardation has been quantified.

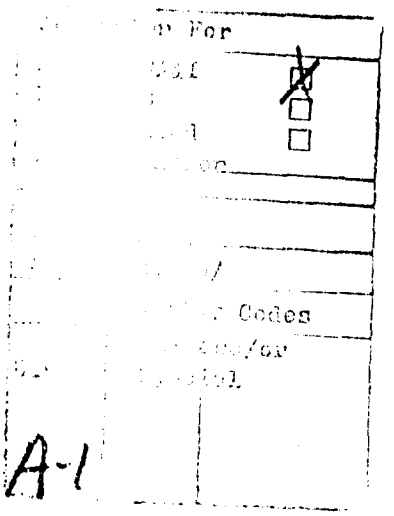

TABLE OF CONTENTS

SUMMARY

This report discusses the results obtained during the study of the process parameters of organometallic vapor phase epitaxy (OMVPE) and their relationship to the properties of Gallium Indium Arsenide (GaInAs) lattice matched to Indium phosphide (InP). The growth phase and electrical characterization of this program was subcontracted to Rensselaer Polytechnic Institute, under Professor S.K. Ghandhi and his doctoral student Mr. J.P. Agnello.

The investigation represents the extension of an earlier study at atmospheric pressure to low pressure conditions and shows that the effects of parasitic reactions can be essentially eliminated by this means. Our work has established ranges of operation (temperature and reactant partial pressures) for high-quality material with a high degree of compositional uniformity over the substrate. Some problem areas have been isolated which can be encountered in the growth of the lattice-matched composition, and methods for their resolution have been presented. Although the problem of growth over large areas (> 1 inch sq.), and the achievement of precise lattice-matched composition from run to run have not been solved by us because it would have represented a major investment in equipment. Specific criteria for scale-up however have been identified, and methods for their implementation have been presented.

A detailed understanding of the kinetics of growth was obtained by the design, construction and attachment of a double

pumped mass spectrometer to the growth system. The results of this phase of the program have shed light on the growth of both GaInAs as well as GaAs, and have allowed us to obtain kinetic data which is not machine-specific. Empirical results on the retardation of the TEI-arsine reaction by the pre-mixing of TMG have been explained, and the extent of retardation has been quantified .

Representative samples for evaluation testing and device development have been delivered to RADC/ESM during the course of this program. These samples represent the highest quality obtained. Characterization results by double crystal x-ray diffraction (DCD) and by Fourier-transform Infrared (FTIR) spectroscopy, both of which are non-invasive methods have been submitted with all these samples.

Many areas are still open candidates for further work. Thus studies of the compositional and thickness uniformities over 2" wafers using a system designed within the specifications that have been developed are required. A second area is the exploration of new chemicals such as diethylmethyl indium and tertiarybutylarsenic, both of which appear to have practical operational advantages over the simple alkyl-hydride system considered here. Finally doping studies of the growing layers would be needed if practical devices using the full potential of OMVPE are to be realized.

BACKGROUND

I IMPORTANCE OF GaInAs/InP

The coming on stream of the fiber-optic communication industry has brought with it two distinct directions in the development of light sources and detectors. Workers in various laboratories throughout the world today are engaged in research to improve light sources and detectors for the short-wavelength region of the spectrum, (0.8-0.9 μm), while others are doing research to improve the sources and detectors for the long-wavelength side of the spectrum (1.0-1.7 μm). For the short-wavelength region (0.8-0.9 μm), the light sources are usually fabricated from the AlGaAs/GaAs alloy system. The long-wavelength light sources are commonly fabricated from the InGaAsP/InP alloy system.

Although the state-of-the-art devices fabricated from the AlGaAs/GaAs system are currently well ahead of those fabricated for long-wave length applications, the demonstration that signals transmitted through silica-based optical fibers are least attenuated and distorted in the 1.0-1.7 μm range (1-3) has spurred major interest in this direction. Fig. 1 shows the attenuation losses for silica-based fibers. From this figure, it is apparrent why the InGaAsP/InP alloy system (which can be used for the fabrication of material that emits in the 1.0-1.7 μm range) is an attractive alternative. Although not important for ordinary applications, it has also been found that signals carried in glass fibers are protected from perturbations due to certain electromagnetic radiation fields if the signals are in

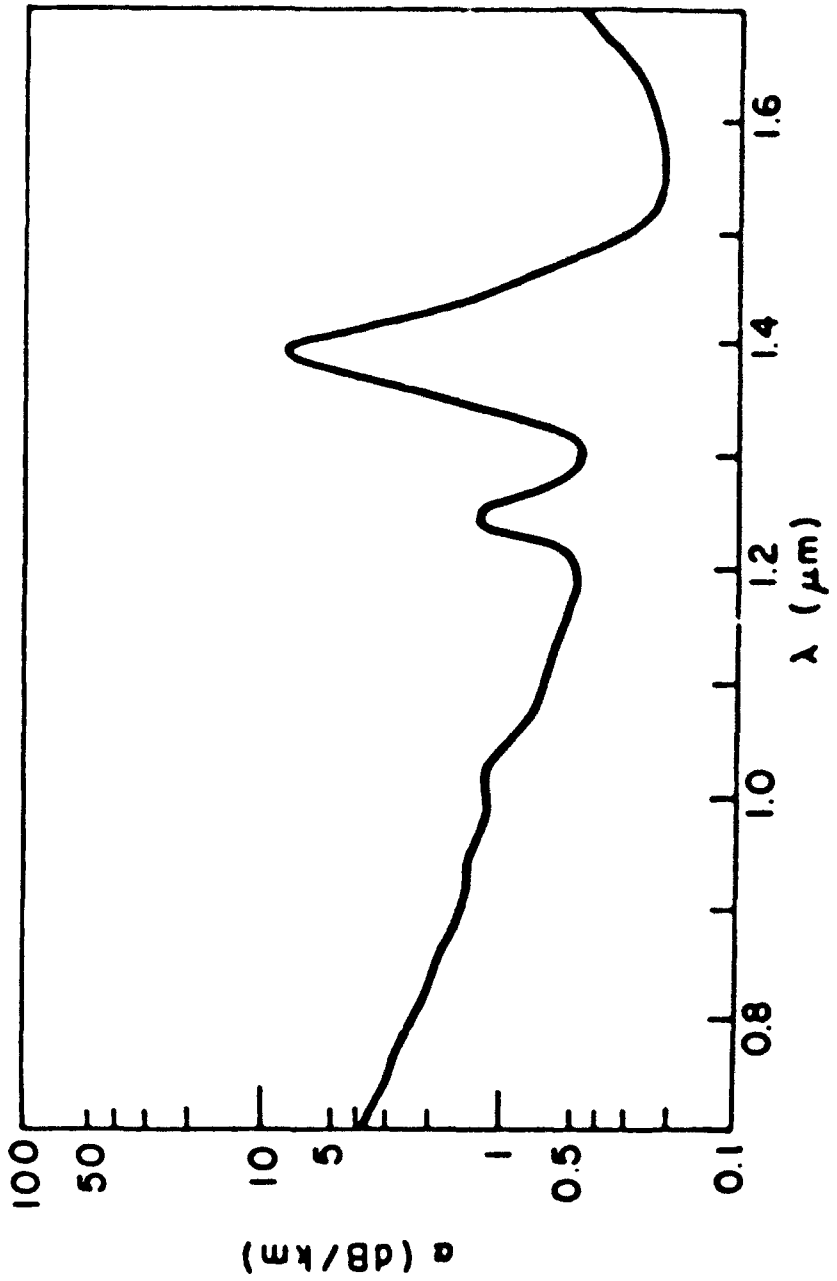

FIGURE 1: Attenuation loss for silica-based fibre in the 1.0 - 1.7μm region

the 1.0-1.7 μm range (4).

The ternary and quaternary alloy compounds involved in the synthesis of the semiconductor for long-wavelength communication come exclusively from the group III elements of In, Ga, Al and the group V elements of P, As and Sb. Appropriate compositions of these elements can be grown lattice-matched on a few select substrates to give direct band-gap compounds of the desired energy and hence emission wave-length. In Fig. 2 (5) we show the lattice parameters of the important III-V compounds as a function of the bandgap along with the corresponding emission wavelengths. A major requirement for any potential semiconductor for use in optical communication is that the bandgap be direct. This amounts to requiring that any radiative transitions from the minimum of the conduction band to the maximum of the valence band be vertical in the (E-k) energy-momentum space. This is important because in nondirect materials, phonon-assisted transitions (for conservation of momentum) reduce their radiative efficiency.

In the synthesis of ternary and quaternary compounds, the lattice parameter of the grown layer and that of the substrate must be the same. Since the growth starts from the substrate, it is the substrate that dictates the lattice parameter to which the grown layer must be matched. In Fig. 2, the solid lines indicate direct-gap compositions and the broken lines show indirect-gap compositions.

Over the entire alloy range of the quaternary $Ga_{1-x}In_xAs_yP_{1-y}$,

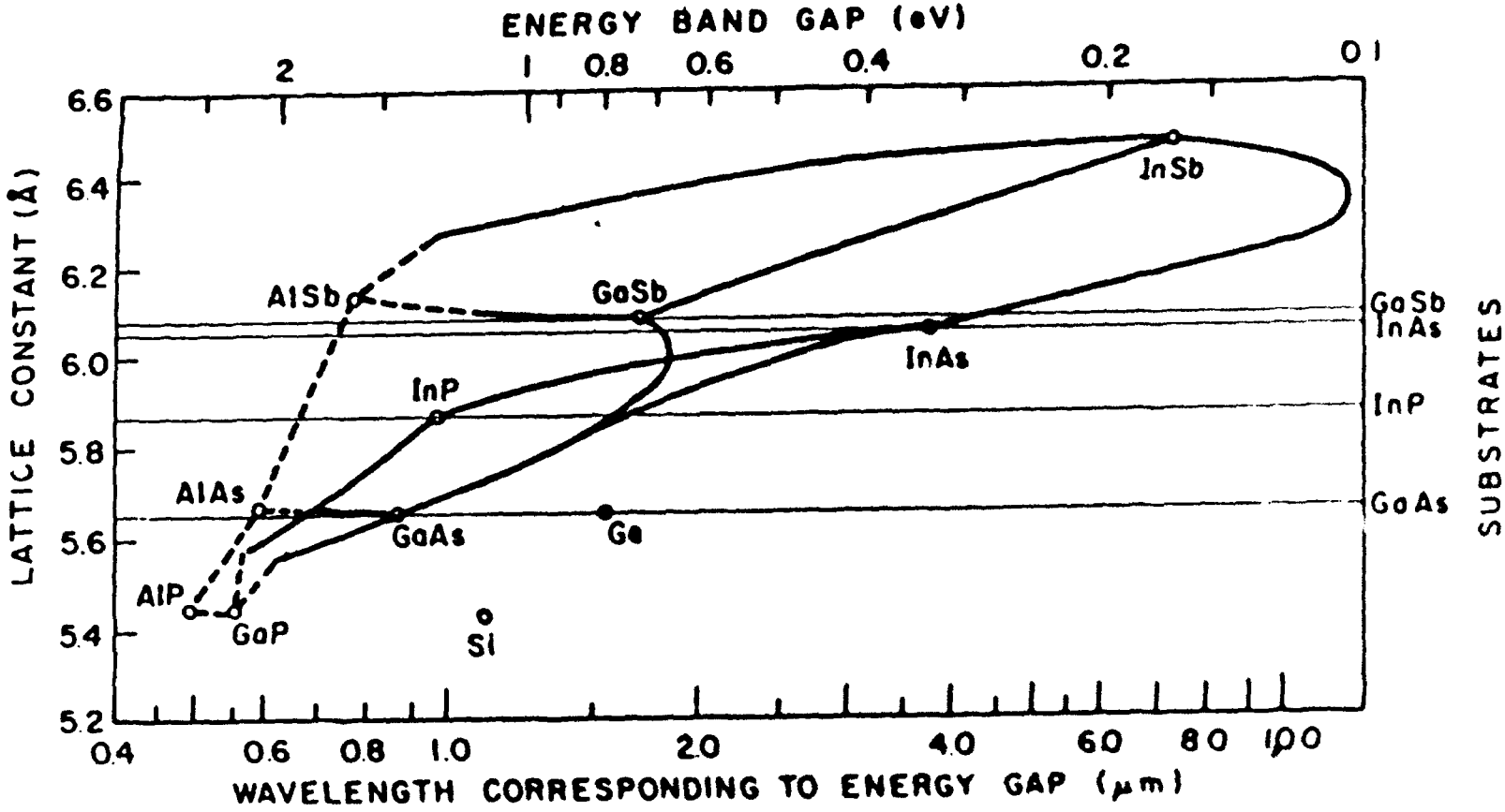

FIGURE 2: III-V compounds with their lattice constants vs. energy band gaps and corresponding wavelengths.

the composition with x = 0.53 shows considerable versatility and promise for both optical communication and microwave applications. It can be used for light sources emitting at approximately 1.65 μm or for detectors that are sensitive to light over the wavelength range of 1.0-1.7 μm. Theoretical and experimental studies (6) have shown that this particular composition should exhibit the highest mobility of all possible compositions over the entire alloy range.

II INCENTIVES FOR OMVPE

The fabrication of many devices described above requires single crystal regions of very different electrical properties to be in contact with each other. The growth of these materials can in principle be achieved by molecular beam (MBE), liquid phase (LPE) and vapour phase epitaxy (VPE).

MBE though a highly controlled physical vapour deposition process has its usefulness limited due to very slow growth rate and the fact that it is performed in a relatively expensive high vacuum apparatus allowing deposition only over small areas. Thus it is very difficult to scale this process up for its commercial utilization. LPE is a relatively simple technique and is well suited for the small scale laboratory efforts but it suffers from several important problems: thickness and compositional non-uniformity both in lateral and vertical directions as well as incomplete melt removal, terraces (7) and miniscus line defects (8). Moreover, modern devices require the sequential growth of extremely thin layers (10 - 1000A) which are impractical with this technique.

Ternary compounds formed by the conventional vapor phase chloride transport process are all grown under conditions close to thermodynamic equilibrium. This results in two very important problems: first some compounds canont be grown because of unfavourable thermodynamic constraints (9) (for example, AlGaAs). Second, and equally important, is the fact that the reversibility of the reaction causes outdoping effect, over about 1.0 micron thickness, so that abrupt transitions of either composition or doping cannot be obtained. This precludes the use of these techniques for many modern device applications.

On the other hand organometallic vapor phase epitaxy (OMVPE) is carried out under conditions that are very far from thermal equilibrium, so that extremely abrupt structures can be readily formed. Moreover, all of the III-V compounds can be grown using this method. Thus, it is perhaps the most versatile of the growth techniques for these films and has the best potential for large scale production.

THE PROBLEM IN PERSPECTIVE

The process of OMVPE typically consists of the transport of an organommetallic group III compound and the hydride of a group V element to the surfce of a heated substrate. The substrate which is contained within a cold wall reaction vessel participates in surface specific pyrolysis of the components to form an epitaxial layer. Systems configured to achieve this transformation consist of a source reactant gas handling section, a gas-solid reaction vessel and an exhaust gas cleaning set-up.

Various laboratory set-ups for the growth of both homoepitaxial GaAs and heteroepitaxial GaInAs/InP have been successfully operated to achieve device quality state of the art epilayers. However multiwafer prduction units are currently only available for the homoepitaxial binary GaAs or the closely related ternary GaAlAs growth. The extension of the OMVPE development to the ternary heteroepitaxial GaInAs/InP growth has been slowed primarily because of two unique constraints: those relating to the homogeneous gas phase (depletion) and those relating to the heterogeneous gas-solid interface (substrate decomposition).

I HOMOGENEOUS GAS PHASE DEPLETION

An important problem related to the intrinsic chemistry of the indium alkyls is associated with an ambient temperature reaction with arsine resulting in a non-volatile product. Deposition of this product upstream from the susceptor surface effectively decreases the indium partial pressures at the interface. This premature loss of indium makes reproducible control of the grown GaInAs film composition especially over large areas difficult.

Two fundamentally different approaches have been taken to solve this problem. The first is based on controlling the chemistry by the use of adduct compounds of indium and arsenic alkyls. As this technique by introducing relatively novel compounds involves fundamentally different reaction chemistry, its evaluation is premature within the scope of this study. The second approach by using conventional group III alkyls and arsine

has its roots within the principle of classical chemical reaction engineering. By changing reactor pressures, susceptor temperatures, gas velocities and partial pressures the intentional or unintentional adjustment of temperature profiles reactant residence times and extent of individual reactions has resulted in the growth of high quality layers. Review and evaluation of the work in this area is covered in subsquent sections of this report.

II InP SUBSTRATE STABILITY

The second problem unique to heteroepitaxy of GaInAs on InP by OMVPE arises during start up of the growth reactor. Typical growth reactors operate with substrate temperatures in the 550 - 650° C range. At these temperatures decomposition of the InP through loss of phosphorus is significant, thus effecting the quality of the subsquent GaInAs layer. The following different approaches have been adopted to circumvent this problem:

Use of phosphine overpressure during the initial heat up cycle.

In situ HCl etching of InP to remove both indium and phosphorus thereby obtaining a polishing etch.

Growth of a buffer layer of InP or GaInAs at low temperatures prior to the higher temperature growth of the formal layer.

Use of a cover piece to prevent the preferential loss of phosphorus during warm up.

All the above methods have managed to minimize the initial heat damage to the substrate material, however their use add

additional factors that need to be addressed. The optimum choice depends largely upon the growth conditions and system that are exployed.

PROGRAM SCOPE

In bridging the gap from research samples to commercially viable production, the OMVPE of GaInAs/InP requires the identification of key process parameters and their relationships to the properties of the grown films. For a specific gas chemistry the design of each section within an integrated growth system determines the capability, controllability and reproducibility of the overall process. Here the specifications of the reaction vessel largely determine the performance capability whereas the lay out of the gas handling section sets the limits on controllability. The effective reproducibility of the process thereby depends largely on an understanding of the true mechanism from which the basic design crieteria for each of the individual sections of the overall process are obtained.

Mechanisms proposed by various authors on the growth of GaAs by Trimethylgallium (TMG) and arsine are often conflicting and non comprehensive (10-16). This lack of consistency has been attributed to the very complex temperature profiles that exist in the gas phase (10,14). These profiles strongly depend on the specific geometry of the reactor and substrate sample support system and in turn affect homogeneous gas phase reactions thereby influencing the course of the surface reaction processes. Due to the non-equilibrium nature of the overall deposition phenomenon

any comprehensive undertanding of the growth mechanism thus demands the consideration of heat, mass and momentum transfer simultaneously with homogeneous and heterogeneous kinetics.

The scope of this program thus covers a combined theoretical amd experimental study providing a descriptive framework suitable for design, control and optimization of the growth environment to meet set performance criteria. The experimental part of the program has been entirely based upon facilities available at Rensselaer Polytechnic Institute and are described in the following subsections.

I GROWTH SYSTEM

The OMVPE system used to conduct the film growth experiments consisted of a gas handling section, the gas-solid reaction vessel and an exhaust gas cleaning set-up.

a. GAS HANDLING SECTION: This section consisted of 1/4" 316 stainless steel tubing with Swagelok fittings, Components for flow control and regulation were Nupro bellow seal pneumatically activated valves and mass flow controllers. In addition a line for anhydrous HCl gas, completely isolated from the rest of the system was also available for in-situ etching as well as for susceptor and reaction vessel clean-up operation.

b. REACTION VESSEL: The cold wall reaction vessel used for the gas solid deposition process was a standard horizontal type 50mm ID quartz tube. It was equipped for front - end loading with separate inputs for the alkyls and hydrides. The r-f heated susceptor was configured to accommodate slices up to 1.5 x 1.75

cm on its front face as shown in Fig. 3.

c. EXHAUST AND CLEAN UP SECTION: The exhaust and gas clean up section consisted of gross and fine control of system pressure. Appropriately sized particulate and oil filteration units together with vacuum pumps allowing operation from 1 atm to 0.1 atm.

d. SOURCE REACTANTS: The commercially available volatile source chemicals during the course of this program consisted of trimethyl gallium (TMG), triethyl gallium (TEG), trimethyl indium (TMI), and triethyl indium (TEI) for group III and arsine for group V. Of these TMG and TEI were available at higher purity levels than TEG and TMI. In addition, the use of TMI, a solid at room temperature, would have added a degree of uncertainity for the Indium flow rate. These considerations dictated the use of TMG, TEI and arsine as source reactants.

III FILM CHARACTERIZATION SET-UP

Characterization of layers on this program involved studies of surface morphology, chemical composition, growth rate, mobility and carrier concentration. The specific set-ups utilized for these measurements are detailed below.

a. SURFACE MORPHOLOGY: Qualitative assessment of the grown layer morphology was carried out under a microscope utilizing Nomorski contrast to assess fine surface features.

b. GROWTH RATE: The following etches were used for delineation of the epitaxial layer:

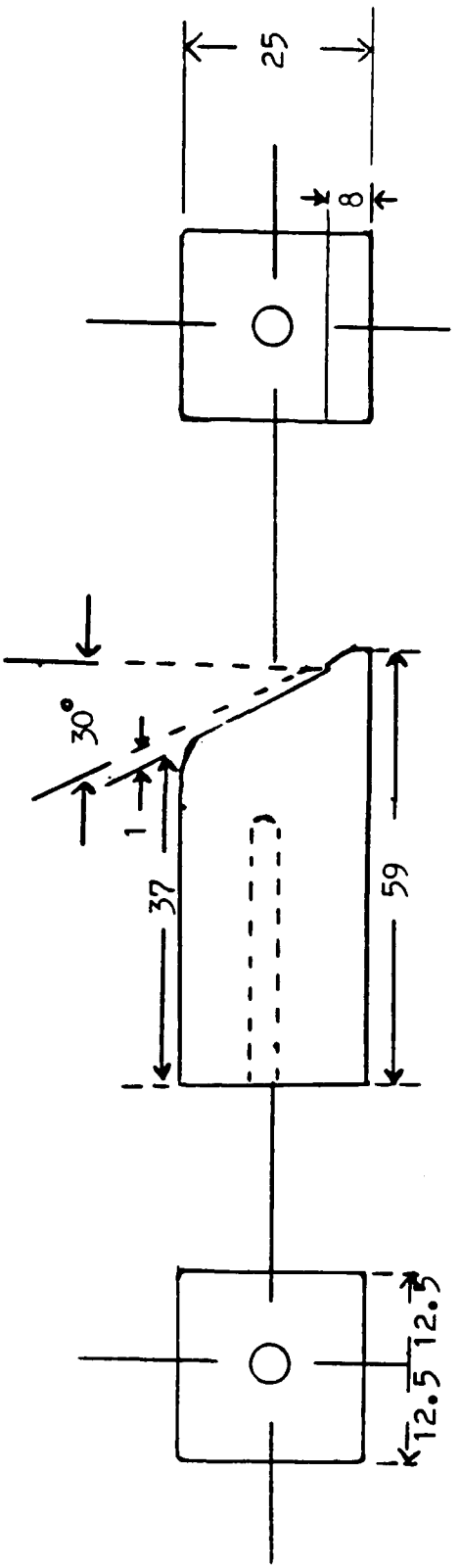

FIGURE 3: GRAPHITE SUSCEPTOR (All dimensions in mm)

1. A two part etch, A and B:

40 ml HF
40 ml H_2O → A
0.3 $AgNO_3$

40 ml H_2O
40 gr Cr_2O_3 → B

2. Another two part etch, A and B:

1 gr $K_3Fe(CN)_6$ in 50ml H_2O ⟶ A

12 ml NH_4OH in 36 ml H_2O ⟶ B

Both of these etches require etching in a fresh 1:1 mixture of A:B

3. Chu etch - HNO_3 :HBr = 1:3 by volume, for 30 secs.

4. Huber etch - H_3PO_4 :HBr = 2:1 by volume, for 2 mins.

Of these etches, the two part systems were the poorest, since they etched the surface GaInAs, and thus gave erroneous results. In one experiment, the entire epilayer was etched off! The Huber etch was found to give a clear indication and to leave the GaInAs surface intact. Thus, it was used in all cases where a precise value of growth rate was required. In day to day runs, an approximate estimate of the growth rate was obtained by using the value of the weight change using an analytical balance assuming edge growth as well as layer growth.

c. ELECTRICAL PROPERTIES: Hall measurements were made in a

conventional dewar system operated at 77 K and 4.5 kG. A van der Pauw configuration was used, with a cloverleaf pattern which was chemically delineated in the epi layer.

d. COMPOSITION: The importance of maintaining tight control over layer composition and its accurate determination was of paramount importance. We have thus utilized various methods for its measurement on a routine basis. Most of these have depended upon obtaining knowledge of energy gap Eg from which the layer composition is calculated based on Vergard's Law,

$$Eg\ (x) = 1.425 - 1.501x + 0.436x2\ (ev)$$

where x is the fractional indium content. These methods are described below.

d1. IR TRANSMISSION: Initially, we explored the conventional method of energy gap measurement, based on determining the IR transmission through InP layers, both with and without the grown GaInAs. The actual transmission of the epi layer is made by taking the ratio of these data, after making allowances for the reflection losses.

The system essentially consisted of an optical source with lenses and chopper, a 0.25 meter Jarrel Ash spectrometer, followed by the test sample, a PbS detector and a lock-in amplifer and x-y recorder. A digital drive was incorporated into this system, which greatly improved its readout accuracy.

The measurement technique is straightforward, but tedious and time consuming. In addition, it is prone to error since it involves the manipulation of two sets of data. Specifically, the

transmission of an InP sample is compared to that of an InP sample with an epi layer, as a function of wavelength. After data manipulation a plot is made of α^2 (optical absorption coefficient) vs. Eg, from which the energy gap is obtained. The composition is directly inferred from this enegy gap value, by the equation given earlier. This requires that assumptions be made about optical properties such as interface reflection . Nevertheless, as long as the α^2 vs. Eg characteristic is sharp, the data can be interpreted with a fair degree of confidence, and the energy gap obtained by projecting the linear portion of this curve. Table 1 presents data on four different samples, and illustrates the use of this approach.

The technique also provides a qualitative measure of compositional uniformity through the layer, by estimating the "steepness" of the absorption characteristic. This steepness has steadily increased as we have developed our growth process.

d2. SPECTRAL RESPONSE: Spectral response measurements are taken on Hall samples which are operated as photoconductors. For this approach, photoresponse measurements are made by illuminating the samples with monochromatic infrared light in the 0.1 to 1.0 micron wavelength region. The light from a tungsten lamp is first passed through a chopper and then through a 0.1 meter Oriel scanning monochromator with a 300 line per mm grating. The light is then focused, using f/3.7 optics onto the sample, which is contacted on opposite edges of the front face with alloyed tin dots.

Next, the sample is hooked up in series with a precision

hν, eV.	Run 208 E(g)=0.762 x=0.520	Run 294 E(g)=0.75 x=0.521	Run 295 E(g)=0.746 x=0.526	Run 298 E(g)=0.722 x=0.559
	(a) ^{2}	(a) ^{2}	(a) ^{2}	(a) ^{2}
1.035	12.71	9.07	9.37	7.85
1.002	11.56	8.14	8.22	6.52
.97	9.88	6.76	7.48	5.59
.941	7.75	5.27	6.14	4.91
.913	7.02	4.93	5.07	4.23
.886	5.53	3.95	4.83	3.66
.863	4.42	2.96	3.71	2.87
.839	3.57	2.72	3.06	2.59
.817	2.41	1.7	2.31	1.84
.796	1.5	1.09	1.53	1.59
.776	.63	.72	1.08	1.25
.757	.05	.21	.32	.76
.739		.06	.07	.43
.722		.01		.16
.705				.02
.69				
.675				

TABLE 1: α^2 as a function of $h\nu$

1 Kilohm resistor and 5 volts applied to the circuit. The a.c. photoresponse voltage induced across the resistor is measured by a lock-in amplifier, with the chopper signal used as a reference. The lock-in amplifier drives the y input of an x-y recorder, while the monochromator drive unit supplies the x input signal. The resulting curve falls from 90% to 10% of peak response in less than 20 meV for "good" samples, and 100 meV for "poorer" samples with a lower peak photo-signal. The band gap is found by extrapolating the curve to zero photoresponse.

d3. FOURIER TRANSFORM INFRARED SPECTROMETRY: During the last year, we were fortunate to acquire a Fourier Transform Infrared Spectrometer (FTIR) on another program. This instrument provides rapid, accurate information concerning the cutoff wavelength of the epi-layer by the conventional transmission method described earlier. Moreover, computer acquisition of data allows its manipulation so that the wavelength can be determined in a relatively convenient and accurate manner. The utility of this instrument is seen in the FTIR data for two layers of slightly different composition, as seen from the difference in the cutoff characteristics in figs. 4 and 5. The excellent uniformity of the composition as a function of layer thickness shows up qualitatively in the steepness of the transmission characteristic. In contrast, Fig. 6 shows the characteristic of a heavily graded layer, which was grown by the transient etch technique described in the film growth section.

d4. DOUBLE CRYSTAL X-RAY DIFFREACTION: Double crystal x-ray diffraction is perhaps the most important technique for stress

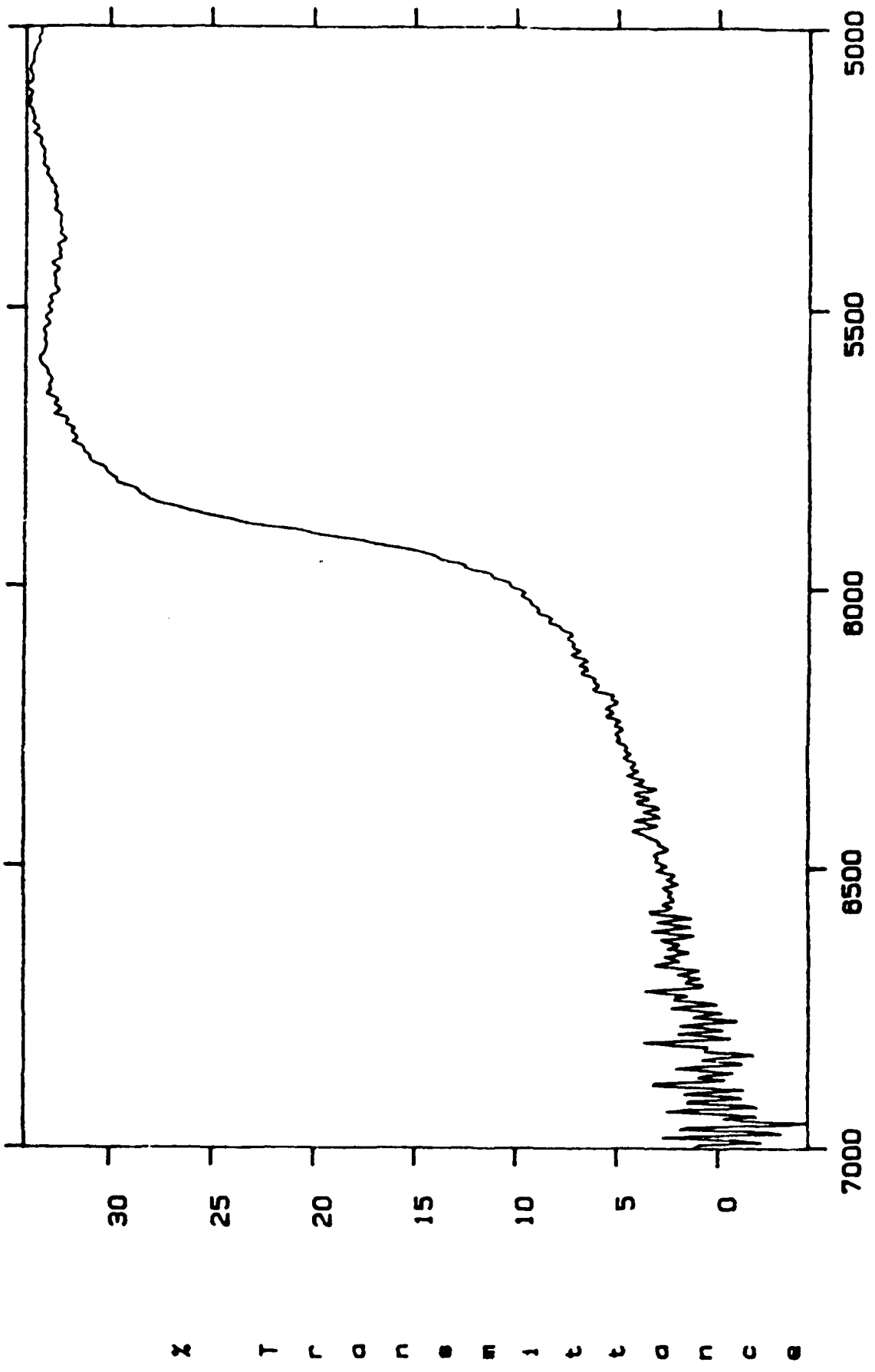

FIGURE 4: FTIR curve for a sample with x=0.545

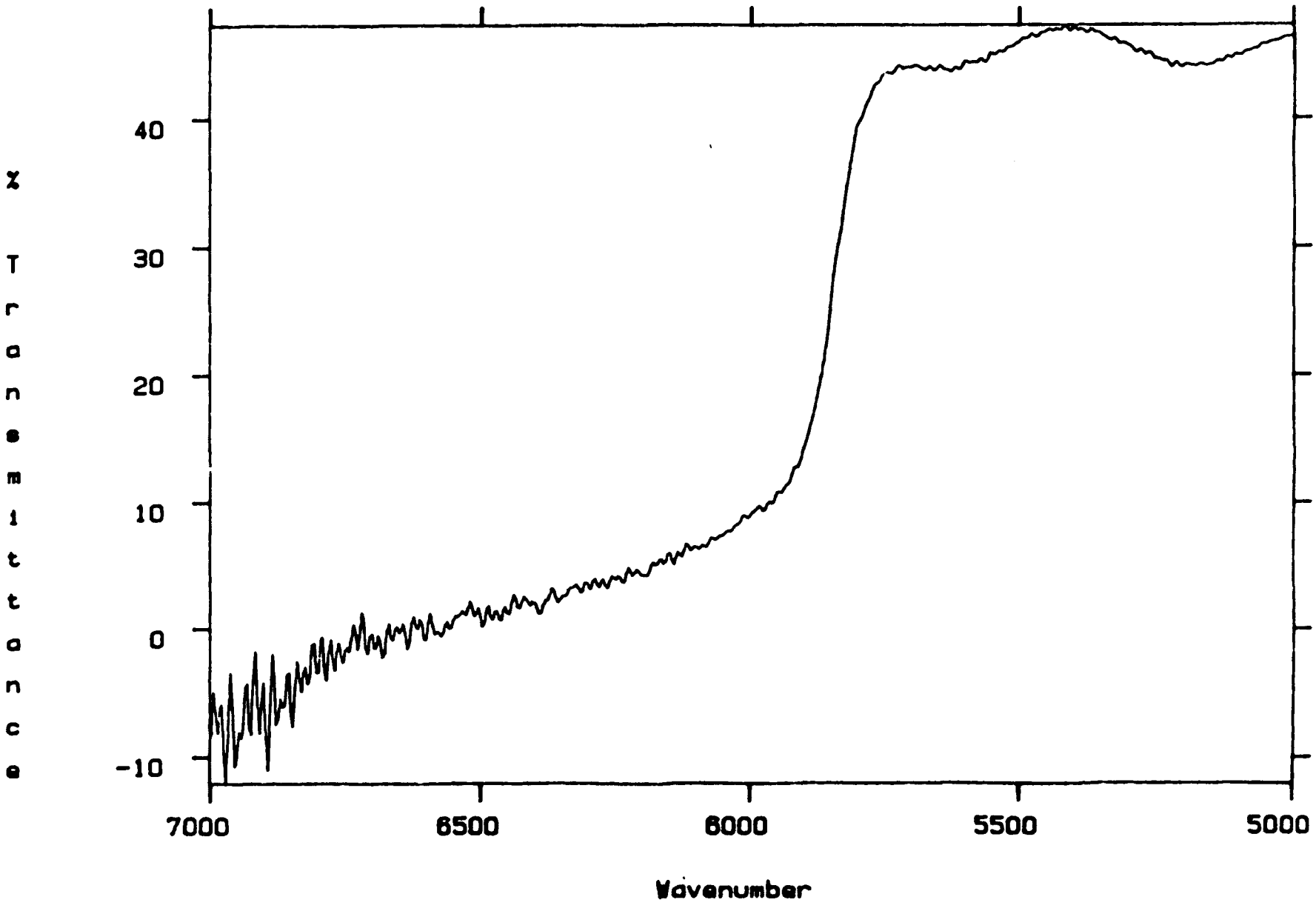

FIGURE 5: FTIR curve for a sample with x = 0.56

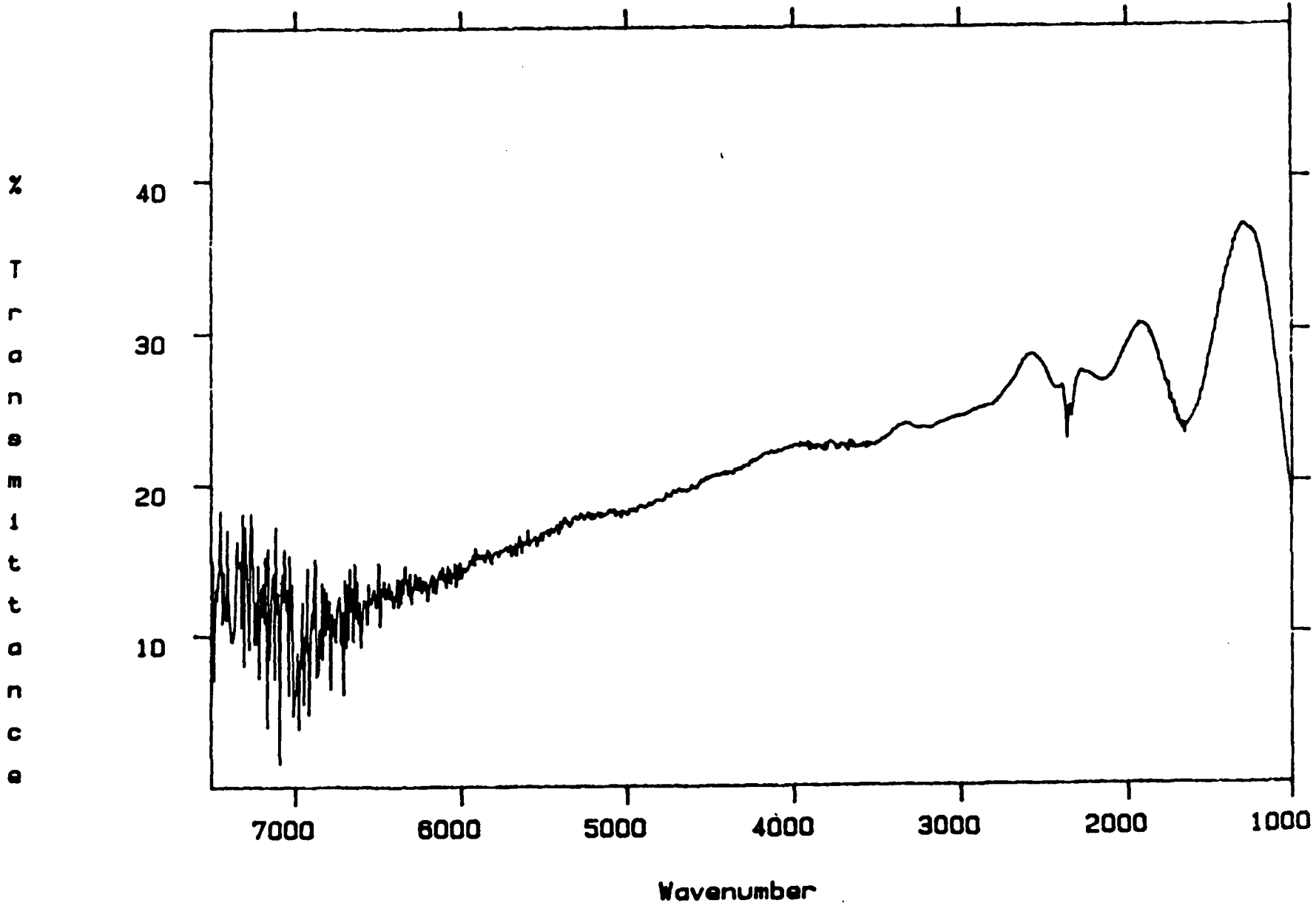

FIGURE 6: FTIR curve for a sample with graded composition

analysis of these epitaxial films. Moreover, this technique gives a direct measure of the amount of lattice mismatch which is present in any specific GaInAs/InP combination.

The system is a Bede 6" double crystal diffractometer (DCD) apparatus, with two crystal axes separated by 6". Each has an angular operating range of $\pm$ 3 degrees. The reference crystal axis has a step size of 0.67 arc seconds and the specimen axis step is 0.43 arc seconds. Each axis is equipped with a tilt goniometer having a range of about $\pm$ 1 degree.

In operation, an x-ray beam, which has been collimated by passing through a stainless tube, impinges on the first, or reference crystal, which is adjusted to its Bragg angle. The reflected beam is highly collimated, and now impinges on a second crystal, which contains the epi-layer under test. Ideally, the first crystal and the epi-layer should be of the same material and orientation (i.e., same lattice parameter). In our case, this is not possible, since we are evaluating GaInAs layers of different composition.

The best choice for the first crystal is bulk InP which is available in sufficient thickness so that it is not unduly stressed by the mounting procedure. Moreover, its lattice parameter is close to that of layers which were grown in this program. Upon reflection from the epi layer, the x-ray beam impinges on a NaI scintillation counter having a circular opening approximately one inch in diameter, which is used as a detector. No slit is used in front of the detector. The source of x-rays is a vertical tube with a copper anode; the maximum

output of the generator is 35kV, 20mA, or 700 Watts. The collimator placed in front of the x-ray tube has a circular aperature, 30 mils in diameter, and is 5.25 inches long, giving a beam divergence of 20 arc minutes. Prior to alignment, the x-ray tube, detector, and two crystal axes are collinear. This is called the zero position. All angles described below are with reference to this zero position.

The experimental setup consists of crystal mounting and system alignment. The technique for careful mounting is extremely difficult, since any stress induced during this process will result in measurement error. First, the reference crystal is mounted, and its axis rotated roughly to the Bragg angle of interest (in all cases here, the Bragg angle for a (400) reflection since all our epi-layers were grown on (100), or slightly misoriented (100) substrates). With the DCD base set to twice the Bragg angle, the detector is swung around to the specimen position and the reference crystal is rotated to that position which gives a maximum diffracted intensity at the detector.

With the first crystal alignment complete, the detector is swung back to its final position at twice the Bragg angle, and the position of the x-ray beam on the speciment crystal mount located using Polaroid film. Now, the specimen is rocked to locate its primary peak. This is done using the "Find" routine contained in the Bede software. Once the peak is found, the specimen tilt is optimized using the Bede "Automatic" routine. The time required for the sample alignment varies from thirty

minutes to several hours.

When taking a rocking curve, it is important that the reference crystal and sample be parallel. If they are not (i.e. the sample tilt is not optimum) then the rocking curve peaks will be broadened. There are three ways to determine the optimum sample tilt. First, if rocking curves are taken at different values of tilt, the value of tilt giving the minimum rocking curve full width half maximum (FWHM) is optimum. Alternatively, one can plot the rocking curve peak position versus sample tilt. This plot is approximately a parabola, concave upwards. The tilt giving the minimum rocking angle peak position is optimum.

The third technique involves a single scan in tilt. Once the peak has been found, a scan in tilt produces two peaks, corresponding to two points on the rocking angle versus tilt parabola. The point midway between these two peaks is the optimum tilt. This third tilt optimization technique is not only faster than the other two, but appears to be more precise ($\pm$ 0.1 mm compared to $\pm$ 1mm for the other two methods).

Another experimental variable which has been investigated is the detector position. It is found that the detector angle is not critical, since its angular cross section is much greater than that of the narrow diffracted beam. However, the radial distance of the detector is important. At distance less than 60 mm, the incoherently scattered (or Compton modified radiation) background becomes significant and increases with the inverse square of the radius. The diffracted peak intensity is

independent of radial distance. Thus, if the detector is placed too close to the sample, the peak/background ratio is decreased and the measured value of peak FWHM increases. We have found that, if the detector is placed 100 mm away from the sample, an accurate FWHM measurement can be made.

Another important parameter is rocking curve count time at each step. Count times of 0.01 second to 50 seconds were used to obtain the (400) peak with Cu $K_{\alpha}1$ radiation. With short count times, the peak intensity/noise standard deviation ratio was as low as ten. This resulted in gross errors in measuring the peak intensity and the FWHM. In all cases, a short count time can cause an overestimate of the peak intensity and underestimate of FWHM. When the count time was sufficiently long so that the peak intensity/noise signal ratio was 100 or greater, both the measured peak intensity and FWHM were independent of count time. For the peak measured, a count time of 10 seconds or greater was required for accurate measurements.

For rapid specimen alignment, it is important to know the precise orientation of the sample. For example, consider a sample which is misoriented 3 deg. from (100) toward (110). If this crystal is mounted randomly, it may be misoriented by three degrees in the tilt axis. With a tilt range of less than three degrees, the peak will never be seen. Even if the tilt range is greater than three degrees, finding the peak may require many hours of trial and error. This is because the crystal must be rocked back and forth at many different values of tilt before any peak can be distinguished.

Misorientation in the rocking axis is less bothersome, since the range of rotation is large, and since the rocking axis postion is optimized first. However, if the misorientation is known precisely before mounting, this angle can be added to the Bragg angle when the specimen is manually positioned. The tilt can also be roughly positioned. As a result, much guesswork is removed from system alignment, which can be completed in half an hour.

We have adapted a laser alignment technique for this purpose. This scheme uses a He-Ne laser, which is reflected from the cleaved (110) edge of a (100) sample. The deflection of the reflected beam on a calibrated scale then gives the amount of misorientation. This aligner was constructed, and used for sample mounting. An alternative approach, using a Laue camera, is more flexiile in that it can be used with odd orientations. However, the apparatus is expensive and measurements require about half an hour.

d5. PHOTOLUMINESCENCE: A PL system was also set up, consisting of a 22 mW argon ion laser and a 3/4 meter single pass spectrometer with a liquid nitrogen cooled detector having a S1 photocathode. Measurements are made on samples at 12-77K in this system. An optical grating, to cover the GaInAs range, was installed on this system. PL data obtained by this technique can be used to determine the room temperature energy gap of these layers.

In actual practice, PL turned out to be less useful than we had expected. Our system did not go down to 4K, so that the PL

response was only obtaained in the high quality samples. Thus, the technique could only be used for determining compositions close to lattice match.

III QUADRAPOLE MASS SPECTRUM ANALYZER

During the course of this program it became increasingly clear that data on the kinetics of the depletion reaction would be needed for developing an effective mechanistic model of the growth process. Since a model UTI 100C mass spectrometer was already available in-house the timely integration of this instrument within the OMVPE growth system became possible.

a. DETECTION: The quadrupole mass spectrometer consisted of a probe, picoammeter, rf generator and control circuitry. Essentially the instrument utilizes electron bombardment to form the positively charged ions that are filtered by a quadrupole. A positive ion is formed if sufficient energy is imparted by an electron during a collision with a molecule. This ion is attracted to the highest electron density at the center of the grid volume and towards the negative potential of the focus plate, injecting a focused beam of ions into the filter section. After filtration by a quadrupole, ion detection is accomplished by a 16 stage 10^{-4} 10^{-6} electron multiplier with a gain of between 10^{-4} and 10^{-6}. The signal from the electron multiplier is fed to an eight decade picoammeter. The entire spectrum may be observed in 75 msec with this instrument.

b. SAMPLING: The design of a practical mass spectrometer

sampling system for the low pressure OMVPE reactor was made after taking into account several factors. The operating pressure of the mass spectrometer is constrained to below 10^{-5} torr to obtain the necessary sensitivity and resolution, while that of the reactor must be near atmospheric pressure. Therefore, some means of dropping the pressure between the reactor and mass-spec was to be provided. This sampling system would have to allow a flexible sampling position within the reaction chamber, without significantly disturbing the flow. The interactions with the gas sample was to be kept to a minimum and the transit time had to be kept short.

We considered a simple orifice system, but concluded that the diameter of the sampler will have to be unmanageably large for sufficient sensitivity. Our calculations showed that a probe extending four inches into the reaction chamber for this purpose would have to be six inches in diameter! This was considerably larger than the reactor diameter itself. To reduce the size of the sampling system, we had to select a differentially -pumped double orifice system.

Commmercial differentially pumped sampling systems were available but the flow up to the first orifice would be essentially stagnant if they were used for sampling at high pressures. Therefore, to sample at near atmospheric pressure in a relatively small flow gas system, it became apparent that a capillary sampling system was necessary. Our design was based on this approach. In this system a quartz capillary was used to introduce the reactants into a skimmer chamber which was pumped

by a forepump. An X-Y micrometer adjustment plate with sliding "O" ring seals was used to align the capillary with an orifice which served as the entrance to the ionizer chamber, and on to the quadrupole. This region was pumped by a turbomolecular pump backed by a forepump. The capillary was supported by a 1/8 inch diameter stainless steel tube in order to reduce noise due to vibrations, and gas flushing was used to keep the region between the capillary and the tube clean.

The capillary passed through a long-throw, welded bellows that were attached between the reactor end seal and sliding "O" ring seal plate. This enabled sampling over a four inch length of the reactor tube without changing any of the characteristics of the probe. Fig. 7 shows the schematic for the sampling system, and its physical relationship with respect to the reactor.

EXPERIMENTAL RESULTS

I SYSTEM MODIFICATION:

A number of modifications had to be made to the OMVPE growth system during the course of this program. These became essential since any variability introduced by the state of the equipment and hardware would have resulted in erroneous interpretation of the data. These aspects plus those relating to overall system callibration are described below under individual sub-headings.

a. TMG FLOW CONTROL: Considerable difficulty was experienced in adjusting the flow through the TMG bubbler, with any degree of

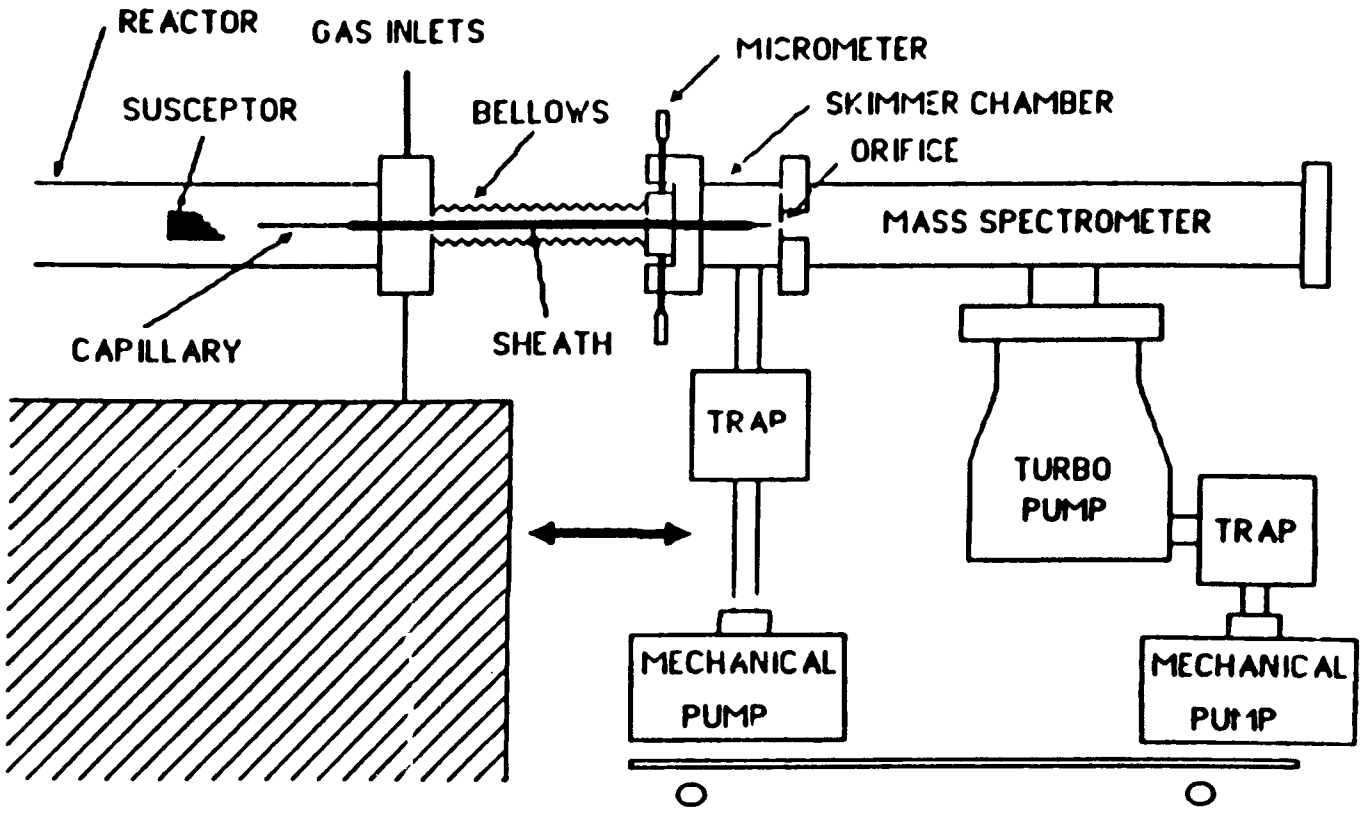

FIGURE 7: Schematic of the sampling system

accuracy, since a typical run called for 5-10 sccm flow when the TMG was held at -10° C. We used a double dilution system using 3 mass flow controllers and a manual valve, which allowed a 10:1 dilution of the TMG flow passing through the main mass flow controller. Although normally stable at both atmmospheric and reduced pressure, this system from time to time, gave us problems which resulted in instability during a run. Primarily, this came about because the system was hard to balance. During the last year, a new line of mass flow controllers, which operate at extremely low flow rates, (5 sccm full scale) became available, allowing us to switch to this simpler approach.

b. INLET BEAMING EFFECT: Many attempts were made to laminarize the flow of input gases, and to prevent a beaming effect at reduced pressures. These included the use of exponential horn systems, and various arrangements of inlet gas configurations. Eventually, we found that a diffuser plate was most effective for this purpose.

c. SUSCEPTOR DESIGN: The susceptor used previously in our earlier study at atmospheric pressure resulted in conditions approaching those of stagnation point reactor. Although reasonably efficient, one problem with such susceptors is that they create eddies in the gas stream in front of the tube. These eddies result in extending the time during which the reactants are resident in the reactor, thus aggravating gas depletion effects. Evidence of this problem is that, upon commencing growth, a freshly cleaned reactor tube becomes rapidly fouled. Long growth runs result in extremely poor surfaces, due

to the incorporation of Lewis reaction products into the growing layer. As a result of this problem, a number of changes were made to the susceptor design. First, its shape was altered along aerodynamic lines to prevent the formation of these eddies. An immediate consequence was that the front end was relatively clean during a growth run. A very faint reddish brown coloration of the tube indicated that there was a small, uniform deposit in this region.

d. REACTION VESSEL CLEAN UP: Growth of GaInAs is accompanied by some fouling of the front end of the reactor, due to premature reactions. Moreover, the susceptor and its environment is fouled during growth because of pyrolysis of the reactants.

A number of modifications were made to the reactor in order to simplify cleaning of the reactor tube annd the susceptor from run to run. First, an internal quartz liner was installed in front of the susceptor. A faint, yellowish tinge was seen on this liner after each run, indicating that some products of the Lewis reaction were being formed. This liner was cleaned in aqua-regia after each run, and blown dry with a hot air gun before it was re-installed.

Next, a mullite tube, of diameter such that it could slide between the reaction tube and the r.f. coil, was installed. The length of this tube was such that it could be slid behind the susceptor during growth. After growth and removal of the sample, this tube was slid over the susceptor and the front end of the reactor. Now, it served as a thermal insulating sleeve during

the reactor/susceptor cleaning process.

Cleaning was done by bringing the suseptor temperature to 1100 C with a hydrogen flow of 6 slm and a HCl (10%) flow of 100 sccm, at atmospheric pressure. A 10 minute etch step served to clean both the susceptor and the "hot" quartz wall. This was followed by a 20 minutes step at 1100 C and a reduced pressure (90 torr) to remove abosorbed chlorine from the susceptor. At this point, the system was brought to room temperature, and the mullite tube slipped to the rear of the reactin chamber.

This simple scheme thus allowed continuous day-to-day operation of the reactor without any dismantling, and was in routine use during the growth runs. As a result, a permanent HCl connection for general clean up, as well as for slice and susceptor etching was in place. However HCl gas had to be handled cautiously , because its presence effectively broke the C-H bond, resulting in carbon incorporation into the growing layer. To avoid these problems, the HCl line had to be isolated from the system to minimize its interaction with the alkyls. Furthermore, the growth procedure had to be modified to ensure the removal of HCl from the system prior to growth of the GaInAs layers.

II SYSTEM CALLIBRATION:

It is well known that both arsine and phosphine are supplied with traces of moisture as a contaminant. This presents a serious problem, since it results in hydrolyzation of the alkyls in the gas phase, as well as incorporation of oxygen in the growing layer. This oxygen is a deep level and thus destroys the

photoluminescence properties of the grown layer. One approach to reducing this problem is to pre-dry these gases, using molecular sieves or ternary melt bubblers (Ga-In-Al alloy) in the gas line. We did not use either approach since the thrust of our work did not emphasize photoluminescence properties, and so would not be affected by these refinements.

On our program, gallium arsenide is grown on GaAs substrates from time to time, to ensure the basic integrity of the arsine gas, and also of the reactor system. This procedure is also followed when any plumbing changes are made, or when any source reactant is replaced. The typical run parameters used in these tests are:

H_2 - 5 slm

TMG - 0.14 torr

ARSINE - 4.2 torr

System pressure - 760 torr

Growth temperature - 700 C

For these condition, the resulting GaAs in a typical run has the following properties:

μ_{300} - 8.3×10^{3} cm^2/V-sec

n_{300} - 1.1×10^{14} $/cm^3$

μ_{77} - 8.03×10^{4} cm^2/V-sec

n_{77} - 6.6×10^{13} $/cm^3$

These values are indicative of a typically clean, tight reactor sytem.

Our arsine gas supplier was originally Matheson, but we switched to Phoenix (California) during the course of this program, because of superior results we had obtained with GaAlAs using this supplier. With this gas, one of our test runs using the system parametes listed above, gave the following results:

$$\mu_{300} - 8.4 \times 10^{3} \text{ cm}^2/\text{V-sec}$$

$$n_{300} - 1.1 \times 10^{14} /\text{cm}^3$$

$$\mu_{77} - 1.199 \times 10^{5} \text{ cm}^2/\text{V-sec}$$

$$n_{77} - 9.6 \times 10^{13} /\text{cm}^3$$

These are some of the best results we had achieved, so we made a complete shift to Phoenix as our arsine supplier for this program.

III SUBSTRATE PREPARATION

a. WET CHEMICAL ETCHING: The etching procedure for InP is considerably more difficult than that for GaAs, because of the formation of regions of indium oxide which are difficult to remove by chemical means. A number of different etches have been tried (Bromine-methanol, Caros' etch etc.) but all result in patchy surfaces. We have found that many etches published in the literature give remarkably poor results. One such etch,

consisting of lactic acid: nitric acid = 5:1 by volume, actually resulted in a weight increase after a 3 minute "etch", probably from the residue which was formed on the slice during this step.

In our experience, clean surfaces, free from these patches, can only be obtained if ultrasonic breakup of these regions is employed in the etch procedure. We have found that a small modification of Duechemin's procedure gives the best results.

Substrates are received pre-polished from the vendor. These are cleaned as follows:

Degrease:	Hot TCE
	Hot ACE
	Methanol Rinse
	Distilled water Rinse
Pre Etch:	Conc. H_2SO_4 in ultrasonic for 5 minutes
	Distilled water Rinse
	Hot Methanol Rinse
Etch:	3% Br/Methanol - 3 minutes
	Methanol Rinse
	Blow Dry N2

Slices are immediately transferred to the reactor at this point.

b. IN-SITU ETCHING: A number of growth runs were conducted using a tansient in-situ etching method explored initially on an earlier program (35) . Unfortunately this technique resulted in a large amount of adsorbed chlorine from the HCl used. This in turn caused a cleavage of the C-H bonds, resulting in carbon incorporation within the grown layer as indicated by the

photoluminescence measurements. Thus this approach was dropped. This of course necessitated the use of phosphine overpressure during the time that the substrate was brought up to growth temperature.

IV EPITAXIAL GROWTH

a. SYSTEM PRESSURE: In an earlier study conducted prior to the undertaking of this program (17) RPI had investigated the growth of GaInAs/InP in an atmospheric pressure OMVPE system. Based on that previous experience we proceeded to evaluate growth behaviour under low pressure conditions. Here the advantages over atmospheric pressure are two fold. First the resultant increase in gas velocity (for the same inlet flow rates) would reduce residence time in the reaction vessel thus further minimizing the effect of premature reactions. Secondly the resulting enhanced diffusion rates would greatly improve layer uniformity, thus making growth over larger areas more feasible. A disadvantage however was that the growth rates would fall off for the same consumption of alkyls, i.e., the growth system would become inefficient. As a result, operation at excessively low pressures would have been counter-productive. Thus a series of runs were made, with a steady decrease in growth pressure. A dramatic improvement was seen around 180 torr, with a near-cessation of premature reaction (as evidenced by an absence of fouling of the reactor liner). All our subsequent work was carried out at 150 torr to provide an additional margin of safety.

b. SUBSTRATE TEMPERATURE: Growth had been carried out at susceptor temperatures of 700-575° C. However the actual substrate temperature was not known for these conditions, and may have been as much as 50 degrees lower because of the combined effects of cooling (by the hydrogen gas) and reduced susceptor-substrate conduction because of operation at low pressures. Optical pyrometry was used to check the temperature of the susceptor during a growth run, i.e., with 5-6 slm of hydrogen gas flow. Assuming that the transmission of quartz is 0.92, and that the emissivity of graphite is 0.66, the surface temperature of the susceptor was detemined to be about 40°C below that which is obtained with no hydrogen gas flow. This cooling effect is due to the high-thermal conductivity of the hydrogen gas, and to poor thermal contact between the sample and the susceptor. The comparable value for atmospheric pressure operation was 20°C. In general, we have found best results for a susceptor temperature of 600 - 650°C (as measured by a quartz sheathed thermocouple in the susceptor). As noted above the actual susbtrate temperature is in all probability about 40°C lower than the measured value. Thus, we estimate that layer quality is optimized at susbstrate temperatures of 560-610°C in our process.

c. REACTANT FLOWS: The composition of the GaInAs layer is a function of the partial pressues of all three of the source reactants, since any premature TEI-arsine reaction (Lewis reaction) results in depletion of the indium species. As a result, the process of achieving growth at the optimum composition (In/Ga = 0.53/.47) is considerably more tedious than

that required for adjusting the composition in the GaAlAs system, where no Lewis depletion reaction occurs. Some 35 runs were necessary to achieve the optimum values of partial pressures for this composition.

The procedure followed was a relatively systematic one. First, a total hydrogen flow of 6 slm was chosen since this is commonly used in our GaAs growth work. TMG and arsine pressures of 0.004 and 1.0 torr respectively were chosen, since these are commonly used for the growth of GaAs in this system. Next the pressure of TEI was varied on a number of runs, which were carried out at a constant temperature (550-700°C, in steps of 50° C) for 60 minutes, with a system pressure of 152 torr.

After each run, the composition was measured by the IR transmission technique. This data was then used to make a rough estimate of the TEI partial pressure to be employed in the next run.

Typical run data is as follows, for a growth temperature of 650°C:

TMG = 0.004 torr

TEI = 0.002 torr

x (indium fraction) = 0.23

For another run:

TMG = 0.004 torr

TEI = 0.004 torr

x = 0.55

and so on. We also observed that increasing the partial pressure of TEI resulted in an increase in the growth rate, with a concurrent deterioration of the surface morphology.

Further runs were carried out by proportionately reducing the partial pressures TMG and TEI. For example:

TMG = 0.003 torr

TEI = 0.006 torr

Arsine = 1 torr

x = 51%

Next, the arsine partial pressure was altered, because this affects the electrical and surface properties of the GaInAs. In addition, it results in a small change in the composition, with x increasing as arsine is reduced, and vice versa. For example,

TMG = 0.002 torr

TEI = 0.004 torr

Arsine = 0.66 torr

x = 0.53

Here, a mirror-like surface was obtained, with the correct composition. A number of additional runs were made, with even lower reactant partial pressures, to see if improvements could be achieved in the quality of the grown layers. We have come to no definitive conclusion from these experiments, however. As a result, our subsequent runs are occasionally made with lower TMG and TEI pressure, by as much as a factor of 2 in some cases. Table 2 shows the data for a number of runs of this type, with x values determined from transmission measurements.

The composition obtained for a number of runs, with only varying the TMG and TEI ratios, has been plotted as a function of TEI/TMG+TEI , and can be approximated by a straight line, with a slope of approximately 0.9, so that

$$x = K\ [TEI/TMG+TEI]$$

where K= 0.9. A simple growth model, based on the assumption of no Lewis reaction, and unity sticking coeffcients, would result in

$$K = [TEI+TMG/TEI+(DTMG/DTEI)TMG]$$

where DTMG and DTEI are the diffusion constants of TMG and TEI in hydrogen respectively. Both DTMG and DTEI can be estimated from considerations of their molecular weights, and are approximately 0.284 and 0.246 cm /sec respectively. Using these values, and partial pressures of 0.001 and 0.002 for TMG and TEI

Run #	H (Flow Rate)	P_{TMG}	P_{TEI}	P_{AsH}	$P_{Sys.}$	x
144	6 slm.	0.002t	0.004t	0.66t	152t	.52
145	6 slm.	0.002t	0.004t	1.0 t	152t	.50
146	6 slm.	0.001t	0.002t	0.66t	152t	.38
147	6 slm.	0.001t	0.003t	0.66t	152t	.48
148	6 slm.	0.001t	0.004t	0.66t	152t	.60
149	6 slm.	0.001t	0.0034t	0.66t	152t	.60
150	6 slm.	0.0015t	0.0032t	0.33t	152t	.40
151	6 slm.	0.002t	0.0041t	0.66t	152t	.57
152	6 slm.	0.001t	0.00205t	0.66t	76t	.56
153	6 slm.	0.001t	0.00205t	0.66t	76t	.40-.53

TABLE 2: Composition as a function of run parameters.

respectively, results in a theoretical value of 0.95 for K in the absence of Lewis reaction effects. An experimental value of 0.9 is thus evidence that operation at reduced pressure and temperature has almost eliminated this problem. We note, in passing, that K values from 0.4 to 0.44 were obtained for GaInAs growth at atmospheric pressure, on an earlier program.

d. GROWTH INITIATION EFFECTS: The optimum sequence to be used during the initiation of growth of GaInAs was also investigated. Here, growth involves heating the susceptor, and turning on the approproate flows of Arsine, TEI and TMG. We have found that the sequence of input fluxes, as well as the temperature at which these are initiated, determines the composition of the first few monolayers of the interface. It is important that this composition be on the GaAs-rich side of the ternary alloy, rather than on the InAs-rich side, to prevent the formation of a low resistivity interface region. (We should emphasize that it is unrealistic to assume that the exact composition can be achieved during this transient phase, hence the need for this investigation.)

Establishing organometallic flows at 300° C to prevent substrate decomposition resulted in Whisker formation together with etch pits, at Arsine/TMG+TEI partial pressure ratios below 20. EDAX analysis of these whiskers showed that they are almost pure indium. We believe that this problem is created during the initiation of growth, since both whiskers and etch pits seem to occur at the same time. The etch pits described are more in the

form of an absence of growth, rather than true pitting, and are of relatively uniform size. They take on the shape of inverted square pyramidal holes, with edges along the [110] directions, and (111) sides. The ratio of the edge length to the epi-layer thickness is about 1.3, and not 1.414 as would be expected for a true stacking fault which starts at the surface. Moreover, observations of cleaved samples, taken with a scanning electron microscope, show that the apex of these pyramidal holes does not coincide with the surface. We believe that the defect does originate at the substrate-epi interface, however, but that slow growth appears to occur along the (111) faces, filling in the pits slightly. This would explain why they were all of reasonably uniform size.

This situation is somewhat simplified when an InP buffer layer is first grown. Now, the substrate is brought to growth temperature in a phosphine atmosphere to prevent decomposition. InP growth is initiated by the introduction of the indium species. The transfer to GaInAs growth then requires turning off the phosphine, and turning on the arsine . Here too, a number of runs were made to determine the optimum sequence. We found that a small overlap in the two flows resulted in the best material. This is because the initial growth is now of GaInAsP, which has a wider gap than the desired GaInAs. Moreover, the absence of phosphine for even a short time led to loss of phosphorus, with pitting of the InP.

e. EFFECT OF SUBSTRATE QUALITY AND ORIENTATION: In our work we used a variety of both semi-insulating (Fe-doped) as well as n+

(S and Sn doped) material (Crystacom California). Here, we observed considerable variability in the surface morphology of samples grown on these substrates. Our results can be summarized as follows:

a. Layer morphology on S and Sn doped substrates was consistantly superior to that obtained on Fe-doped material.

b. With Fe-doped material, layer morphology was often highly variable for layers grown side by side during the same run.

c. Layer morphology with Fe-doped material was also a function of how early this material was purchased during the course of this program. Thus, recently acquired substrates (during the last one year) were considerably superior to those obtained earlier.

It is known that Czochralski grown InP has a W-shaped radial dislocation pattern, because of stresses set up during crystal growth from the melt. This means that slices will have poor regions in the center and on the perimeter, and a thin torus of good material. Presently purchased substrates have this same basic radial distribution of defects. However, the useful torus is considerably wider. Thus, substrate quality of SI-InP has considerably improved over the last year. Even so, the EPD for these substrates is typically around 5×10^4 /cm .

It is a generally accepted tenet of epitaxy that layers grown on slightly misoriented substrates are more specular than those grown on precisely oriented material. Certainly, all our work with other material systems such as GaAs and CdTe have shown this to be the case. As a result, our early work focussed on the use

of (100) material, 2° misoriented towards the (110). We have found, surprisingly, that growth on oriented InP substrates results in considerably superior morphology. We do not understand why this is the case; certainly, theories for morphology vs. mis-orientation will need revision. All our results over the last year are based on oriented material.

V LATTICE MATCHED FILM GROWTH

A total of 460 runs were made during the course of this program. These included runs during the shakedown phase, GaAs and arsine gas calibration runs, runs with different gas entry configurations and runs with different susceptor designs. Finally, a large number of runs were made to adjust the composition to the lattice-match conditions.

In order to minimize the formation of intefacial defects in the growth of heteroepitaxial structures, the matching of crystal structure, lattice parameter and thermal expansion properties is highly desirable. Lattice mismatch between an epitaxial layer and its substrate will be accommodated by some combination of elastic strain, associated stress, and the formation of dislocations. The lattice mismatch between GaInAs and InP at 300 K is shown in Figure 8. Strains are induced in the epitaxial layer due to lattice-mismatch and this results in the formation of dislocations if the associated stress exceeds the elastic limit.

When an epilayer has been grown with a small mismatch it undergoes tetragonal distortion, with the misfit accommodated

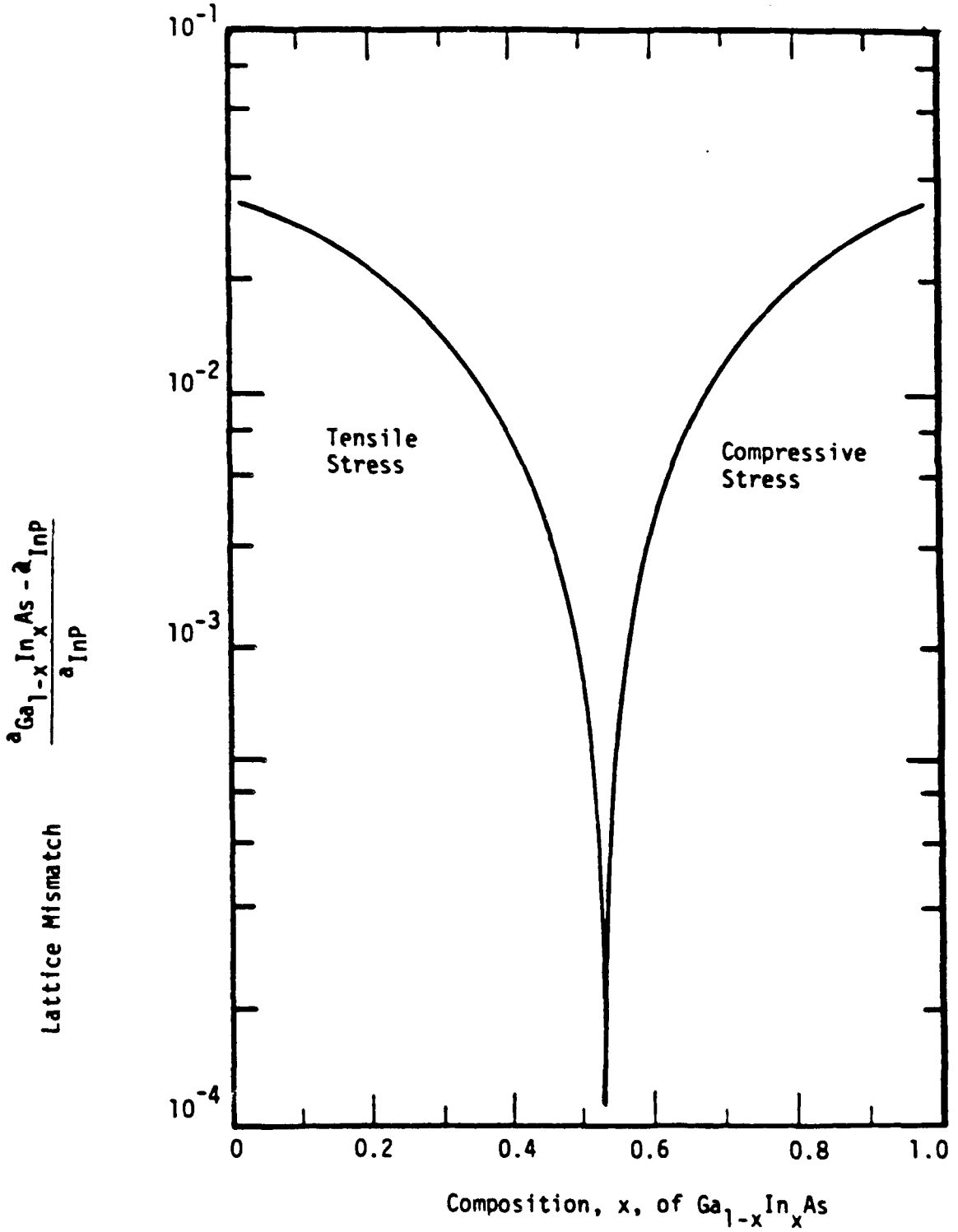

FIGURE 8: Lattice Mismatch of GaInAs grown on InP as a function of composition

primarily by a change in the lattice constant perpendicular to the substrate. Larger values of mismatch result in the generation of misfit dislocations along the <110> directions. Finally, at high values of mismatch, a dense dislocation array is formed, and the material becomes highly defected. In practice, the epitaxial layer is considered lattice matched if the lattice mismatch ($\Delta a/a$) is less than 10^{-3} .

Epitaxial layers are grown at elevated temperatures and than cooled following growth. Since the thermal expansion characteristics of the epilayer differs from those of the substrate, the combination will not be lattice matched at both growth temperature and room temperature. The thermal expansion coefficient of InP is 4.67×10^{-6} (C^{-1}) while that for $Ga_{.47}In_{.53}As$ is 5.66×10^{-6} (C^{-1}).

To minimize dislocation formation, epitaxial layers should be grown lattice matched at growth temperature since dislocations form most easily at high temperatures. Consequently, a strain will result upon cooling due to the difference in thermal expansion coefficients. Unfortunately for the GaInAs/InP system, if the epitaxial layer is lattice-matched at growth temperature, it will be in a state of tensile stress at room temperature.

Although elementary theory predicts that it is only the magnitude of the strain that causes dislocations, in practice tensile stress is much more detrimental to an epitaxial layer than is compressive stress, especially for thin layers. This can

be seen in Figure 9 where the theoretical and experimmental curves for the initiation of misfit dislocations are plotted as a function of epitaxial layer thickness for GaInAs on InP. Here, curve (a) is the theoretical curve for dislocations formed at room temperature and curve (b) is the theoretical curve for dislocations formed at the growth temperature of 600°C in terms of the lattice misfit at room temperature. The dashed curve represents the experimentally determined threshold region for the initiation of misfit dislocations. Note that it is in the vicinity of the theoretical curve for dislocations formed at the growth temperature, but is highly asymmetric, especially at low values of d. It shows that at the growth temperature, dislocations were much more easily introduced for layers in tension than in compression.

In summary, it is apparent that tension is much worse than compression for both the creation of dislocations in the epitaxial layer and the reduction of the mobility in the alloy. In fact, layers with somewhat more InAs than required for lattice-matching at room temperature (53%) or at typical growth temperatures (52%) may have superior electrical properties.

Evidence of lattice mismatch to the InP substrates has been observed in many runs. For large lattice mismatch, where $\Delta a/a < 10^{-3}$ (corresponding to .505 <x< .555) the GaInAs surface appears shiny and free from features. Within the above range, a cross hatch pattern in observed. This pattern vanishes, however, as the composition approaches 0.53 ± 0.01.

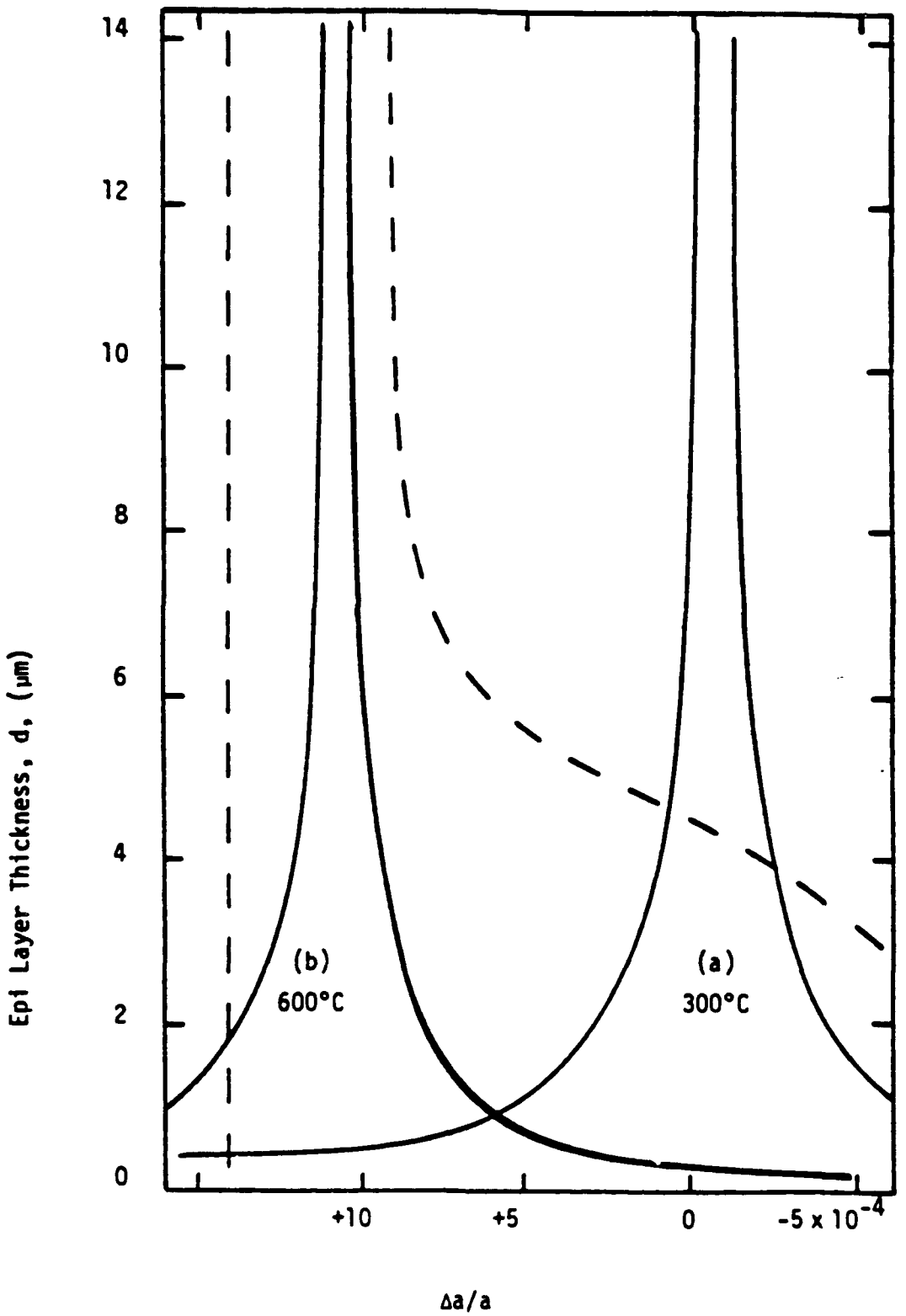

FIGURE 9: Calculated threshold region for the initiation of misfit dislocations in GaInAs on InP. Broken line-experimental.

The electrical properties of the grown layer are strongly dependent on the composition, and thus on the degree of lattice mismatch. Assuming that a (InP) = 5.8686 A, a (GaAs) = 5.64613 A, a (InAs) = 6.0584 A, and that all misfit dislocations are accommodated uniformly within a 2 um layer, we obtain a dislocation concentration of 1.3×10^{16} /cm for a layer of composition x = 0.5. This calculation results in a low value, since dislocations are usually confined to a much thinner layer, so that the local dislocation content is probably higher.

A second problem area is that layers of composition x <0.53 are in tension while those with x > 0.53 are in compression. As a result, the electrical properties of mismatched layers with an excess of indium are considerably superior to layers with an indium deficit. Consistently, we have noticed an extremely rapid fall off in layer mobility as x falls below 0.53. On the other hand, values of x>0.53 result in a gradual fall off in this parameter. This, in effect, results in a window of compositions with acceptable electrical properties. This is seen in the data of Table 3, for layers grown on an InP buffer. The growth of layers of x > 0.53 has the disadvantage, however, in that this results in a shift in the wavelength response of the resulting detector. This is seen in Table 4, where the values of Energy gap and cutoff wavelength are listed as a function of the composition.

a. COMPOSITION CONTROL: Only one specific GaInAs composition is lattice matched to the InP substrate. As a result, the composition of this material must be precisely maintained from run to run, in order to obtain a reasonable yield of useful epitaxial layers. This is because mismatch results in material with a high defect concentration. (It is worth mentioning, in passing, that this problem does not exist during the growth of GaAlAs on GaAs. With this system, lattice-match is achieved over the full composition range; hence changes in composition do not result in defected material.)

We have experienced a large amount of scatter in our layer compositions from run to run, and some time has been spent trying to determine its cause. This has been directly traced to the fact that the chiller temperature varies by about 1° C during the course of a run, but must be kept to within 0.1° C. Typically, this resulted in x values from 0.52 to 0.54, for "identical" runs. This has been achieved by two methods. First, the chiller has been physically moved away from the equipment chamber, to avoid undue heating of the bubbler by the pyrolysis furnace, the r-f. generator, and the chiller refrigerator itself. Next, the feedback sensor has been moved into the bubbler well to give control at the point-of-use. A combination of these approaches has resulted in a chiller control to 0.1° C as required.

A third cause for scatter in layer compositions from run to run lies in the fact that the control accuracy of a mass flow controller (MFC) is specified as a certain percentage of full

scale (FS) (0.2% for our units). This means that the MFC's should be preferably operating near 100% FS to minimize this error. Thus, it is a mistake to assume that these units can be operated over their full range without error. In our reactor, the indium channel operated around 33% FS, the gallium channel was at 50% FS. We calculated that this would result in a change of composition by as much as $\pm$ 0.008 from run to run. On the other hand, operation of all controllers around 100% FS would reduce composition variations to $\pm$ 0.002 from run to run.

A fourth cause for loss of composition control is the inability to maintain saturated flow through the alkyl bubblers, as a function of time. This is especially true as the bubbler approaches its end of life. We have discussed this problem with the vendor, and proposed a number of bubbler design changes (small diameter, deep vessels; low diameter dip tubes with multiple orifices, etc). They are taking these under advisement. An alternative approach, used for doping in commercial siiicon epitaxy, is to use computer control to vary the flow through the bubbler from run to run. Our system did not allow this feature to be incorporated.

A final problem is that of compositional control over the area of a substrate. Again, loss of control here results in poor yield of devices on a slice. In our own experiments with our susceptor, we have been able to demonstrate a composition control of better than $\pm$ 0.1 over a 1.5 cm x 1.75 cm substrate area, not withstanding the fact that a small diameter (51 mm ID) reactor was used.

Run #	x	μ_{300}
381	.5	2370
382	.52	6723
384	.53	9079
383	.54	9398
388	.54	8874
385	.57	7490

TABLE 3: Variation of the room temperature mobility with x

Ga	In	Eg(10K)	λ nm(10K)
.37	.63	.709832	1.74534
.38	.62	.719732	1.72134
.39	.61	.729726	1.69776
.4	.6	.739816	1.67461
.41	.59	.75	1.65187
.42	.58	.76028	1.62953
.43	.57	.770654	1.6076
.44	.56	.781124	1.58605
.45	.55	.791688	1.56488
.46	.54	.802348	1.54409
.47	.53	.813102	1.52367
.48	.52	.823952	1.50361
.49	.51	.834896	1.4839
.5	.5	.845936	1.46453
.51	.49	.85707	1.44551
.52	.48	.8683	1.42681
.53	.47	.879624	1.40844
.54	.46	.891044	1.39039
.55	.45	.902558	1.37265
.56	.44	.914168	1.35522

TABLE 4: Eg and λ as a function of composition.

VI GROWN LAYER CHARACTERIZATION

a. COMPARISON OF COMPOSITION MEASUREMENT TECHNIQUES:

In light of the large scatter in our data on layer composition from run to run we conducted a careful comparison of the composition value obtained by IR transmission and spectral response measurement techniques. Fig. 10 shows the correlation between x values obtained by these two different methods. We note that as long as the input excitation is kept low, there is good correlation between these methods. With large signals however there appears to be a linear shift in values. Thus it is important to verify that we are in the small signal mode when this measurement is made. This is accomplished by reducing the excitation until the Eg value becomes independent of changes in the excitation level.

b. DETERMINATION OF LATTICE-MISMATCH INDUCED STRESS

A large number of rocking curves were taken during the course of this program. A few of the rocking curve results for GaInAs on InP samples are shown in Figs. 11-16. One sample was measured after successive rotation by 90 , 180 , and 270 deg . Since the InP-GaInAs peak separation was found to be independent of the rotation angle (550 arc seconds, $\pm$ 80 arc seconds), we conclude that this epilayer was deposited with the same orientation as its substrate (to within 80 arc seconds). The 80 arc seconds variation may be due to composition nonuniformity of the layer, since the x-ray beam reflects off different spots on the sample for all four measurements.

Data taken by this system has been analyzed, and a computer

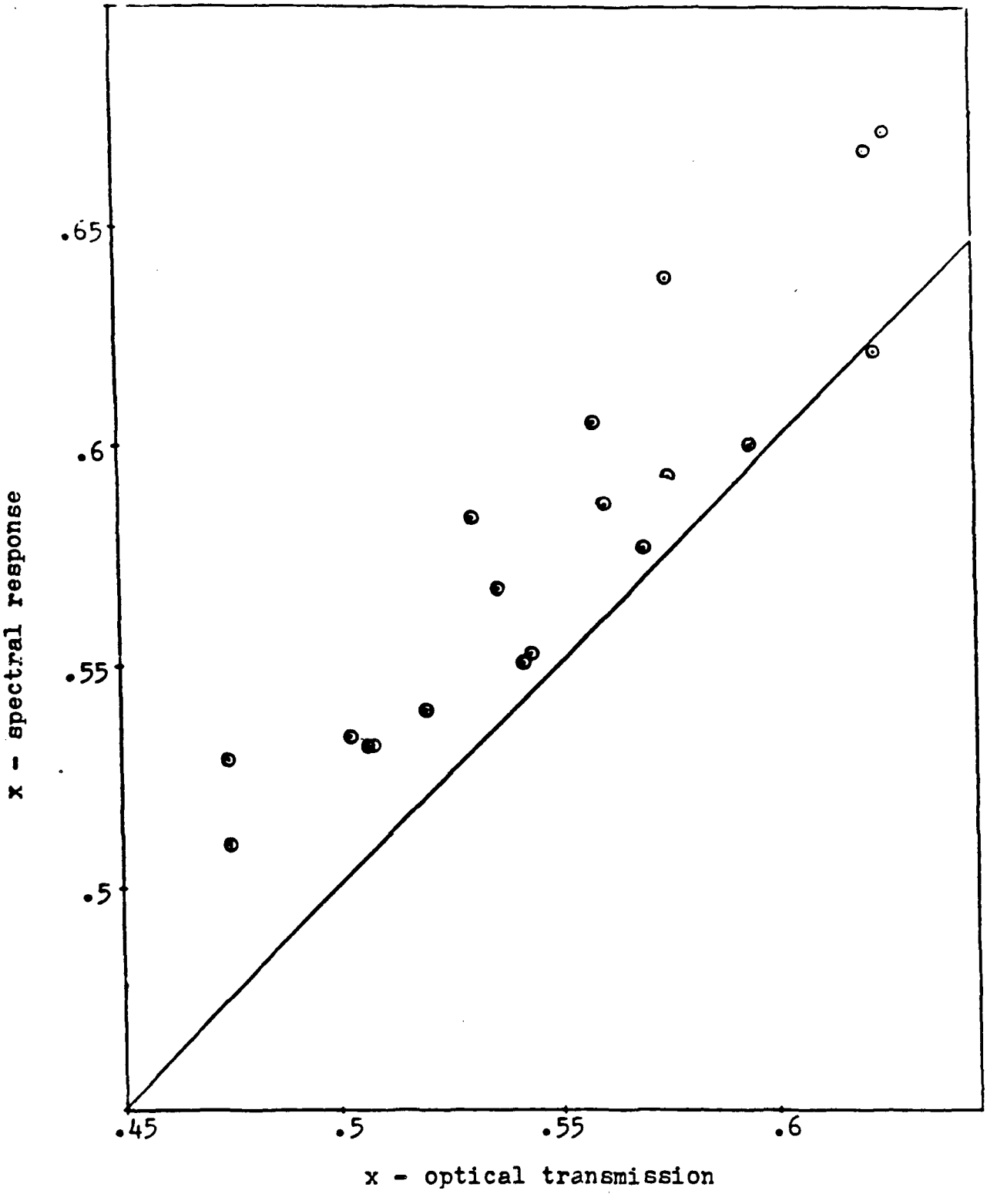

FIGURE 10: Comparison of the absorption and spectral response methods.

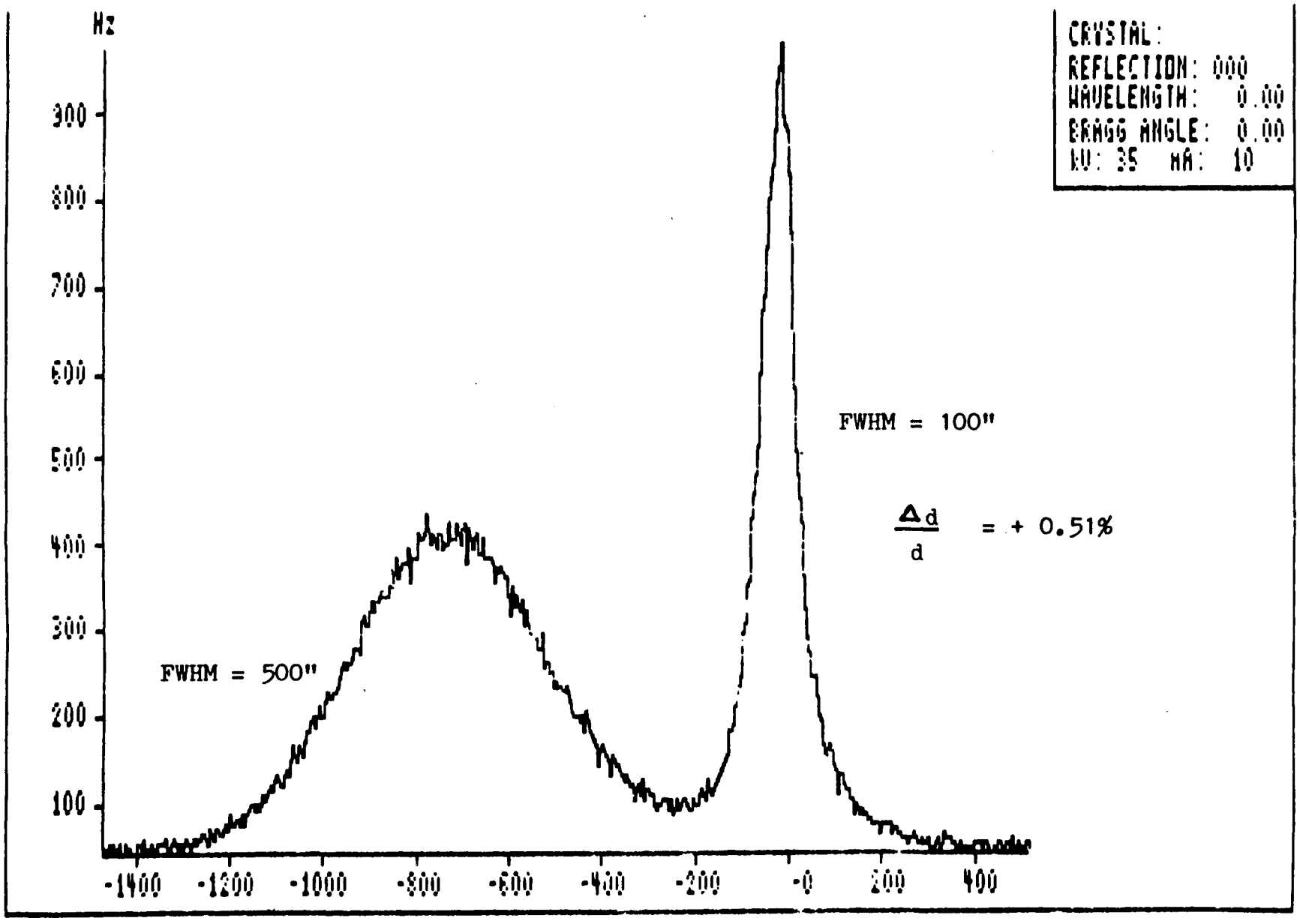
Hz
300
800
700
600
500
400
300
200
100
-1400
-1200
-1000
-800
-600
-400
-200
-0
200
400
CRYSTAL:
REFLECTION: 000
WAVELENGTH: 0.00
BRAGG ANGLE: 0.00
KV: 35 MA: 10
FWHM = 100"
Δd/d = + 0.51%
FWHM = 500"

FIGURE 11

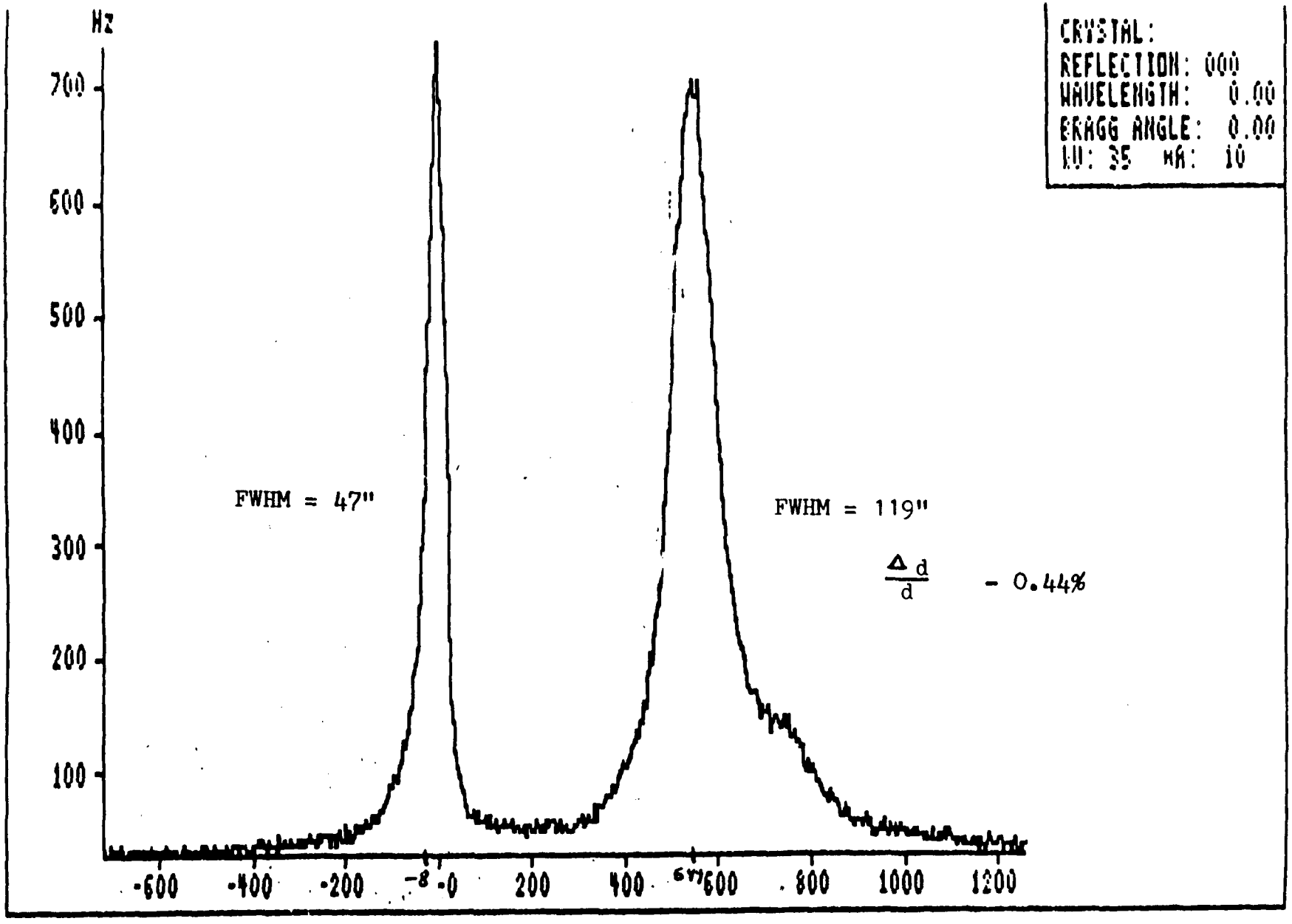
Hz
700
600
500
400
300
200
100
CRYSTAL:
REFLECTION: 000
WAVELENGTH: 0.00
BRAGG ANGLE: 0.00
KV: 35 MA: 10
FWHM = 47"
FWHM = 119"
Δd/d - 0.44%
-600
-400
-200
-8
-0
200
400
600
800
1000
1200

FIGURE 12

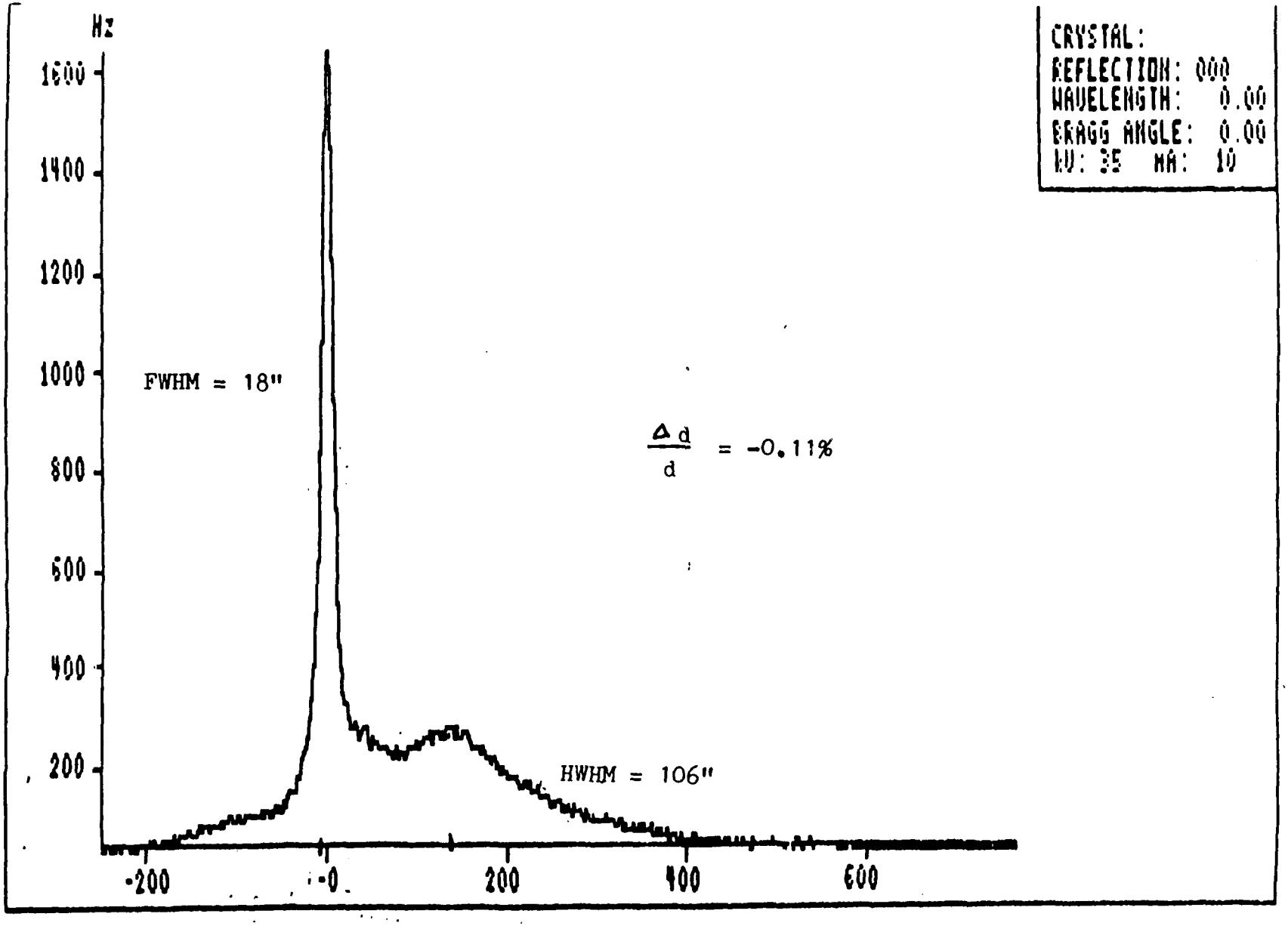

$$\frac{\Delta d}{d} = -0.11\%$$

FIGURE 13

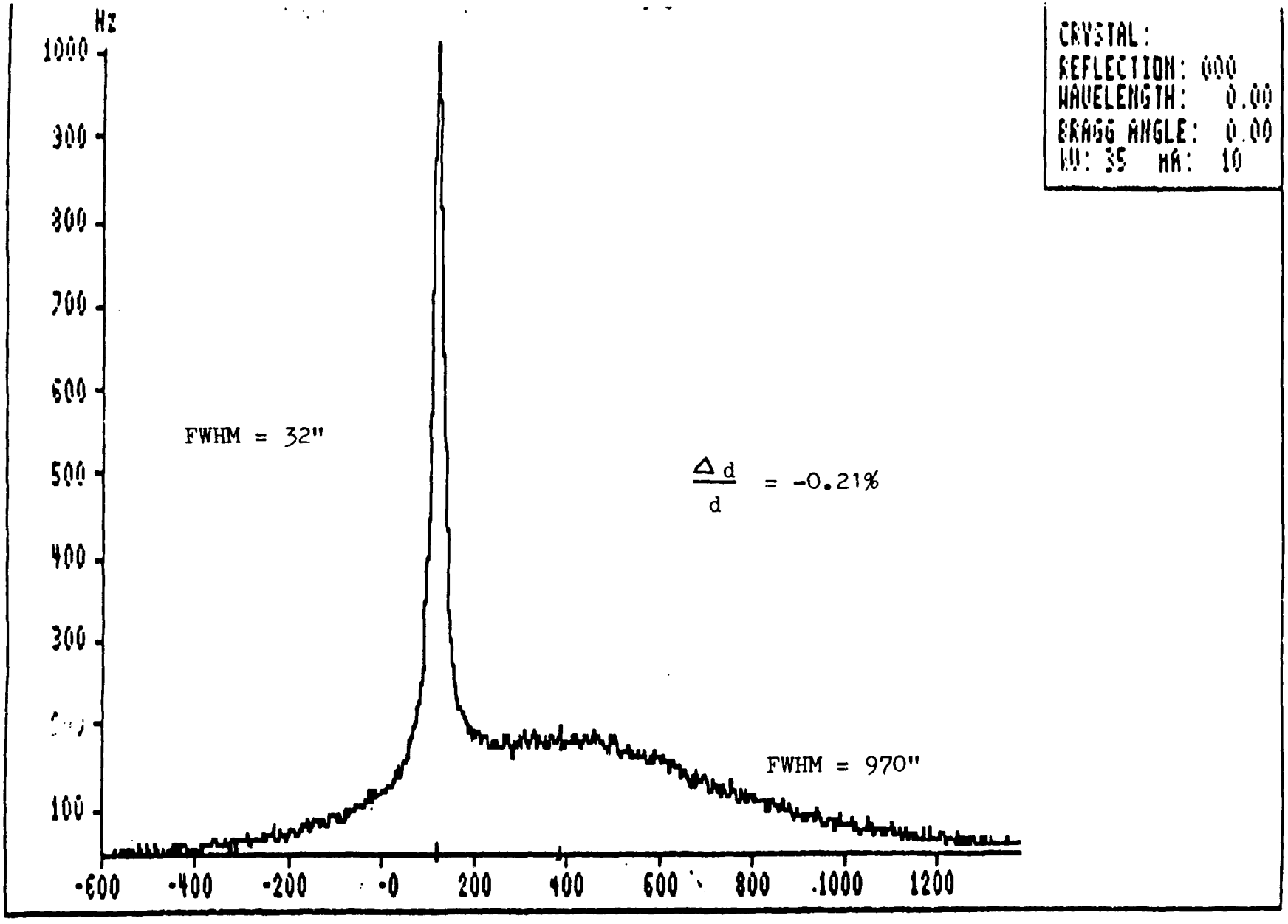
Hz
1000
900
800
700
600
500
400
300
200
100
-600
-400
-200
-0
200
400
600
800
1000
1200
CRYSTAL:
REFLECTION: 000
WAVELENGTH: 0.00
BRAGG ANGLE: 0.00
KV: 35 MA: 10
FWHM = 32"
Δd/d = -0.21%
FWHM = 970"

FIGURE 14

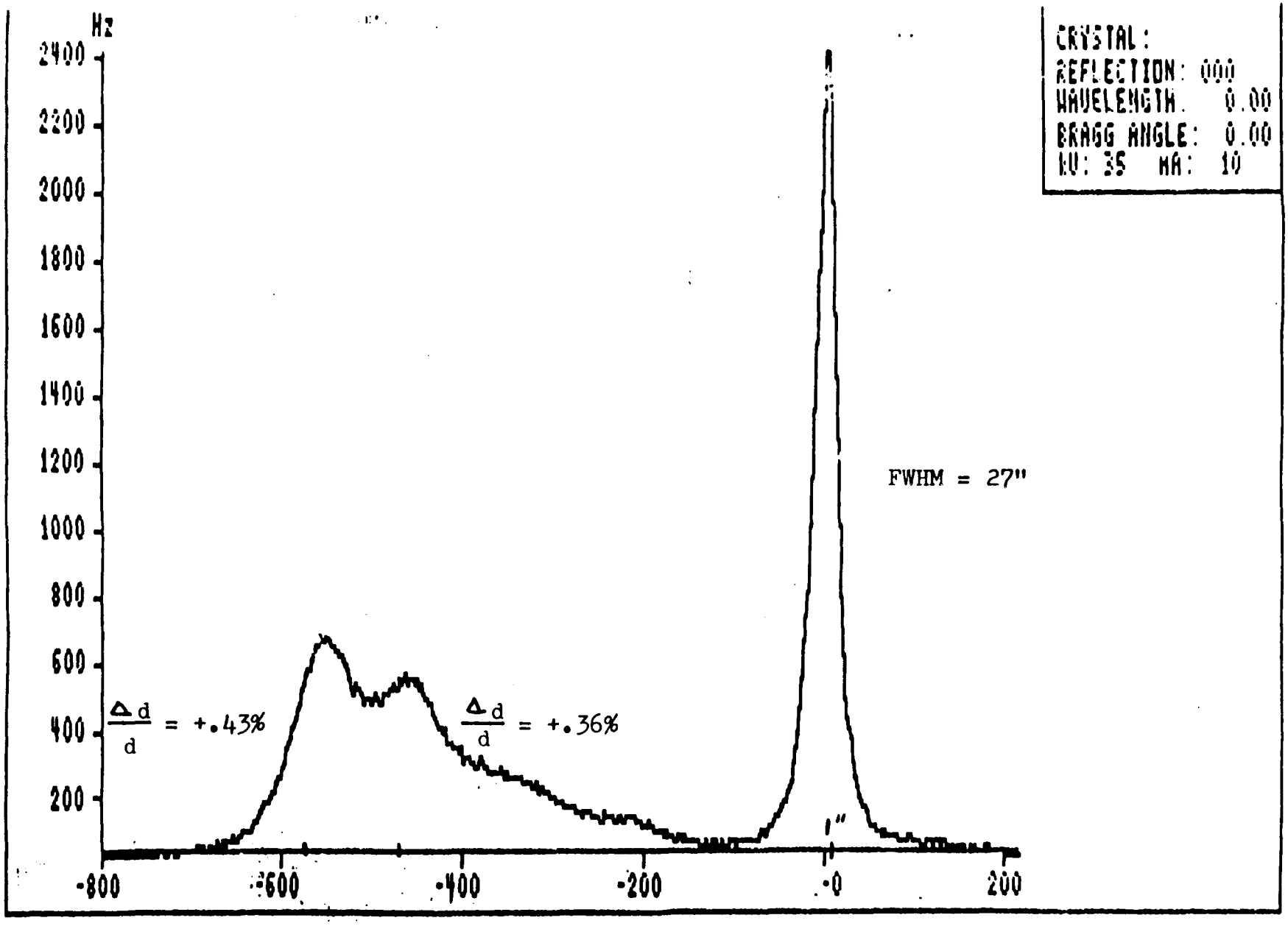
Hz
2400
2200
2000
1800
1600
1400
1200
1000
800
600
400
200
-800
-600
-400
-200
-0
200
CRYSTAL:
REFLECTION: 000
WAVELENGTH. 0.00
BRAGG ANGLE: 0.00
KV: 35 MA: 10
FWHM = 27"
Δd/d = +.43%
Δd/d = +.36%
1"

FIGURE 15

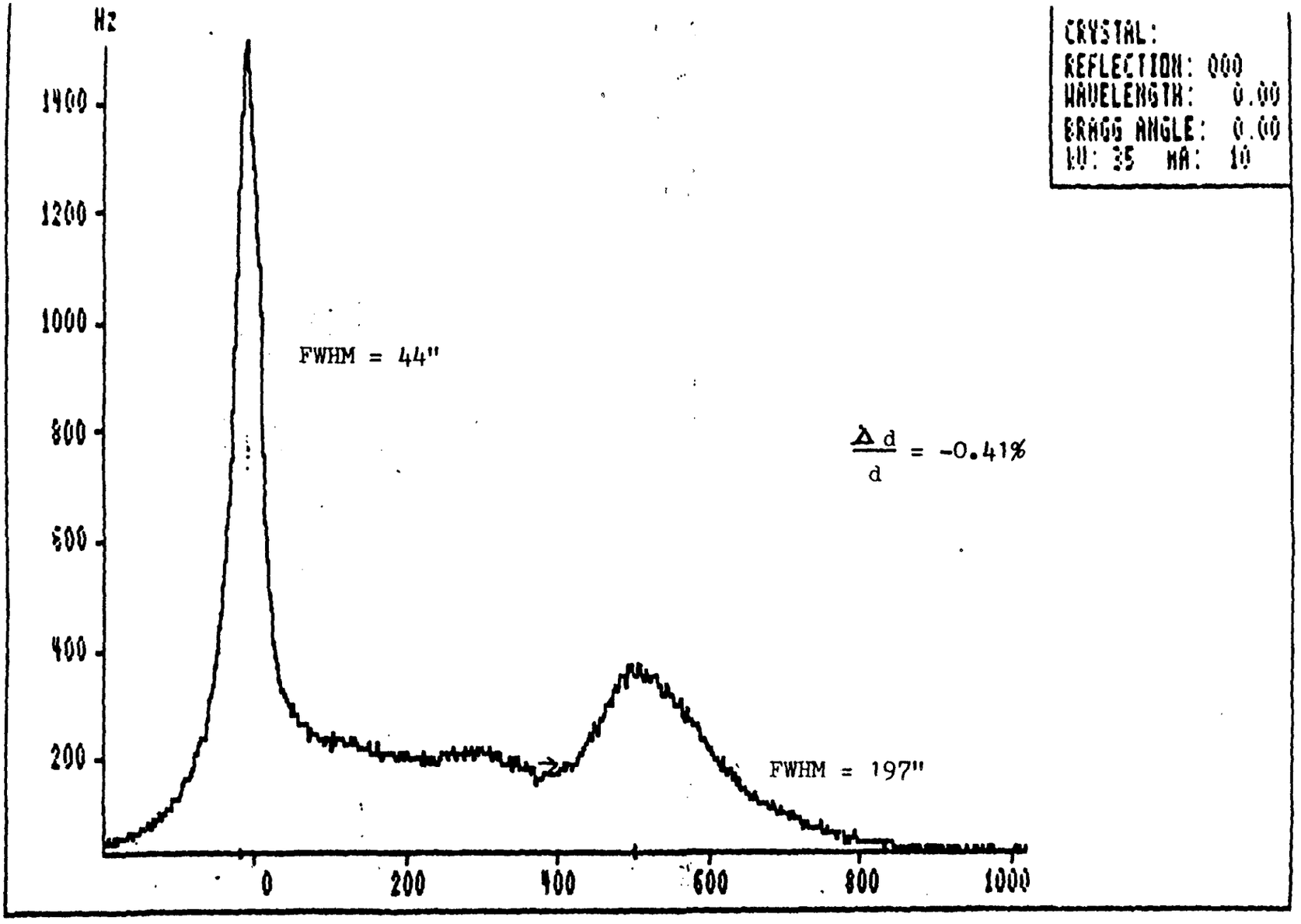
Hz
1400
1200
1000
800
600
400
200
0
200
400
600
800
1000
CRYSTAL:
REFLECTION: 000
WAVELENGTH: 0.00
BRAGG ANGLE: 0.00
KV: 35 MA: 10
FWHM = 44"
FWHM = 197"
Δd/d = -0.41%

FIGURE 16

program written to de-convolute the peaks, to obtain a more accurate value of FWHM when peaks are close. Our analysis of the data indicates that, for the case of layers in which the mismatch is negative [a (GaInAs) < a (InP)], the FWHM of both the peaks falls as the mismatch is lessened. Thus, there is firm evidence of stress in the InP as well as in the GaInAs layer.

Linewidths of the GaInAs layer are seen to increase with mismatch. Moreover, layers with positive mismatch exhibit considerably broder line widths than layers with negative mismatch. The reasons for this are not clear at the present time.

In one case, (Fig. 15) double peaks were observed for the GaInAs layer. We believe that this is due to twinning of the epilayer in the region where the beam is placed. This form of gross defect mey be caused by a large mismatch between the substrate and the GaInAs layer. Finally, one layer (Fig. 17) shows a single peak. Since this layer is definitely GaInAs (as seen by PL), we believe it represents an exact match to the substrate.

c. MOBILITY AND CARRIER CONCENTRATION

The electronic aspect of our layer growth is that the electron concentration of the layer increases as the ratio of the arsine overpressure to the OM overpressure is increased. To a first order, this come about because an increase of arsine overpressure results in an increase in the gallium vacancy concentration and thus in the incorporation of silicon, a common

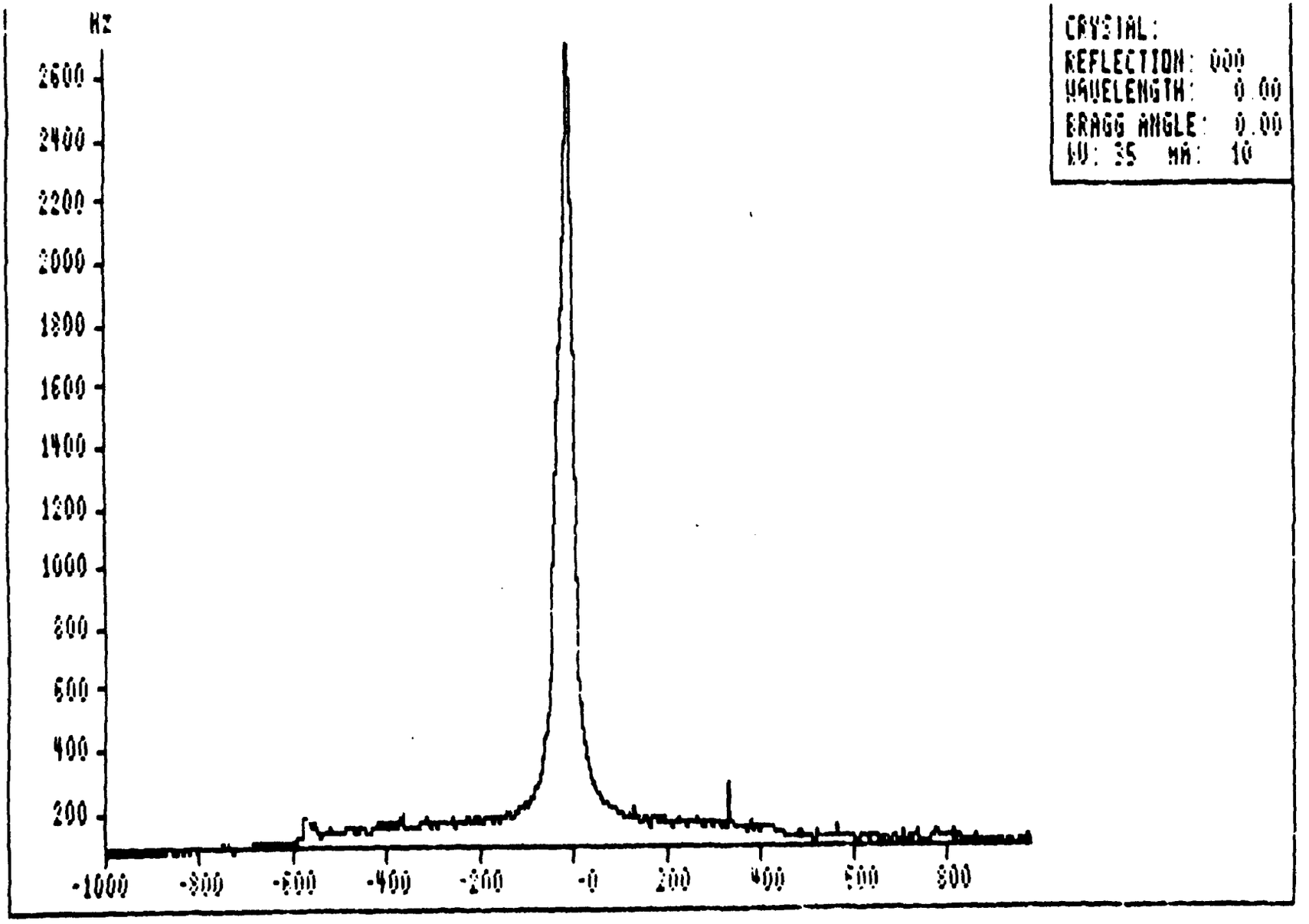
HZ
2600
2400
2200
2000
1800
1600
1400
1200
1000
800
600
400
200
-1000
-800
-600
-400
-200
-0
200
400
600
800
CRYSTAL:
REFLECTION: 000
WAVELENGTH: 0.00
BRAGG ANGLE: 0.00
KV: 35 MA: 10

FIGURE 17

contaminant which is n-type for this site occupancy. This is not the whole picture, however, since increase in the arsenic pressure also results in a slight fall in the composition and thus a change in the electron concentration. As a result, the data of n vs Arsine/TMG+TEI shows considerable scatter, and any interpretations of it must be viewed with caution.

The mobility of the grown layer has, in general, been found to decrease with increasing electron concentration, as seen in Fig.18. This emphasizes the need for careful control of both the composition as well as the doping concentration if high quality layers are to be grown.

VII MASS SPECTROMETER STUDIES OF VAPOR REACTANTS

The mass spectrometer was fully leak checked and put into operation. Upon start-up, the system was pumped down to 5×10^{-7} torr, the primary constituents of the residual gaseous species were H_2, N_2, CO_2, O_2, CH_4, C_2H_6 and Ar in decreasing order of abundance. The nitrogen was not present in a 4:1 ratio with oxygen, but was much more abundant. Thus, it was probably the result of a leak from the nitrogen supply on the system, or caused by adsorption on the walls of the vacuum system. Some pumping oil fractions at higher masses were also observed in very small quantities.

The system was then baked out at about 200 C for six hours, after which the base pressure was less than 1×10^{-8} torr. The reduction was mainly due to a decrease in the water vapor and nitrogen peaks, indicating that the N_2 was probably adsorbed on

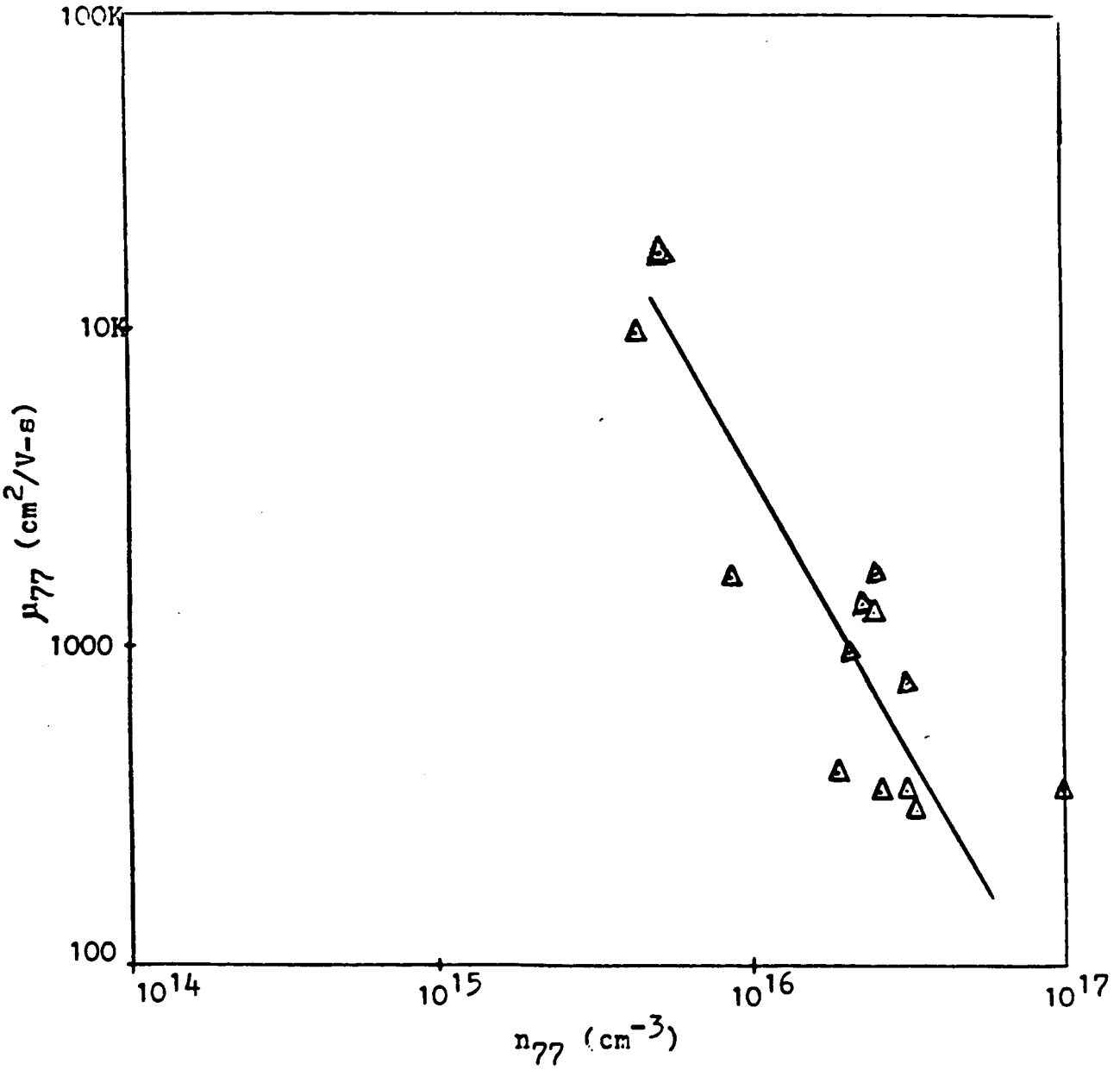

FIGURE 18: Mobility as a function of electron concentration

the walls of the vacuum system and was out-gassing. A reduction in pump oil fractions was also noted.

The probe position with respect to the orifice was then optimized through the use of the adjustment micrometers. The N_2 peak was increased by a factor of 20 (with 152 torr of N_2 in the reactor) while the H_2O peak remained constant. This indicates that the H_2O was in the mass spectrometer and not in the reactor.

Measurements were then made with four different partial pressures of AsH_3 in the reactor (with the susceptor cold). Four arsine fraction peaks were observed at 78, 77, 76 and 75 AMU corresponding to AsH_3, AsH_2, AsH and As respectively. The relative abundance of the species was about 12 : 4 : 17 : 7. No peaks were observed for As_2 or As_4. Intuitively, it is reasonable that AsH should be the most abundant species because the last As-H bond is the strongest.

Figure 19 shows the ion current versus inlet partial pressure for AsH_3 and its fractions. The curves do not pass through the origin because of a small amount of residual hydrocarbons at those mass numbers and/or AsH_3 absorbed on the mass spectrometer walls. No change in any of the background peaks from 0 to 300 AMU was observed with the addition of the AsH_3. The curves show very little deviation from linearity. Even more accurcy could be achieved if fewer mass units were scanned if we hold the scan on one particular peak. Using this data, and knowledge of the ionization efficiency for the various species (and the electron multiplier gain), the partial pressures

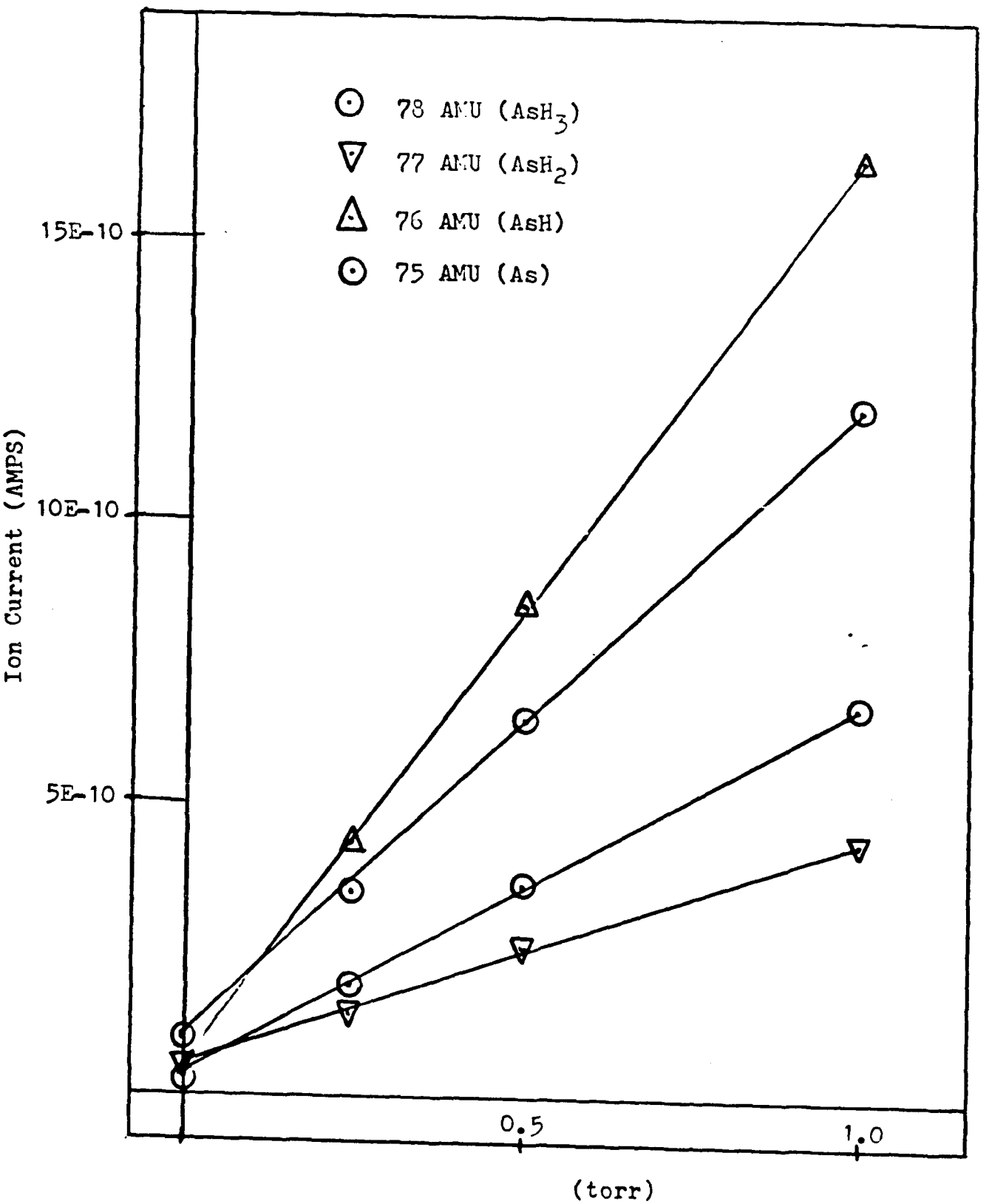

FIGURE 19: Ion Current vs Arsine Pressure

of the individual species can be determined.

The response speed of the sampling system was also observed in a qualitative manner during the investigation of the arsine peaks. The response was found to be so fast that the response of the mass flow controller could be observed; unfortunately this proved to be quite poor. Figures 20 and 21 show roughly the response of the mass flow controller (MFC) to a step change in the set point. The curves show that not only is the MFC flow reading heavily filtered, but that its controlling action closely resembles a hi/lo controller. Also note that, when going from 100% to 50% flow, the reactor is without arsine for several seconds.

At this point the mass spectrometer was used to observe TEI in the reactor. Fig. 22 shows the signature of the TEI signal, which is not available in the literature. Next, a detailed study was made of the reactions of TEI, TMG and AsH3.

Experiments were carried out in a system with digitally controlled flow meters, to obtain as high an accuracy ($\pm$ 2%) as possible. As far as it was possible, the actual flows used were close to those encountered under practical operating conditions. The sampling system was completely bakeable, and was designed with double pumping to obtain as short a transit time as possible (0.2 secs).

The sampling speed achieved here was quite satisfactory for a study of the TEI-AsH3 reaction, which was the main problem area to be investigated. Here, it was first determined that the $EtIn^+$

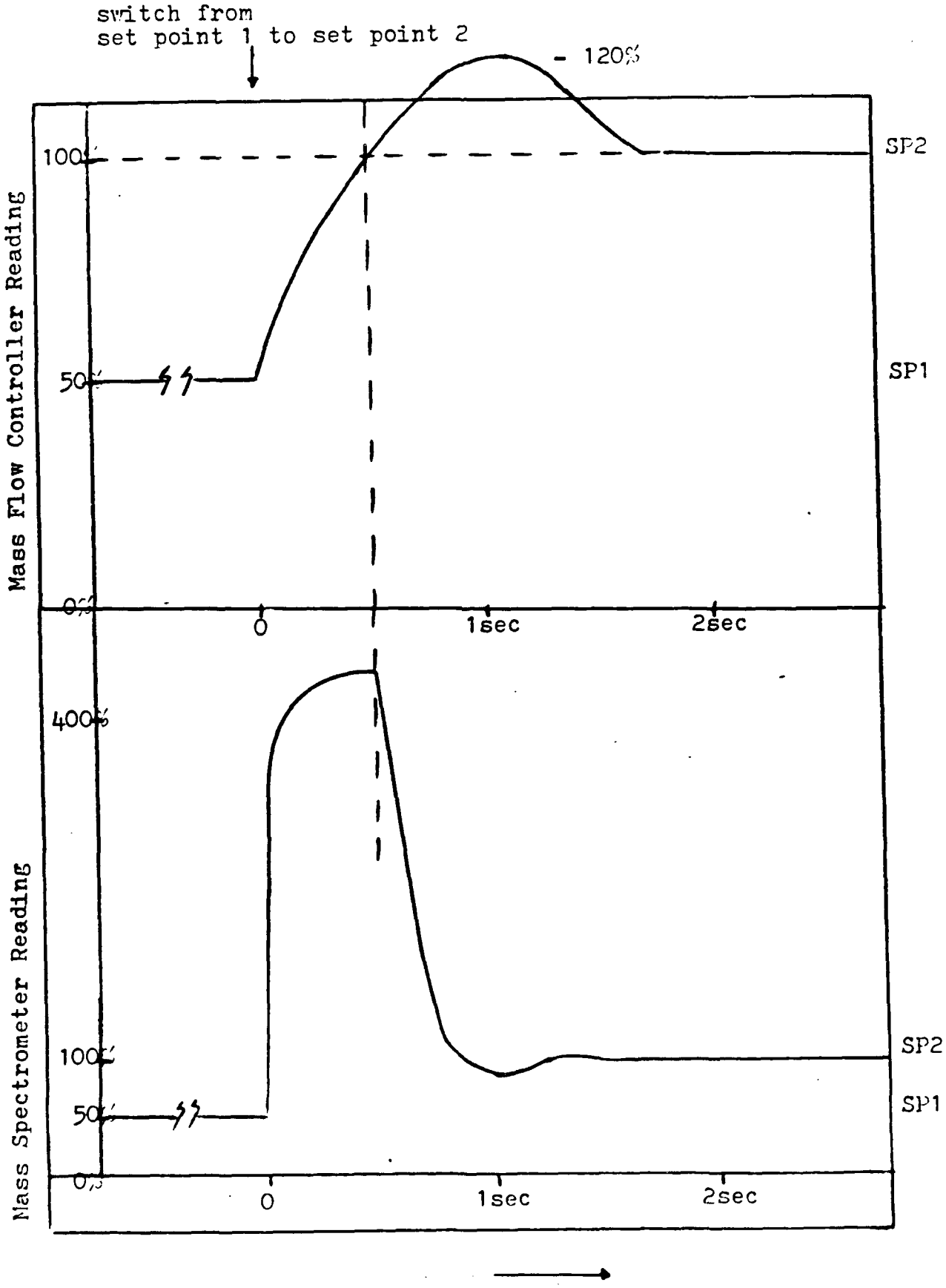

FIGURE 20: Response time of a MFC

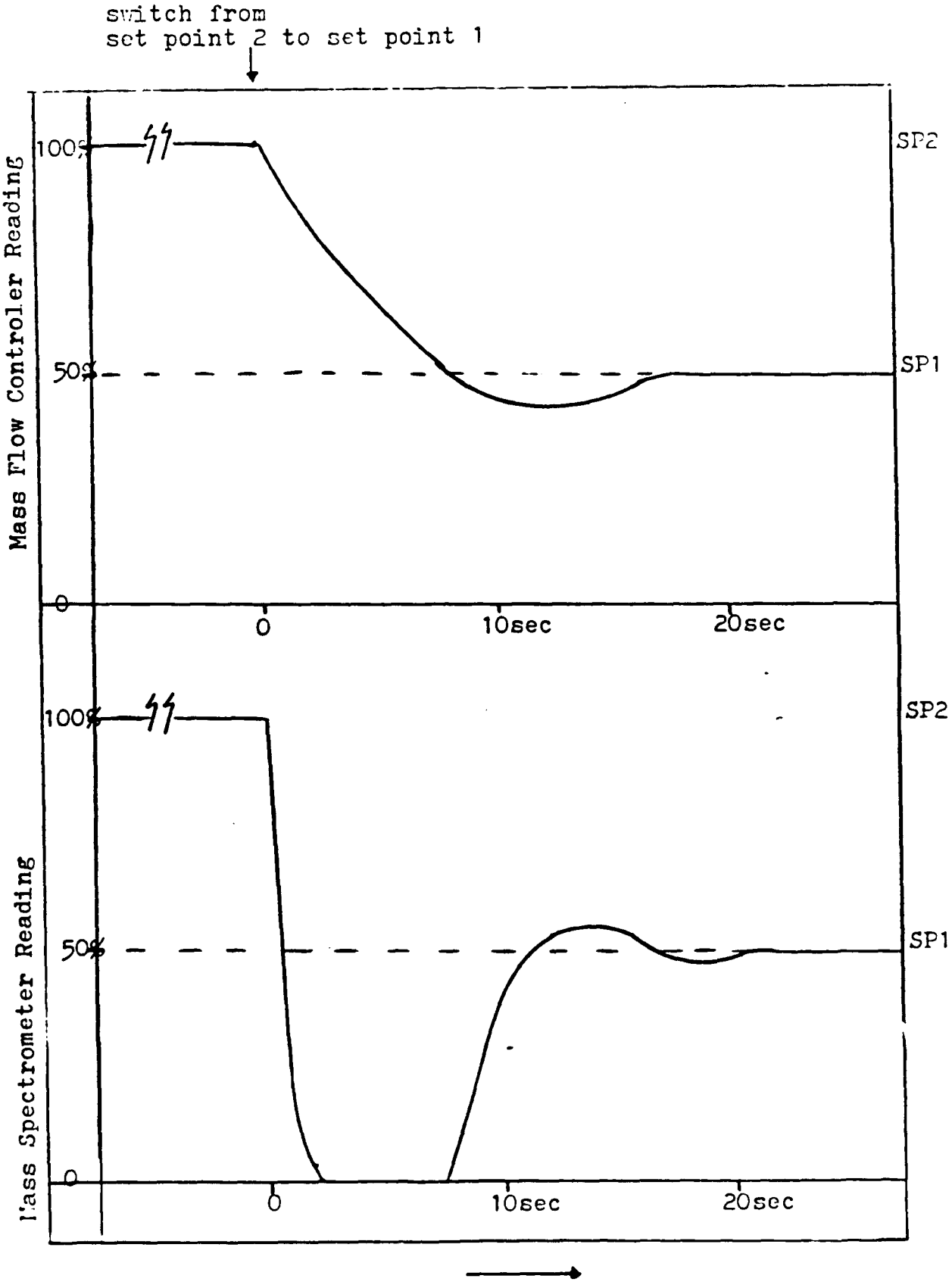

FIGURE 21: Response time of a MFC

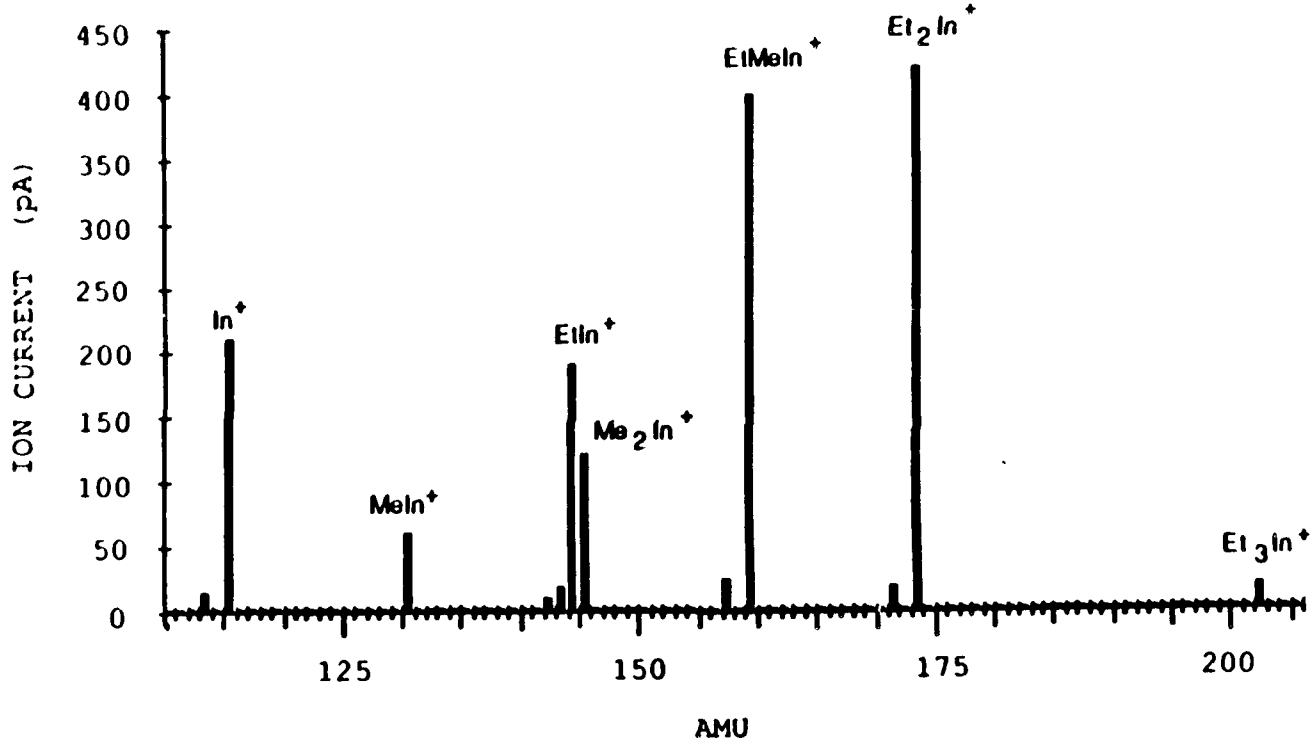

FIGURE 22: Signature of Triethylindium

fragment was truly the representative of the Et_3In remaining in the reactor at any point in time. This parameter was plotted as a function of AsH_3 overpressure, and also as a function of probe distance. An analysis of the results gave the equilibrium constant, as well as the rates of forward and back reaction (Appendix A).

An important consequence of these measurements is the ability to predict what will occur in any reactor, i.e., the results are not machine-specific. Simulations at atmospheric and reduced pressure showed that adduct formation is complete in either case, before the reactants arrive at the susceptor. Thus, the rate of formation of the adduct is not the rate limiter in the growth mechanism within our process.

Results for the TMG-AsH_3 reaction have not been as complete as those outlined above. This is because of a basic limitation to the interpretation of mass spectrometric data in this case. Specifically, analysis requires monitoring an individual daughter fragment which is produced in the reactor, but not in the ionizer as well. This can be ensured if a set of conditions can be arranged for which the signal can be made to drop completely to zero. This occurs in the case of the TEI-AsH_3 reaction, where $EnIn^+$ drops to zero under conditions of excess AsH_3 pressure, and long transit time. With the TMG-AsH_3 reaction, however, this does not occur and the Me_3Ga^+ (or any other fragment) signal never drops completely to zero. Consequently, data resulting from this set of experiments can, at best, be used to set an

upper bound to the Me_2Ga^+ fragment. This, in turn only allows lower bounds to be determined for the equilibrium constant and for the rate of forward reaction (APPENDIX B).

Even so, the results were useful in providing insights to the growth of GaAs by the reaction of TMG and AsH3. For example, it is generally assumed that the growth of GaAs from the reaction of TMG and AsH3 presents no problem because there is no pre-reaction. Our work has shown that there is considerable pre-reaction. However, the reaction product has a high vapor pressure, under normal operating conditions, and does not eliminate methyl groups to eventually form polymers, so that it is easily transported to the susceptor and participates in the growth process. Finally, the bond energy for the adduct formation reaction between TMG and AsH3 is probably very small (about 6 kcals/mole), since it breaks down completely in the vicinity of the growing surface.

We have also noted significant interchange effects when mixtures of the alkyls have been used with AsH3. This problem has been studied during the course of our work, using the mass spectrometer system.

One set of experiments were based on a study of the TEG-TEI alkyl mixture. Here, we have monitored the fragments due to 0.02 torr of TEI,TEG and the mixture of these organometallic compounds, in the absence of Arsine. Figure 23(a-d) shows the ion current signals for these species over the AMU ranges of interest. Figure 23(a) shows the mass spectrum for TEG alone

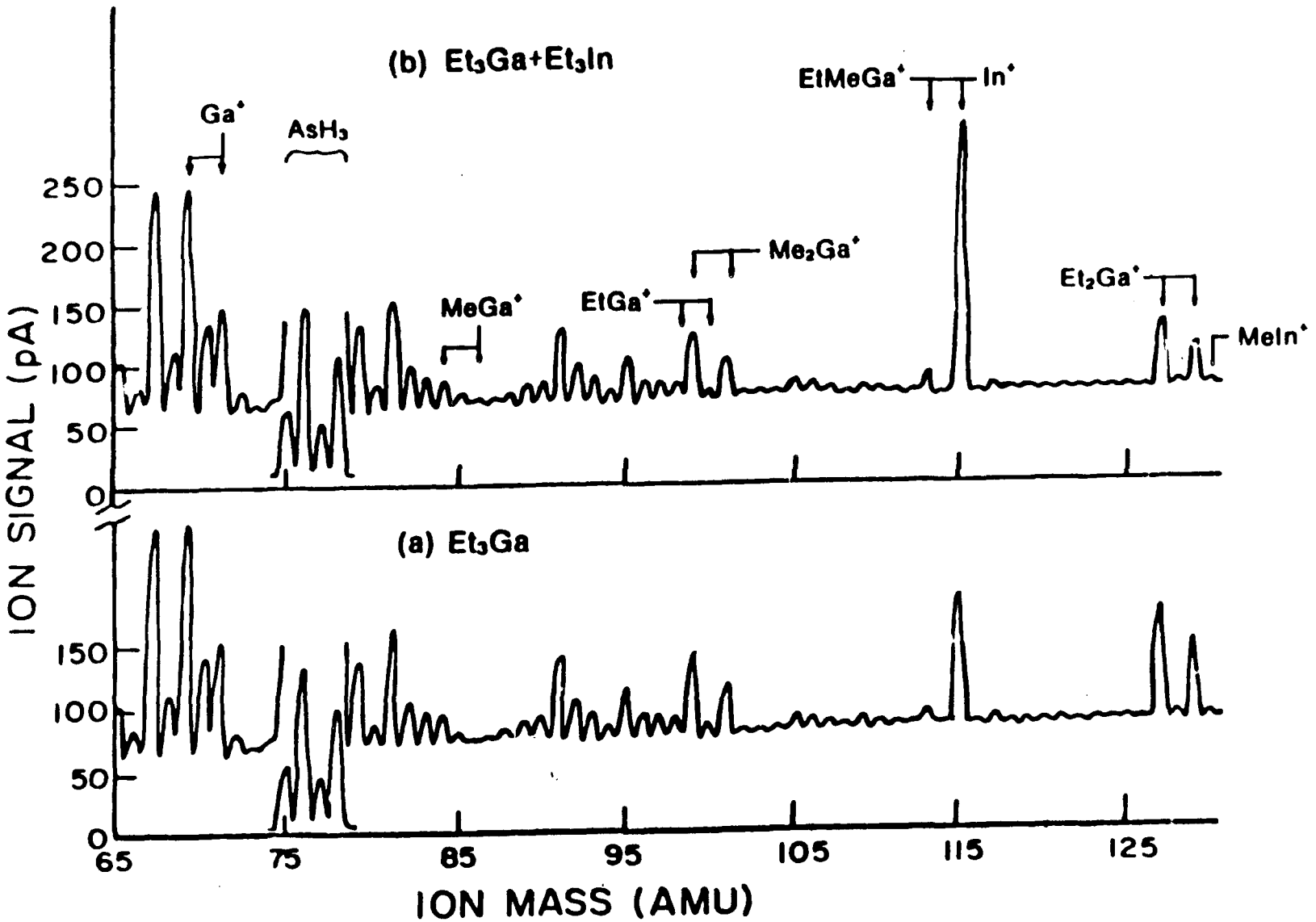

FIGURE 23: Mass spectra: a) 0.02 torr Triethylgallium
b) 0.02 torr Triethylgallium plus .02 torr TriethylIndium

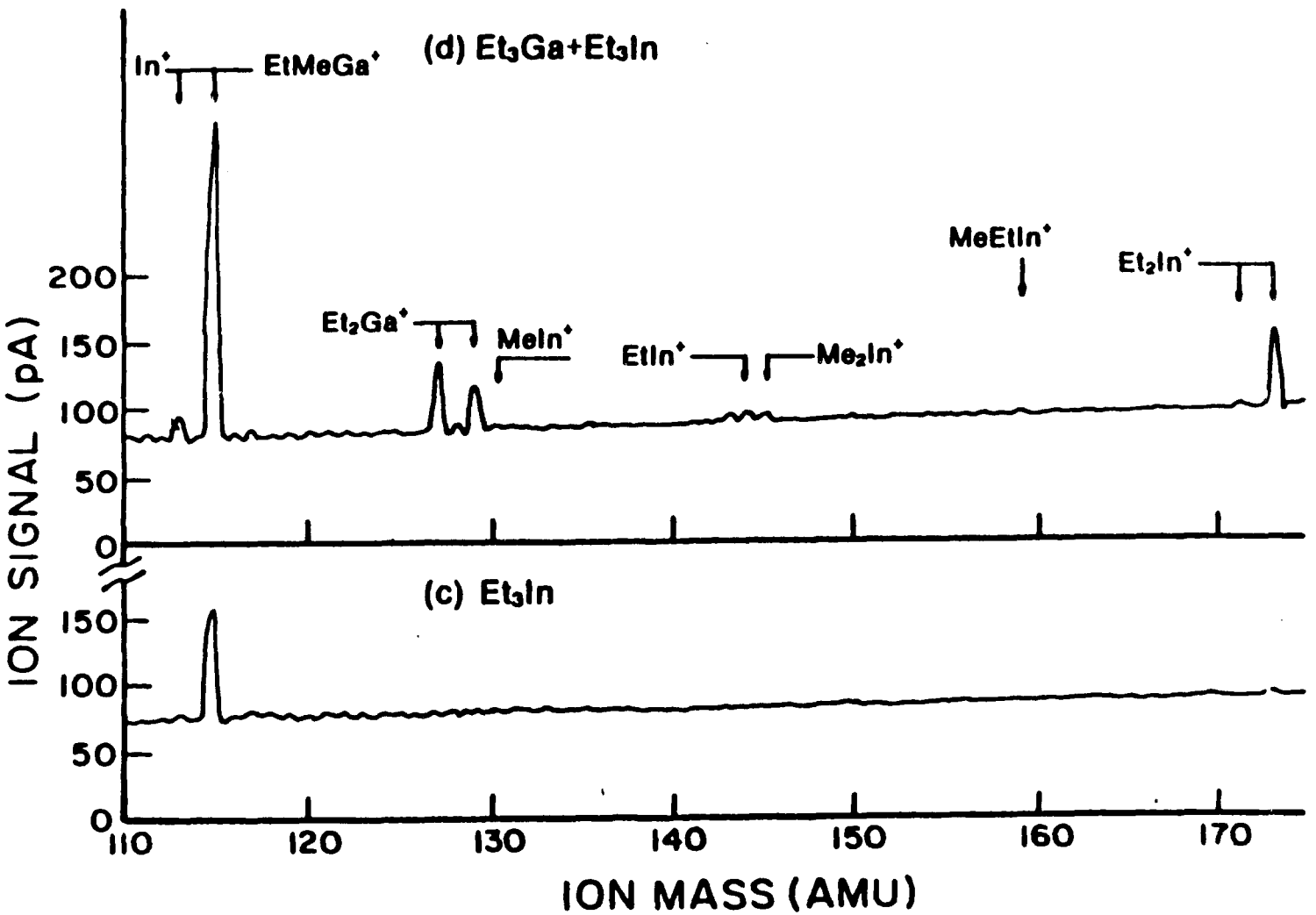

FIGURE 23: Mass spectra: c) 0.002 torr TriethylIndium
d) 0.02 torr TriethylIndium and 0.02 torr Triethylgallium

over the range from 65 to 130 AMU, where the fragments ranging from Ga^+ to Et_2Ga^+ are located. Likewise, Fig. 23(c) shows the mass spectrum for TEI alone over the range from 110 to 175 AMU, where the fragments ranging from In+ to $EtIn^+$ are located. The spectrum for the mixture is shown in Figs. 23(b) and (d) over the entire 65-175 AMU range. This data is also listed in Table 5, corrected for multiplier gain and quadrupole transmission, where it is seen that the dialkyl metal fragments (Et_2In^+ and Et_2Ga^+) provide the largest signals.

When TEG was added to the TEI the Et_2In^+ signal doubled. In addition, the Et_2Ga^+ signal from the mixture was about a factor of two lower when compared to an equivalent amount of TEG alone. We have studied the possibility that these changes may be caused by a process where TEG can displace the TEI, which may be adsorbed on the walls of the reactor and the sampling probe. (This displacive adsorption process can be expected, since TEG is more acidic than TEI) This process can be discounted since it would result in a change in all the gallium and indium alkyl fragments by an equal amount, which is not the case for our data.

The mass spectra for the mixture of TEI and TEG contains no peaks which are not also observed in the spectra of the individual organometallics. (In the spectrum for TEI alone, Fig. 23 (c), it is difficult to see the EtMeIn+, EtIn+ and Me_2In^+ peaks at the low TEI partial pressure (0.02 torr) used in this experiment. At higher partial pressures (0.13 torr), however, these signals are easily resolved as seen in Fig. 24 (c). Moreover, because the spectrum for the mixture is not a

FRAGMENT	MASS AMU	Et_3Ga	Et_3In	Et_3Ga-Et_3In
		Ion Signal ($\times 10^{-10}$ A)	Ion Signal ($\times 10^{-10}$ A)	Ion Signal ($\times 10^{-10}$ A)
Ga^+	69	6.03	0	6.27
	71	3.10	0	3.10
$MeGa^+$	84	0.91	0	0.95
	86	0.24	0	0.24
$EtGa^+$	98	0.88	0	0.69
	100	0.53	0	0.53
Me_2Ga^+	99	3.94	0	3.44
	101	2.87	0	2.33
In^+	113	0	0.39	0.60
or	115	0	7.73	12.00
$EtMeGa^+$	113	1.08	0	1.09
	115	0.72	0	0.73
Et_2Ga^+	127	10.00	0	6.44
	129	7.00	0	3.89
$MeIn^+$	130	0	0.89	0.56
$EtIn^+$	144	0	0	1.43
Me_2In^+	145	0	0	1.43
$MeEtIn^+$	159	0	0	1.00
Et_2In^+	171	0	0.44	1.25
	173	0	8.75	16.25

TABLE 5: Ion current signals for .02 torr each of Et_3Ga, Et_3In and their mixture.

superposition of the individual spectra (i.e., the peak ratios have changed) we conclude that weak bonding or interaction has occurred between the organometallic species. Note however , that the parent ion peak of the adduct is not observable because it would occur at 316 and 318 AMU, which is beyond the range of the mass spectrometer (300 AMU).

A detailed examination of the spectra, before and after mixing, has been made on a fragment by fragment basis. By subtracting the spectra of the individual species from the spectrum of the mixture, we calculate that a maximum of 65% of the initial reactants remain in the mixture. Thus, at least 35% of the end products are in the form of addition compounds.

Next, we considered the TMG-TEI mixture. When TMG and TEI are mixed together prior to their introduction into the reactor, they not only form an addition compound, but some alkyl exchange occurs. Figures 24(a-d) show scans over a wide range of masses for 0.13 torr of each of the individual reactants TMG and TEI and for the mixture of the two, in the absence of arsine gas. Again, we note that the ion pattern of the mixture is not a superposition of the individual ion peaks. The parent ion peaks of the individual organometallic compounds are not shown because they are small. but they can be detected. As before, the parent ion peak of the adduct is not observable because it would occur beyond the upper range of our mass spectrometer (300 AMU).

Table 6 lists mass spectrometric data for TMG,TEI and for the mixture, corrected for the effect of the electron

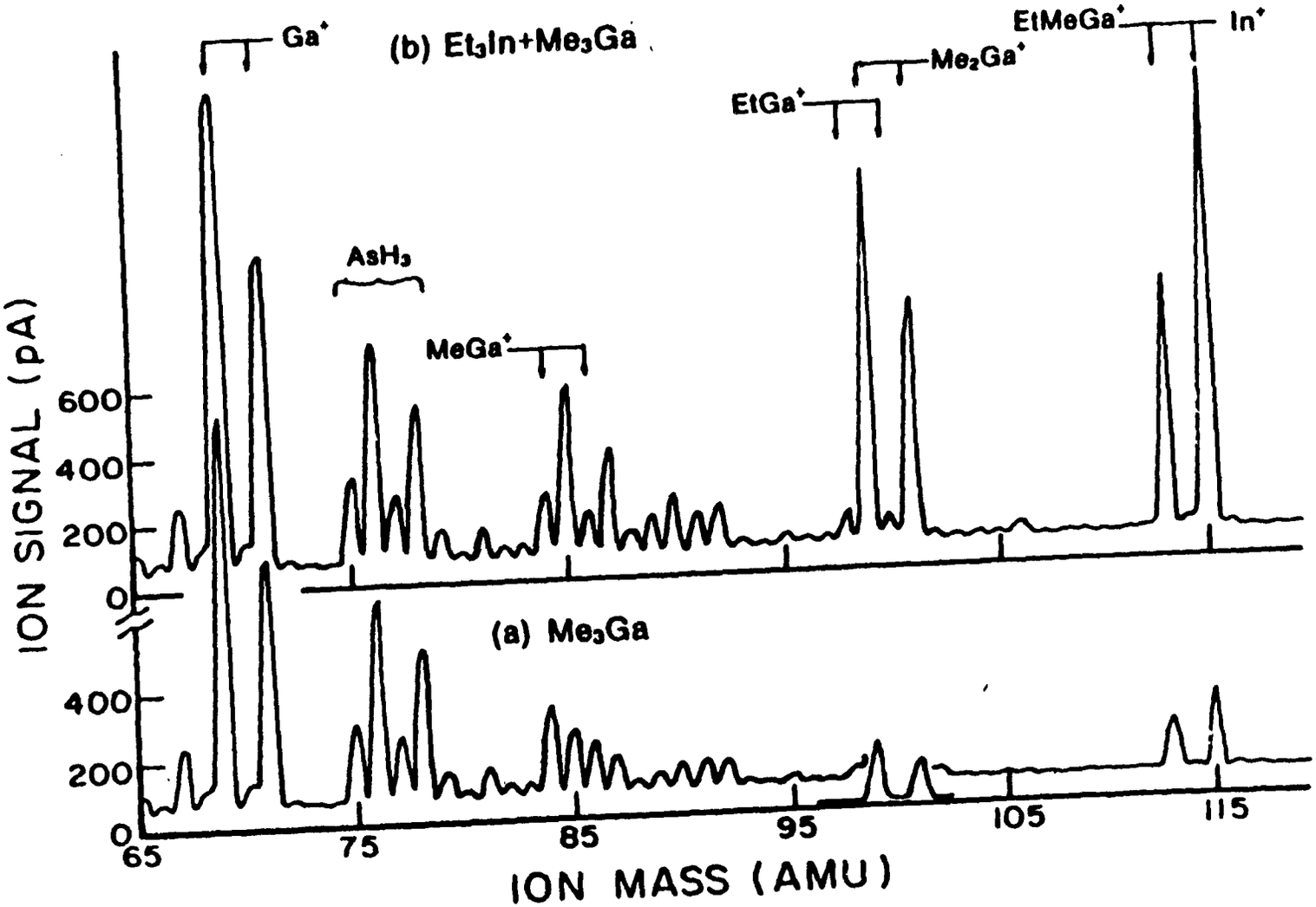

FIGURE 24: Mass spectra a) 0.13 torr Trimethylgallium
b) 0.13 torr Trimethylgallium and 0.13 torr TriethylIndium

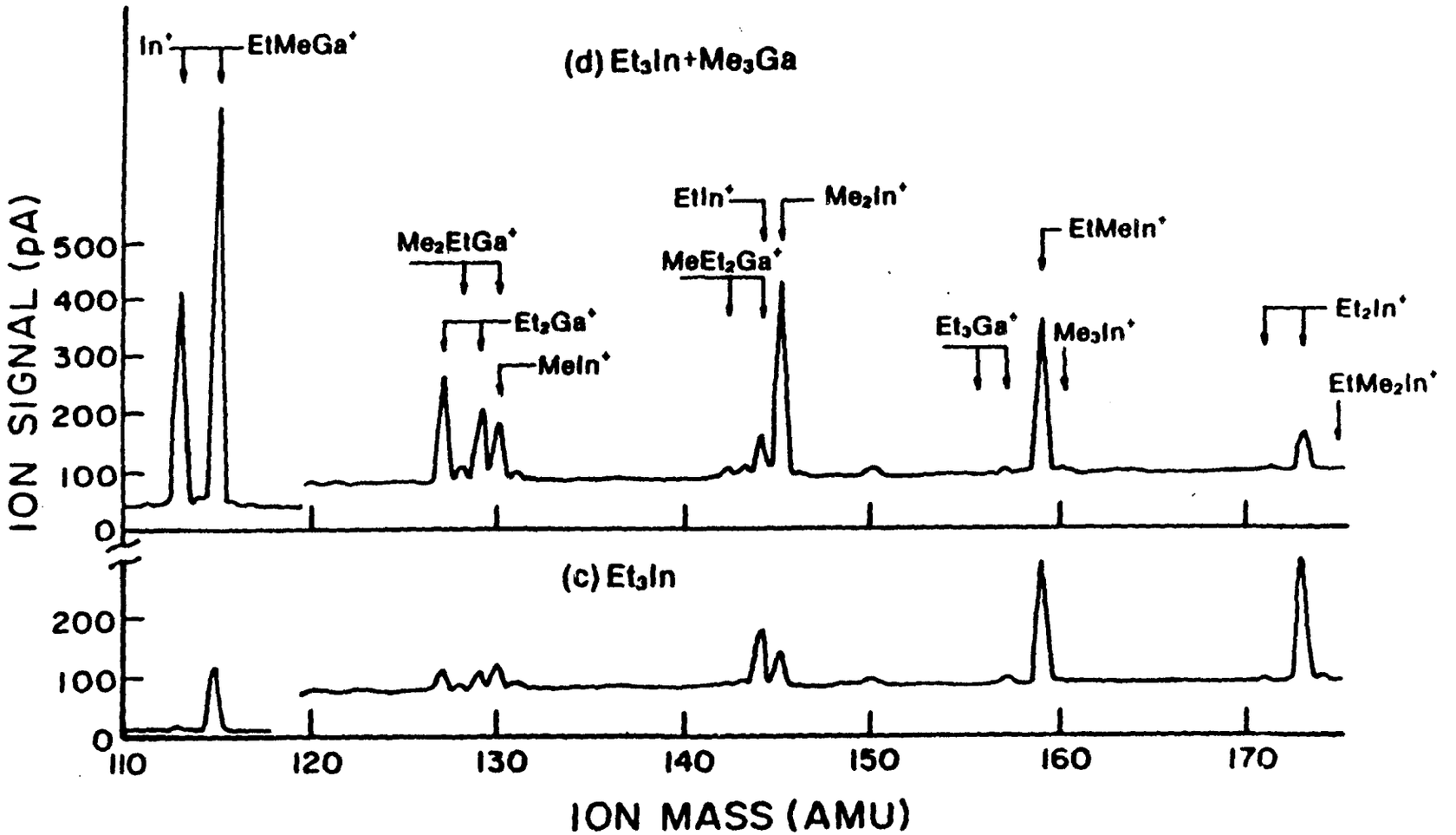

FIGURE 24: Mass spectra: c) 0.13 torr TriethylIndium
d) 0.13 torr TriethylIndium and 0.13 torr Trimethylgallium

FRAGMENT	MASS AMU	Me_3Ga	Et_3In	Me_3Ga-Et_3In
		Ion Signal ($\times 10^{-10}$ A)	Ion Signal ($\times 10^{-10}$ A)	Ion Signal ($\times 10^{-10}$ A)
Ga^+	69	36.5	0	44.8
	71	24.5	0	31.7
$MeGa^+$	84	11.1	0	8.4
	86	7.6	0	5.7
$EtGa^+$	98	2.5	0	6.3
	100	1.3	0	4.7
Me_2Ga^+	99	112.5	0	70.6
	101	76.0	0	54.7
In^+ or $EtMeGa^+$	113	0	4.2	3.4
	115	0	83.6	68.2
	113	11.7	0	63.3
	115	9.1	0	45.5
Et_2Ga^+	127	0	0	16.7
	129	0	0	11.7
$MeIn^+$	130	0	3.9	20.6
$EtIn^+$	144	0	13.6	11.4
Me_2In^+	145	0	8.6	48.6
$MeEtIn^+$	159	0	38.0	54.0
Et_2In^+	171	0	2.5	1.3
	173	0	52.5	16.3

TABLE 6: Ion current signals for 0.13 torr each of Me_3Ga, Et_3In and their mixture.

multiplier gain and quadrupole transmission. Here, the first notable observation is the appearance of a series of Me-In and Et-Ga peaks, accompanied by a reduction in the Me-Ga and Et-In peaks. As expected, the spectrum of pure TEI contains some methyl fragments due to ionization. However the spectrum of pure TMG does not contain ethyl fragments as their creation during the ionization process would be highly improbable.

The signals at 113 and 115 AMU could result from both indium and gallium fragments. However, the separate contributions can be evaluated by taking into account the natural isotropic proportions of Ga^{69} to Ga^{71}, which is 3:2, and those of In^{113} to In^{115} (4 : 96).

The spectrometer data of Table 6 shows that, upon mixing TEI and TMG there is an increase in the Me_2In^+ signal with a concurrent decrease in the Et_2In^+ peak. The behavior of the gallium signals shows an opposite trend, i.e., a decrease in the Me_2Ga^+ signal and a concurrent increas in the Et_2Ga^+ signal.

The parent ion signal of the exchange product Et_3Ga^+ falls at masses 156/158. Although weak, this signal is clearly observed, since it is not obstructed by other signals. Parent ion signals of the exchange products $EtMe_2Ga^+$ and $MeEt_2Ga^+$ fall at 128/130 and 142/144 AMU respectively, which are close to (or coincide with) other strong fragment signals. Again, some of these exchange products can be identified if we take into account the isotropic proportions of Ga^{69} to Ga^{71}, and of In^{113} to In^{115}. Thus, we can show that the signal at 138 AMU is due to

$EtMe_2Ga^+$ alone. The signal at 130 AMU is due to a combination of $EtMe_2Ga^+$ and $MeIn^+$, and the relative magnitudes of these fragments can also be established by the same method.

The $MeEt_2Ga^+$ fragment is also clearly identifiable by using these arguments. Small peaks were also observed at 160 and 174 AMU and may be due to TMI and $EtMe_2In$. No attempt was made to observe $MeEt_2In^+$ at 188 AMU.

Based on the above experiments, we conclude that there is a significant amount of alkyl interchange when TMG and TEI are mixed, prior to entering the reactor. Moreover, a detailed calculation of the spectra of Table 6 , on a fragment by fragment basis, shows that at least 69% of the end products are in the form of addition compounds.

Reactions with arsine and the alkyl mixtures were also considered. As before, the Et_2In^+ fragment was used to monitor the TEI remaining in the reactor.

Figure 25 shows the ratio of the Et_2In^+ fragment, before and after the addition of Arsine to TEI as a function of the arsine overpressure. These measurements were made with the sampling capillary placed at a distance of 9.0 cm beyond the reactor inlet. We believe that this represents the equilibrium state, since the same curves were obtained with the capillary positioned at 6.5 cm from the inlet.

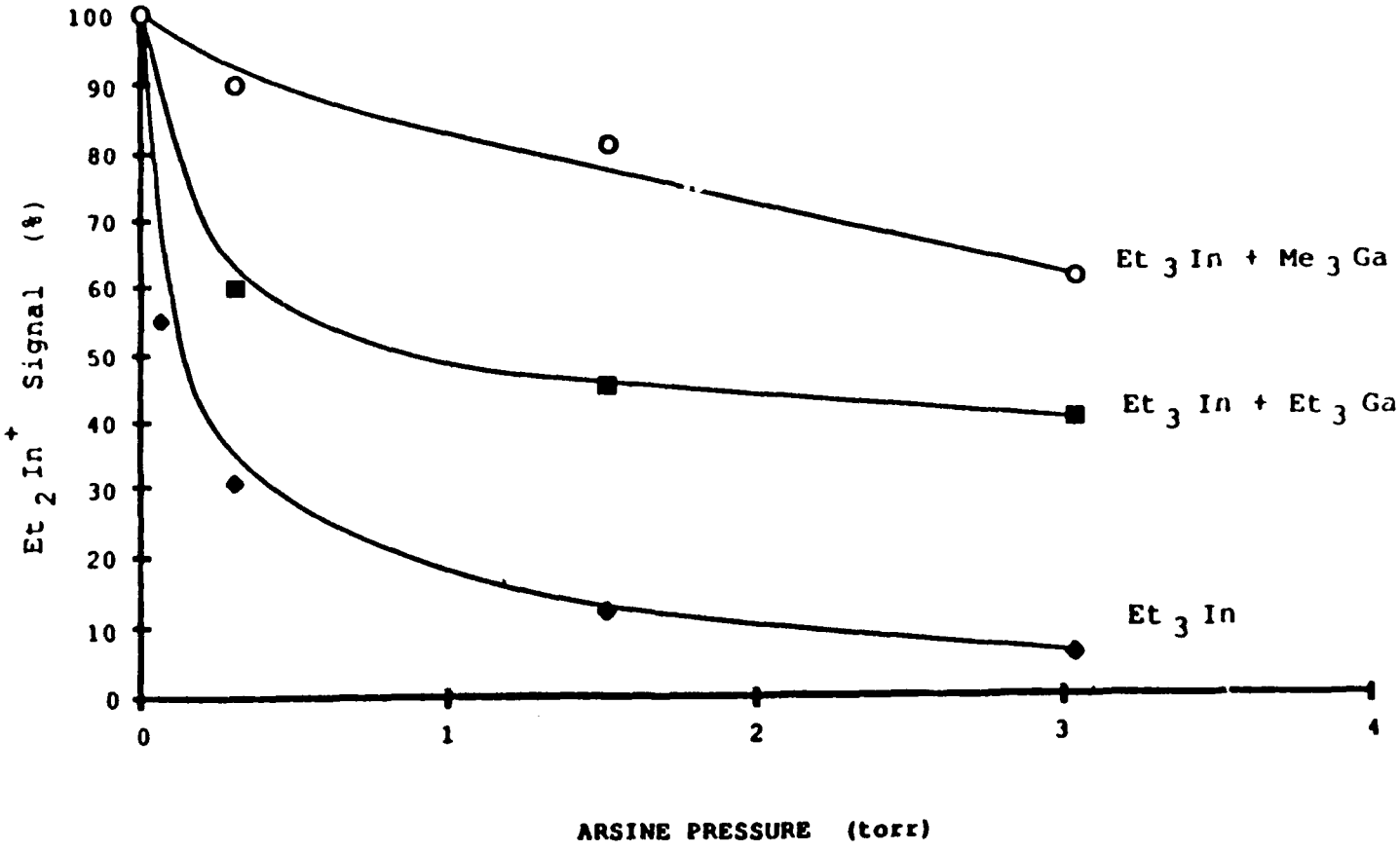

FIGURE 25: Percentage of Et_2In+ fragment remaining in steady state as a function of arsine pressure for Triethylindium alone and its mixture with Triethylgallium or Trimethylgallium.

Similar sets of data are shown for the Et_2In^+ fragment when equal amounts of TMG or TEI are added prior to combining with arsine. All of these experiments were performed at a system pressure of 152 torr, and 3 slm hydrogen.

In the last two instances, it is possible that the Et_2In^+ ion may be a fragment of the indium-gallium addition compound as well as of the unreacted TEI . This is a reasonable assumption because additional bonding is involved, so that these compounds are probably less reactive towards Lewis bases. Moreover, there are probably some unreacted organometallic species in equilibrium with the addition compound. Thus, the net reaction with arsine, would be dominated by the reaction with the individual organometallic compounds. Finally, as outlined in the comments which follow, the direct reaction of arsine with the organometallic addition compound would be unlikely.

From this figure, it is seen that the extent of reaction increases with the arsine pressue, but it is considerably less for both the alkyl mixtures than for the case when TEI reacts with arsine alone. We note that, in the presence of 3.04 torr arsine, all of the TEI was consumed in 0.7 secs (i.e., 9.0 cm from the inlet) as a result of the Lewis reaction. On the other hand, if an equal amount of TEG was mixed with the TEI prior to its entrance to the reactor (i.e. prior to its reaction with Arsine), then only 60% of the TEI was reacted after the same interval of time. In effect, the presence of TEG has reduced the extent of the reaction between TEI and Arsine . This is

further evidence that the two organometallic species form some type of addition compound. Moreover, analysis of the data shows that at least 40% of the TEI is tied up in this way, and is less susceptible to reaction with arsine in this form.

The TMG-TEI mixture is even less reactive with Arsine than the TEG - TEI mixture. Here, the Et_2In^+ signal is reduced by less than 40% upon the addition of arsine, indicating that at least 60% of the TEI is in the form of an addition compound.

The results described here are particularly significant, since they provide a quantitative basis for explaining experimental results which workers have observed during the growth of GaInAs. Typically, it has been seen that thorough mixing of the indium and gallium species, prior to combining with arsine and admission to the reaction chamber, tended to inhibit the parasitic reaction of TEI and Arsine. However, no physical reasons were advanced for this behavior and no attempts made to quantify it. Our study has shown that the reaction between TEI and arsine was indeed reduced when a comparable amount of TEG or TMG was added prior to its introduction into the reactor, and the extent of this retardation has been quantified.

The results described here indicate that both TEG and TMG show definite signs of association with TEI in the gas phase. This addition compound formation must be occurring in the reactor or gas handling system, because the extremely low pressures and the very low probability of ionization make such reactions unlikely in the mass spectrometer. Since all these

organometallic compounds are Lewis acids in nature, an adduct similar to the Lewis acid-Lewis base TEI-arsine reaction is not expected. We propose that the gallium-indium association is in a form similar to the gas phase dimerization of Trimethylalluminum which involves two bridging alkyl groups as shown in Fig. 26(a) and (b) (18).

Studies of mixtures of Trimethylthallium and Triethylthallium (19) have shown alkyl exchange via a structure of the type proposed here. The stuctures of Fig. 26 would be less acidic and therefore less likely to react with arsine. Further, the dynamic nature of the structure depicted in Fig. 26 (a) would provide a mechanism for alkyl exchange of the type observed in the mass spectrometer data. Repeated formation and dissociation of such a structure could eventually form TEG and TMI from TMG and TEI . The three centered bond arrangements shown here for the association of TEI with TMG and TEG would be unlikely to react with arsine, because indium has a coordination of three in the alkyl. The dashed lines shown are half bonds which attempt to satisfy the tendency of the indium to achieve a closed shell electronic configuration such as that of xenon.

Indium and gallium , with electronic structures $[Kr]4d^{10}5s^{2}5p^{1}$ and $[Ar]3d^{10}4s^{2}p^{1}$ respectively, each have 13 valence electrons. In structures such as TEI , TEG and TMG, 16 electrons can be associated with the metal so these structures are coordinatively unsaturated. In Lewis acid-Lewis base adducts such as $Et_3In : AsH_3$, the metal is coordinatively saturated with 18 valence electrons. The structures shown in Fig. 26 are

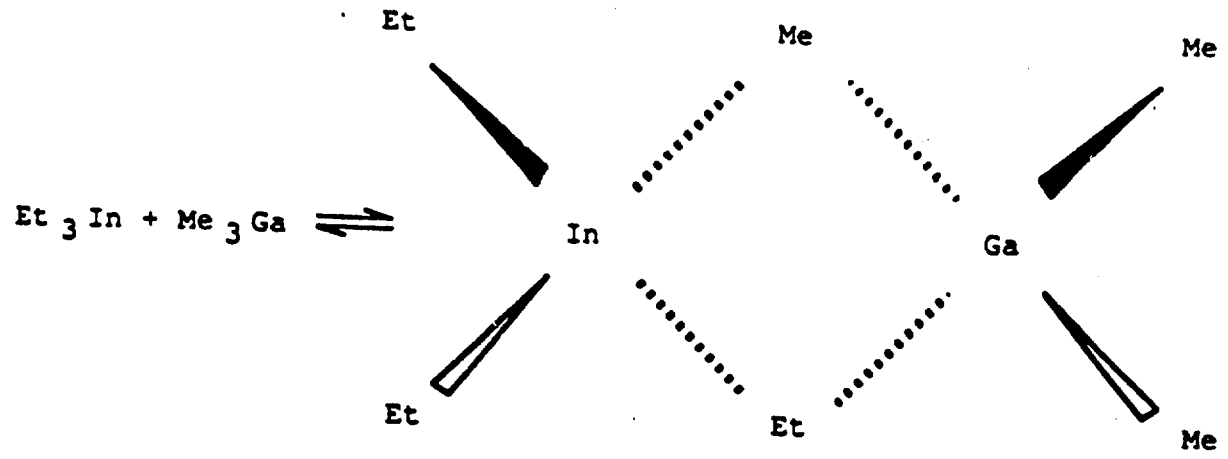

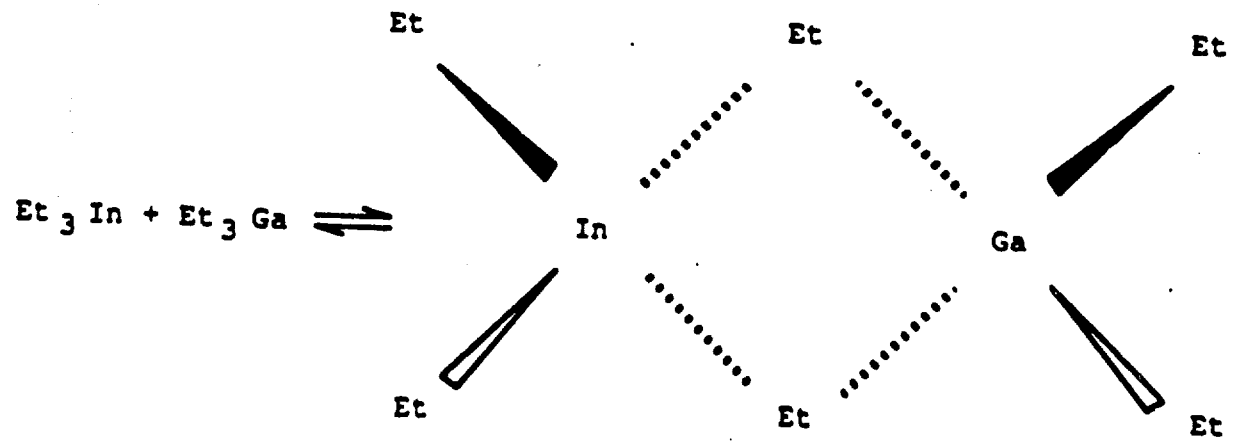

FIGURE 26: Proposed structure of a) the Me_3Ga - Et_3In addition compound and b) the Et_3Ga - Et_3In addition compound.

coordinatively unsaturated with 16 electrons associated with each metal. However the metals in these structures have a coordination of four and may be sterically hindered from further reaction, unless they dissociate.

The fact that some reaction between arsine and TEI still occurs with these structures is evidence that either some of the TEI is dissociated from the gallium species or that the arsine is still somewhat reactive towards the indium, even when it is bonded to the gallium, because the 18 electron rule is not strictly satisfied.

PROCESS ANALYSIS

Adequate understanding of the actual growth process lays the foundation for an effective system design. It is thus important that the initial framework adapted to pursue this objective is comprehensive in its ability to support experimental observations.

Our attempt to structure an understanding of the growth mechanism is based on the consideration of the basic chemistry of the reactants in both the homogeneous gas phase as well as within the heterogeneous region at the gas-substrate interface. In addition the charateristics of the transport processes as they relate to velocity and temperature profiles and thereby impact and influence rates and extent of individual reactions are also defined. Integration of the above thus provides the necessary

interrelationships for structuring the needed framework.

I GAS PHASE REACTIONS

Experimental evidence of the alkyl exchange effects has clearly demonstrated that the process chemistry of OMVPE is initiated from the point of transportation of the source reactants. Adequate mixing of the two group III alkyl's, TEI and TMG, within the gas flow system allows for the bridging of these reactants into the dimer structures represented by reaction R1. As this mixture of non-bridged and bridged alkyls enters the reactor chamber, contact with arsine takes place. The carbon-metal bond in the group III alkyls imparts an electron pair acceptor characteristic to the overall compound i.e. a Lewis acid. Arsine on the other hand possesses the ability to donate such pairs. Thus, the unbridged group III alkyls participate in a reaction with arsine to form a Lewis acid base adduct represented by reaction scheme R2 and R3. All three reaction steps R1a, R2a and R3a are reversible homogeneous reactions and as verified by our mass spectrometer studies achieve equilibrium prior to the contact of the gas mixture with the heated substrate. An estimate as to the extent of each reaction can be made from the observations of our mass spectrometer studies . Under conditions of excess arsine, TEI is essentially all exhausted by reaction R3a, however in the presence of TMG only 40% of TEI is involved in reaction R3a. Therefore it can be approximated that reaction R1a involves 60% of the TEI introduced under conditions of equal partial pressures of TMG. Similar calculations on TMG indicate that less then 20% of TMG is

$$(CH_3)_3Ga + (C_2H_5)_2In \rightleftharpoons$$

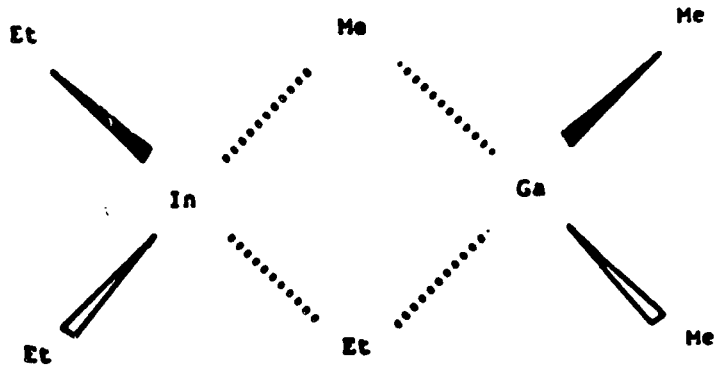

R1a

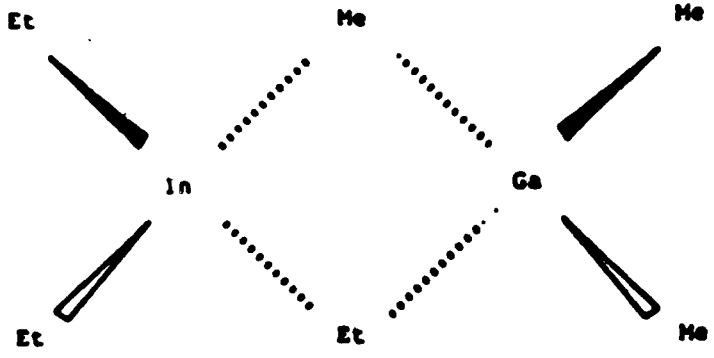

$$\rightleftharpoons (CH_3)_2C_2H_5Ga + (C_2H_5)_2CH_3In$$ R1b

$$(CH_3)_2C_2H_5Ga + (C_2H_5)_2CH_3In \rightleftharpoons CH_3(C_2H_5)_2Ga + (CH_3)_2C_2H_5In$$ R1c

$$CH_3(C_2H_5)_2Ga + (CH_3)_2C_2H_5In \rightleftharpoons (C_2H_5)_3Ga + (CH_3)_3In$$ R1d

$$(CH_3)_3Ga + AsH_3 \rightleftharpoons (CH_3)_3GaAsH_3 \quad \text{R2a}$$

$$(CH_3)_3GaAsH_3 \longrightarrow (CH_3)_2GaAsH_2 + CH_4 \quad \text{R2b}$$

$$(CH_3)_2GaAsH_2 \longrightarrow (CH_3)GaAsH + CH_4 \quad \text{R2c}$$

$$n\ CH_3GaAsH \longrightarrow (CH_3GaAsH)_n \quad \text{R2d}$$

$$(C_2H_5)_3In + AsH_3 \rightleftharpoons (C_2H_5)_3InAsH_3 \quad \text{R3a}$$

$$(C_2H_5)_3InAsH_3 \longrightarrow (C_2H_5)_2InAsH_2 + C_2H_6 \quad \text{R3b}$$

$$(C_2H_5)_2InAsH_2 \longrightarrow (C_2H_5)InAsH + C_2H_6 \quad \text{R3c}$$

$$nC_2H_5InAsH \longrightarrow (C_2H_5InAsH)_n \quad \text{R3d}$$

involved in reaction R2a with arsine which implies that under conditions of excess TEI relative to TMG, reaction R1a would proceed to exhaust TMG, reaction R2a would proceed to a negligible extent and reaction R3a would essentially tie up the remaining TEI.

On its approach towards the substrate the bulk gas temperature is continously increased providing the necessary activation energy for initiating the subsequent alkyl exchange reactions in scheme R1 and hydrocarbon elimination reactions in schemes R2 and R3. The extent to which these subsequent in-series reactions occur within the bulk gas depends upon the time and temperature history of the gas mixture prior to its contact with the heated substrate. For the growth run conditions in our system this time is on the order of approximately 2 seconds. Thus it is highly unlikely that reactions R1c, R1d and R3d occur to a significant extent since these involve bimolecular collisions of intermediates under low pressure conditions. Reactions R1b , R3b and R3c however can proceed to a significant extent since these essentially involve unicomponent dissociation.

At the heated substrate surface the high temperature and resulting increase in gas viscocity together with the retarding effect of the solid surface to bulk gas motion creates a boundary layer region within which movement of reactant species takes place by diffusion rather then forced convection. We believe that it is in this region that the nutrient species responsible for growth are generated. Conventional decomposition

steps for the pyrolysis of individual compounds TMG, TEG and arsine have been studied (20-24).

For the case of TMG-H_2 an irreversible hydrogenolysis reaction lead to the formation of methane whereas the pyrolysis of TEG-H_2 followed a reversible beta elimination mechanism forming ethylene. In both cases however the reactions went to completion below 500 C. Specifically the TMG-H2 reaction took place between 370-460 C whereas the TEG-H_2 decomposition covered 220-330 C. Within this context another study conducted by Den Baars et al, (20) specifically determined the release of all 3 methyl radicals from the TMG-H_2 decomposition. Assuming that decomposition mechanism for TEI would follow a similar route to that taken by TEG, reaction schemes R4 and R5 would then represent the mechanism for decomposition for TMG and TEI in the absence of arsine a hydrogen environment.

Adequate support for the heterogeneous decomposition of arsine in H_2 has been recently presented (23). Based on this data the decomposition of arsine in the absence of TMG or TEI follows the mechanism provided by reaction R6. However, Dan Baars et al,(20) while studying the homogeneous and heterogeneous thermal decomposition rates of TMG and arsine observed that the presence of TMG in the gas phase increased the rate of arsine decomposition but did not substantially alter the activation of the process. Although they conceded that this observed low temperature arsine decomposition probably was dominant during OMVPE, they were unable to provide a complete explanation. Their results are reproduced in Figure 27 .

$$(CH_3)_3Ga \longrightarrow CH_3\cdot + (CH_3)_2Ga \qquad \text{R4a}$$

$$(CH_3)_2Ga \longrightarrow CH_3\cdot + (CH_3)Ga \qquad \text{R4b}$$

$$2CH_3\cdot + AsH_3 \longrightarrow 2CH_4 + AsH \qquad \text{R4c}$$

$$n(CH_3)Ga \longrightarrow (CH_3Ga)_n \qquad \text{R4d}$$

$(C_2H_5)_3In$ ——— $C_2H_4 + (C_2H_5)_2InH$ R5a

$(C_2H_5)_2InH$ ——— $C_2H_6 + C_2H_5In$ R5b

C_2H_5In ——— $C_2H_5 + In$ R5c

$$AsH_3(g) + S \rightleftharpoons AsH_3(ad) \qquad R6a$$

$$AsH_3(ad) \rightleftharpoons AsH + H_2(g) \qquad R6b$$

$$2AsH(ad) \rightleftharpoons As_2 + H_2 \qquad R6c$$

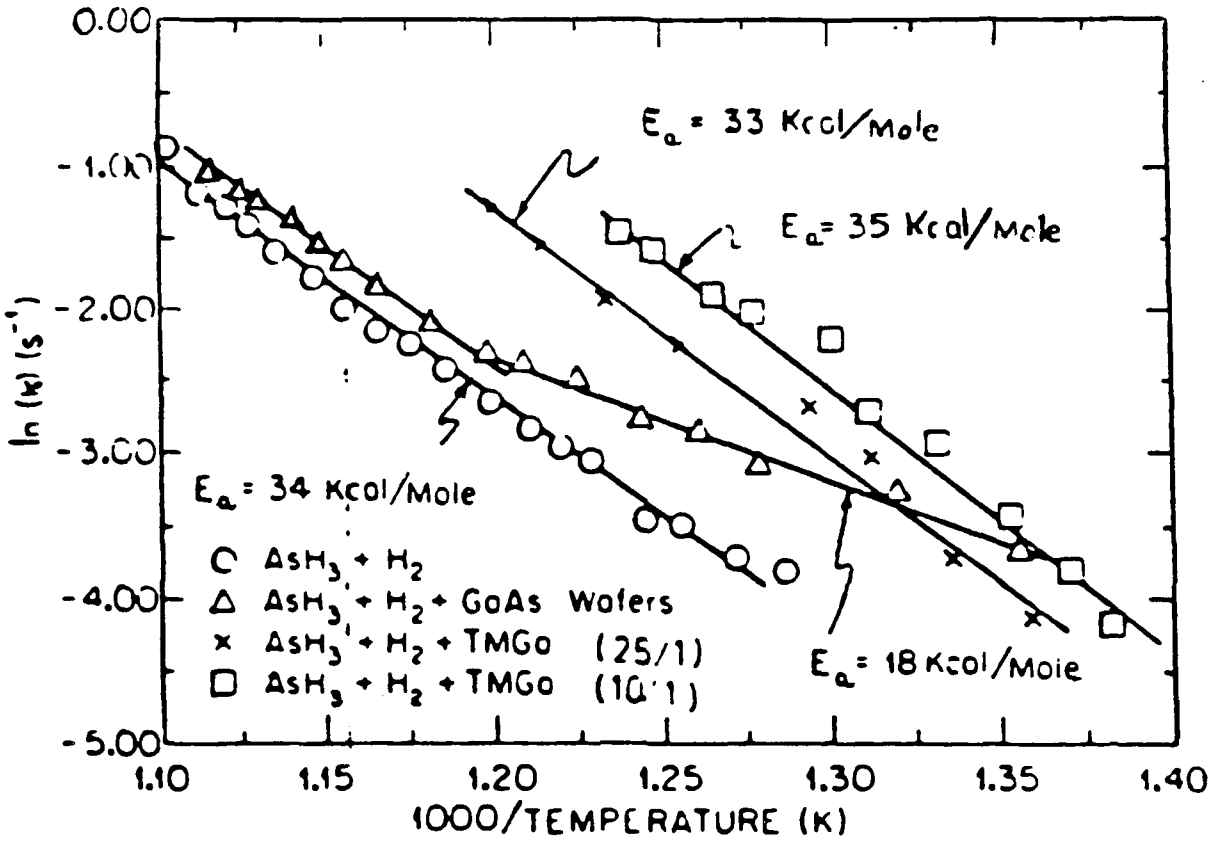

FIGURE 27: Effective rate constant for decomposition of Arsine in H_2, H_2 + TMG and H_2 with GaAs wafers present (20).

During an investigation on the pyrolysis temperature of TEG and arsine Mashita et al (21) observed that the pyrolysis of TEG with and without the presence of arsine resulted in not only lowering the decomposition temperature for the TEG/arsine mixture but also resulted in different hydrocarbon products. In the case of TEG-H_2 system at 400°C ethylene and butane were the main by products. TEG-arsine-H_2 mixture on the other hand resulted in ethane as the dominant hydrocarbon with almost no butane. In addition significant amounts of ethylarsine were also observed.

It thus seems that for the case of TMG in the presence of arsine, the methyl radicals released during decomposition interact with arsine via reaction R4c. Whereas for the case of TEG in the presence of excess arsine, the adduct undergoes decomposition reactions to ethylarsines. Whether the same would apply to TEI is unclear. In any case, this would only be of secondary importance for the growth of GaInAs in our growth system. Since the indium nutrient for the growing film would primarily be supplied from the products of the alkyl exchange reaction scheme R1.

II SUBSTRATE SURFACE REACTIONS

Homogeneous nucleation of GaInAs is highly unlikely under growth conditions resulting in single crystal materials with specular surfaces. It thus seems that the species supplying the nutrient elements are the decomposition products of the group III alkyls and arsine (26,27,28). Although the method of surface incorporation has not been conclusively established, results obtained on the orientation dependence of GaAs growth rate (27)

strongly support an independent reaction of the As bearing and Ga bearing species with the substrate surface.

Work carried out on the OMVPE of GaAs on foreign substrates (29) has shown that this growth involves an intermediate liquid phase that subsequently saturates with arsenic to form GaAs. However the single crystal growth of homoepitaxial GaAs obviously occurs without the formation of any liquid intermediate state or discrete nucleii. It thus seems that vapor solid transformation during OMVPE involves a chemical reaction between surface absorbed species. This form of transformation requires chemisorption of gas phase radicals as opposed to adsorption of reactants.

Based on the gas phase process chemistry for GaInAs presented in the previous section, such group III alkyl radicals would primarily be provided by the products of Reaction R1b. Although reaction R1c could proceed, its influence would be much less significant since it involves the interaction of two intermediate species in the gas phase at low pressures. Thus following the reaction pathways established by reaction schemes R4 and R5 the most likely group III radicals would be monomethyl gallium, monoethyl indium and monomethyl indium generated in the hot zone near the substrate surface. Arsine absorption on to the heated substrate as well as its homogeneous reaction with methyl radicals via reactions R4c and R6a and b would produce the AsH nutrient for the group V radical. Reaction between these radicals on the substrate surface would then be responsible for epitaxial growth. The availability of the above nutrients to

$$CH_3Ga + C_2H_5In + 2AsH \longrightarrow GaInAs + CH_4 + C_2H_6 \qquad \text{R7a}$$

$$CH_3Ga + CH_3In + 2AsH \longrightarrow GaInAs + 2CH_4 \qquad \text{R7b}$$

participate in the growth reaction R7 essentially determines the growth process. This availability is not only effected by the generation rates of the nutrient species but also by their depletion via any parallel reactions.

Alternate reaction pathways available to the above nutrients for the group III alkyls are polymer formation for the gallium alkyl (30) and decomposition for the Indium alkyl (31) as represented by reactions R4d and R5c. Since reaction R5c is a unimolecular dissociation it is of much more significance than reaction R4d which involves a bimolecular collision between an intermediate species at low pressures. For the group V hydride nutrient AsH the most likely alternative pathway is essentially heterogeneous association to form the elemental dimer since the bond dissociation energy of AsH is relatively high (≈272kJ/mol) preventing participation in any homogeneous reactions.

III TRANSPORT PROCESSES

The generation of nutrient species within the hot zone above the heated substrate imparts significant importance to the fluid transport aspect of the system design and operation. Analysis of the transport processes involved during our OMVPE growth of GaInAs can be considered as resulting from the combination of two distinct categories:

gas flows normal to the substrate surface

gas flows parallel to the substrate surface

a. GAS FLOWS NORMAL TO THE SUBSTRATE SURFACE

This mode of transport is characterized by the following

salient features:

1. a two dimensional forced convective flow pattern whereby the main axial flow is divided across the plane along the substrate surface at the stagnation point (32)

2. Imposition of a thermal convection flow pattern on to the forced convective flow, creating stagnant regions resulting in vortices.

3. lower spread around the mean residence time within the diffusion layer due to the two dimensional flow across the plane of the substrate

b. GAS FLOWS PARALLEL TO THE SUBSTRATTE SURFACE

The parallel mode relative to the normal mode of transport is characterized by the following salient features:

1. a unidimensional forced convective flow pattern whereby the gas flow along the substrate surface at most experiences only a potential field displacement rather than a flow direction change.

2. insignificant thermal convection effects away from the leading edge thereby avoiding vortex generation above the substrate surface.

3. variable residence time along the substrate surface due to the changing diffusion layer thickness in the direction of gas flow.

Our method of reactant transport in a horizontal reactor with a vertical susceptor essentially resulted in a combination of the above two flow patterns. This essentially allowed for the maintanance of uniformity of growth thickness provided by the normal mode of operation but at the same time avoided the

generation of stagnant regions that lead to the loss of control over the gas phase reactions.

IV GROWTH MECHANISM

Justification that the process chemistry described above adequately supports the results obtained during the course of this program is based upon the following observations.

Firstly, the growth of GaInAs with solid concentration ratio of Ga:In relatively insensitive to the input partial pressures of TMG, TEI and arsine is obtained over a wide range as shown in Figures 28 and 29, respectively. This can only come about if the nutrient species providing the chemisorbing radicals are not the input TMG & TEI reactants but a product of a reaction between the two. The fact that the alkyl exchange dimer between the two compounds involves a 1:1 ratio of Ga to In atoms it is the most likely candidate . In addition, the insensitivity of the x value to the relative concentration of arsine also makes it unlikely that the nutrient species could be a product of a reaction between the group III alkyls and arsine.

The chemisorbing radicals are a product of a gas phase reaction and are themselves an intermediate both for the growth reaction R7 as well as alternate homogeneous reactions R4d and R5c. As such if and only if R7 is the slowest step in the overall process it would be possible to correlate the data generated on growth rates and composition with the partial pressures of the input reactants and operating conditions of the growth reactor. However, this is highly unlikely since reaction

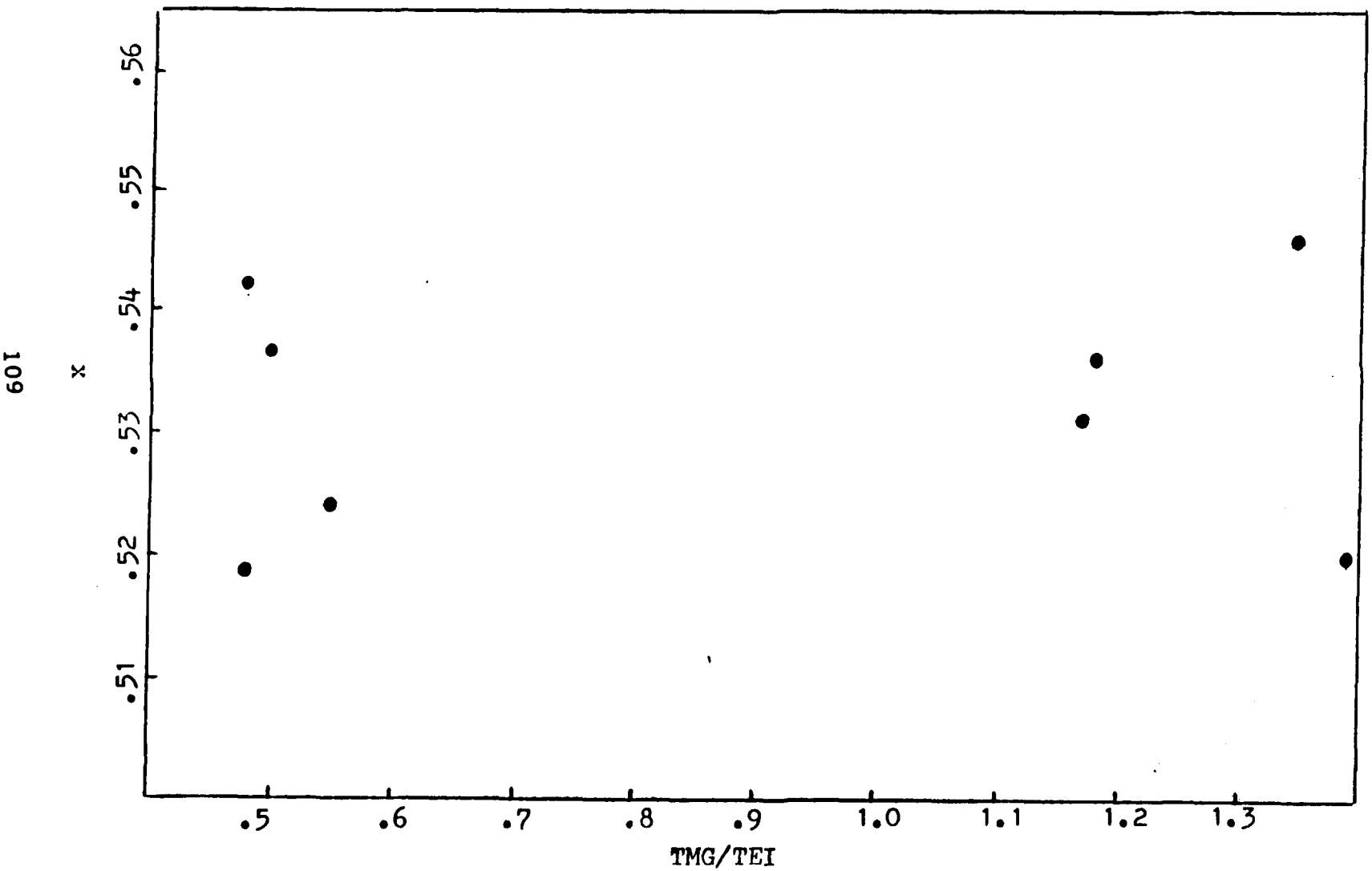

FIGURE 23: Solid composition (x) vs inlet ratio of TMG/TEI

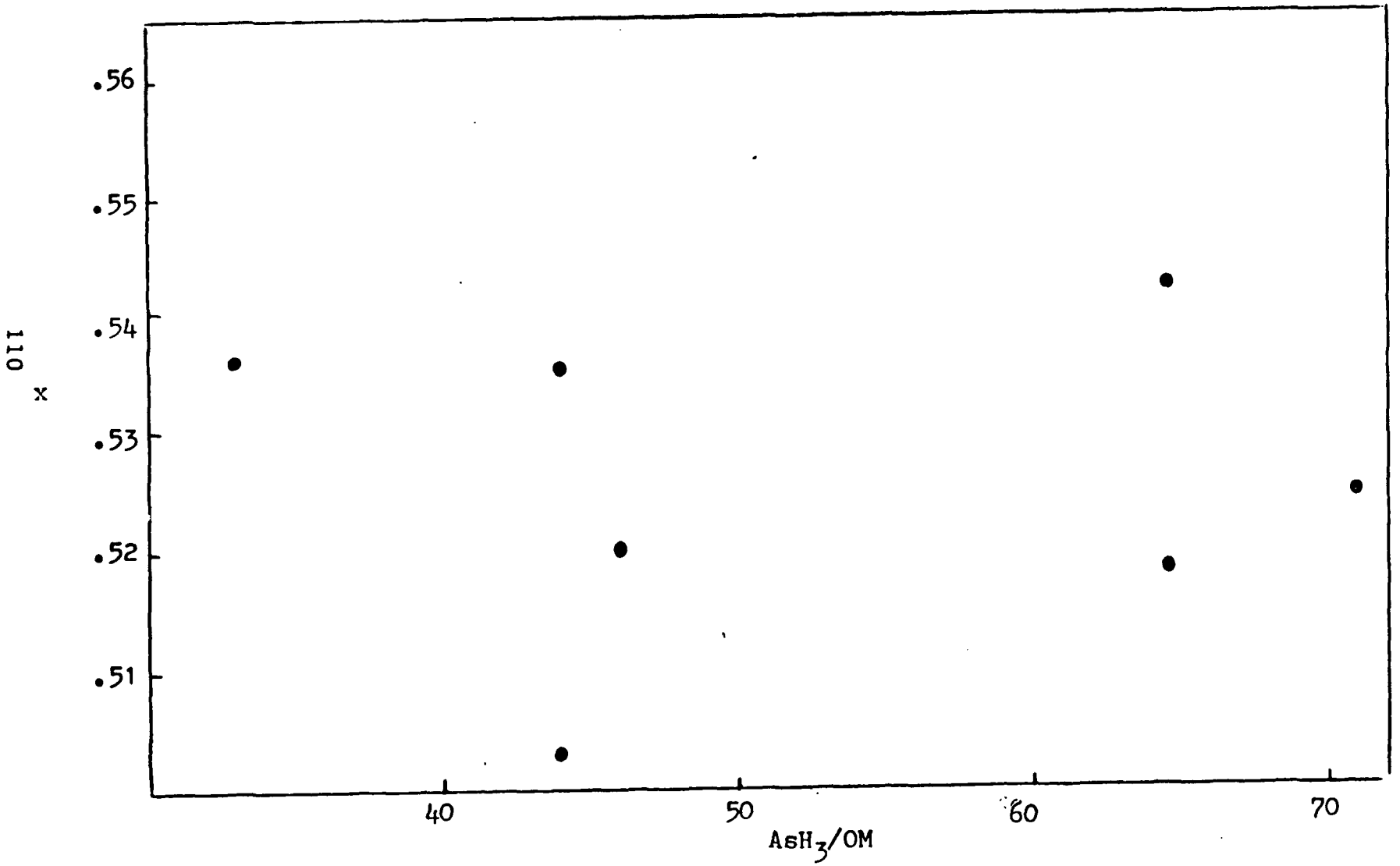

FIGURE 29: Solid composition (x) vs inlet ratio of Arsine/Total Organometallics

R7 is thermodynamically much more favoured then the group III monoalkyl generative reactions R4 and R5 and even the group V hydride decomposition reaction R6.

Within reactions R4 and R5 vs R6 the insensitivity of growth rate to arsine partial pressures as shown in Figure 29 suggests that reaction R6 is probably not the slowest step. This therefore implies that either reactions R4 and R5 are the rate controlling kinetic steps or that diffusion of the monoalkyl radicals through the stagnant boundary layer is the rate limiting step. Since reaction R4 and R5 involve both activation energy, initiated monoalkyl generation as well as an activation energy dependent homogeneous decomposition of the monoalkyl for TMI the effect of susceptor temperature would have a compensating effect on the growth reaction R7 and would therefore provide limited effect on growth. This can be seen by the data presented in Table 7 . However, the indium incorporation into the growing layer would then be expected to go up for lower susceptor temperatures. This trend is also observed in the data presented for fixed arsine to group III alkyl input ratio.

We have discounted the possibility of diffusion limited growth since any changes in the diffusion driving force does not significally influence the growth rates. This can be seen in Figure 30 where the concentrations of the dimer formed in reaction R1 is plotted against the growth rates measured. Although some scatter can be seen there does not appear to be any dependence of one on the other.

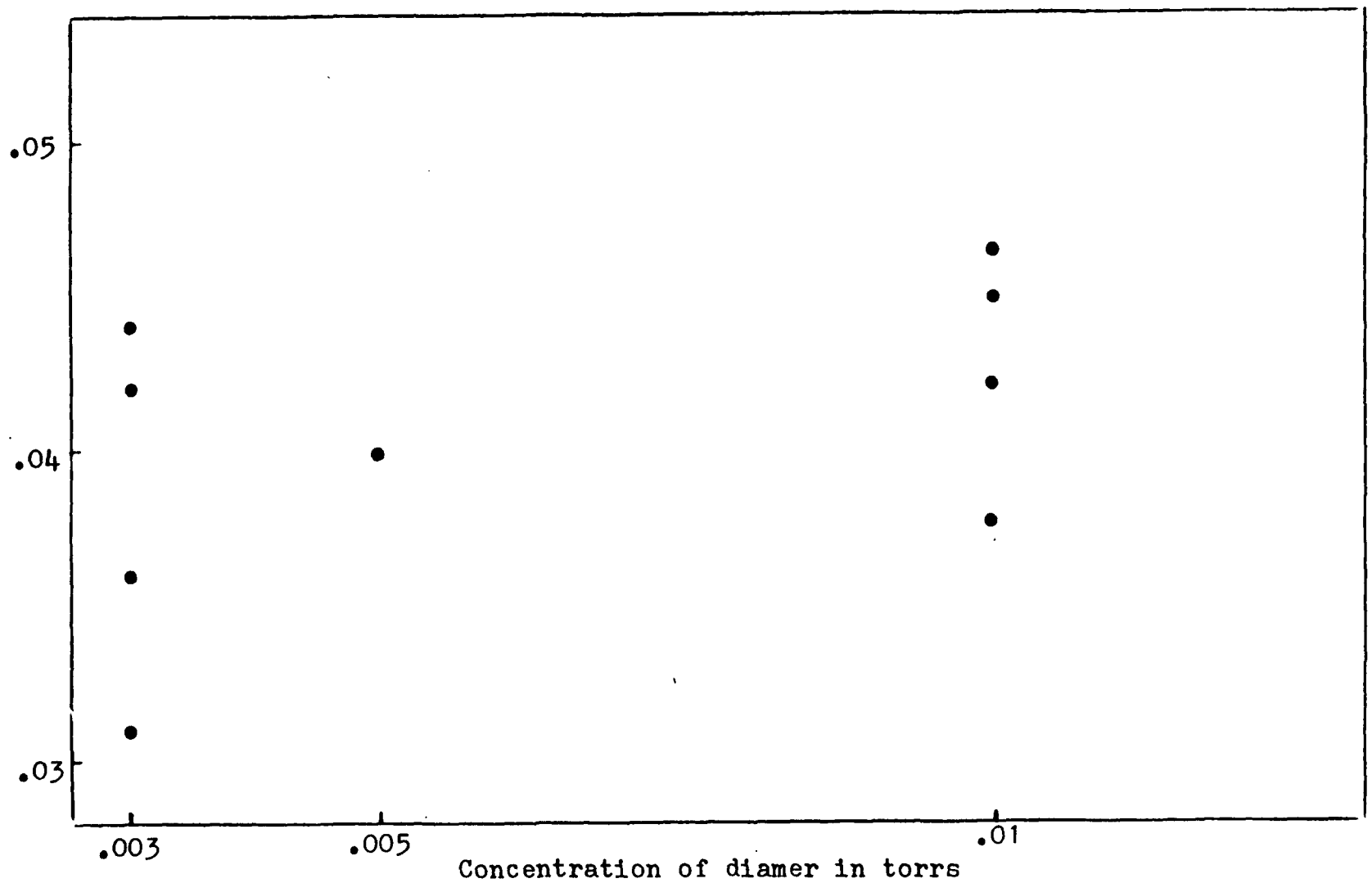

FIGURE 30: Growth rate vs the concentration of the diamer in torrs.

	A	B	C	D	E	F	G
1	Run	444	448	450	452	454	457
2	t1	6000	6000	6000	6000	6000	6000
3	pTMGa	0.01	0.01	0.01	0.01	0.01	0.005
4	pTEIn	0.02	0.021	0.021	0.021	0.021	0.0091
5	pTEIn/pOM	0.667	0.677	0.677	0.677	0.677	0.645
6	pAsH3	1	2	2	2	2	1
7	pPH3	2	2	2	2	2	1
8	As/OM	33.33	64.52	64.52	64.52	64.52	70.92
9	pR	152	152	152	152	152	76
10	Susc	60	60	60	81	60	60
11	Ts	650	650	600	600	650	625
12	1000/Ts °K	1.083	1.083	1.145	1.145	1.083	1.114
13	Tga	263	263	263	263	263	263
14	Tin	298	298	298	298	298	298
15	Time	60	60	60	30	60	60
16	B Layer Time	2	2	2	2	2	2
17	Thickness	2.69	2.69	2.78	1.13	2.52	2.49
18	Growth R	0.0448	0.0448	0.0463	0.0377	0.0420	0.0415
19	u300		2541	5895	8513		1043
20	l/r300		1.74E-04	9.70E-04	1.10E-03		1.59E-04
21	n300 °K		1.59E+15	3.70E+15	7.15E+15		3.83E+15
22	u77			21300	40700		
23	l/r77			1.40E-03	4.00E-03		
24	n77			1.48E+15	5.44E+15		
25	WNc	6000	6150	5700	5950	5950	6400
26	x	0.5365	0.5186	0.5731	0.5425	0.5425	0.4894
27	Morph	Exc	Exc	Exc	Exc	Exc	
28	Susc Etch	Y	N	N	N	Y	
29							
30	Comments	Cross Hatch	Cross Hatch		Plasma	Large Sample	
31	Comments					Cross Hatch	
32	Comments						
33							
34							
35							
36							
37							
38							

TABLE 7: Comprehensive data of optimized growth runs.

Based on the above arguments we believe that for the growth of GaInAs in our program the growth mechanism proposed by R1- R7 is the most plausible.

PROCESS PARAMETERS

I CARRIER GAS

Establishing the relevent process parameters for the growth of GaInAs lattice matched to InP, it is important that these be considered within the context of the source reactants as well as the carrier gas that is utilized. From the gas phase reaction scheme developed earlier it is clear that the carrier gas does not participate in the various reaction pathways through which the input source reactants travel. This does not imply that the carrier gas is of only secondary importance in the overall transformation process, on the contrary it is the carrier gas that determines the velocity and temperature profiles within the growth reactor. These factors primarily determine the extent of most if not all the reactions within the gas phase R1 - R7. The main properties of the carrier gas that are relevent to determining its impact on the growth process are density, viscosity, heat capacity at constant pressure, and thermal conductivity as functions of temperature. Although hydrogen has been normally used as a carrier gas helium and nitrogen mixtures with hydrogen have also been utilized. Figure 31-34 show the relative values of the above parameters for these gases. It can thus be seen that the use of the mix ratio of these gases can be an effective control parameter for influencing the gas phase

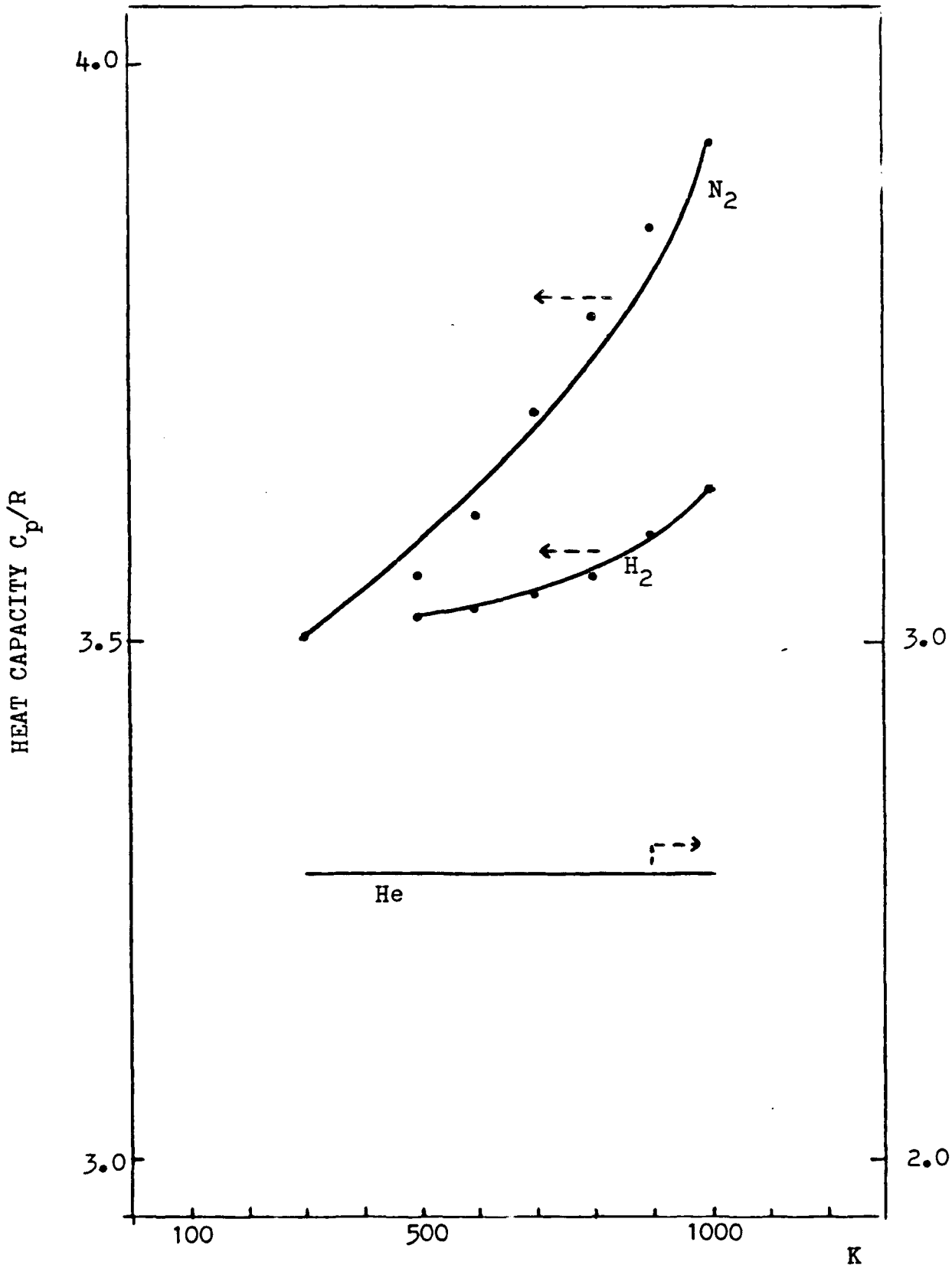

FIGURE 31: Heat capacity vs temperature

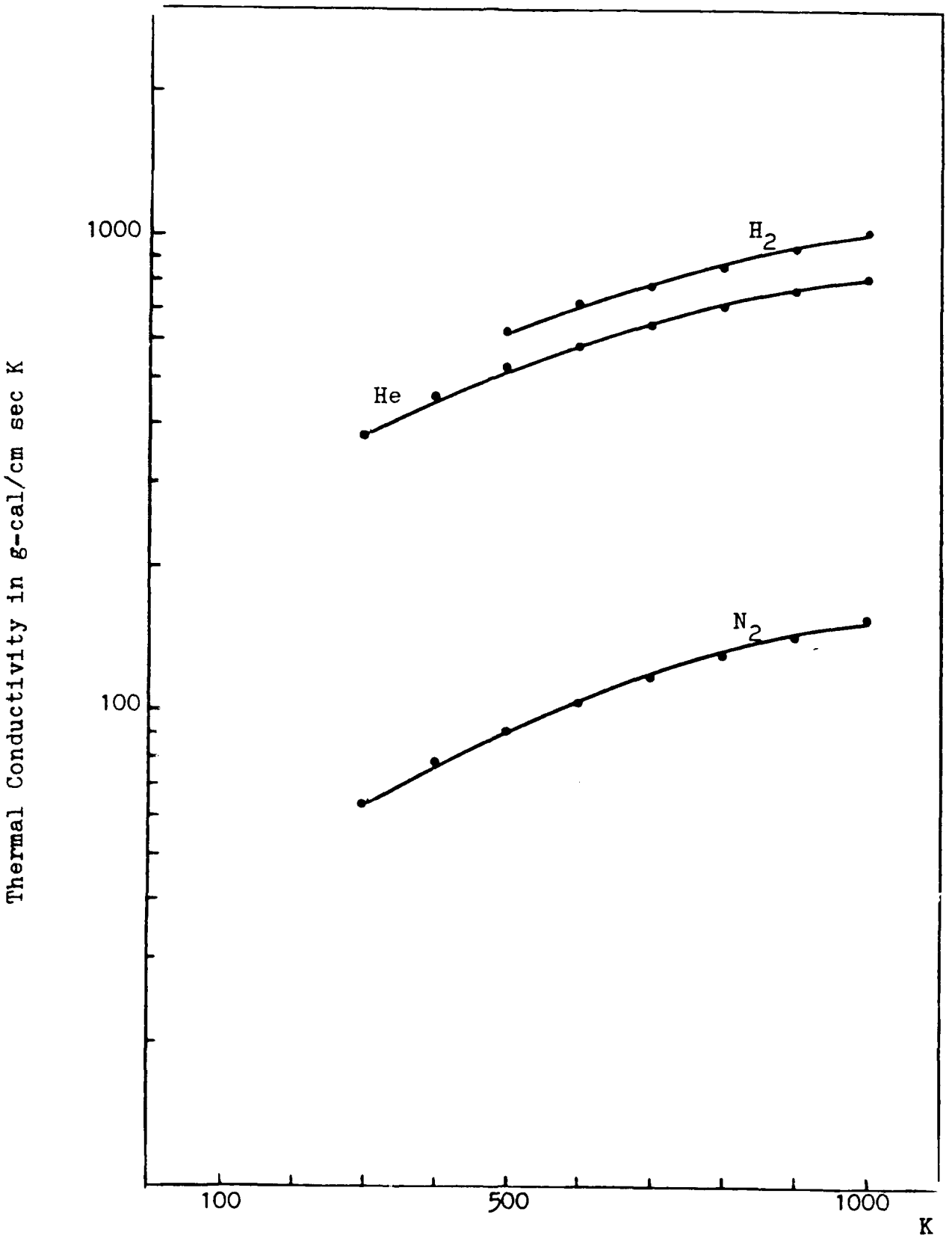

FIGURE 32: Thermal conductivity vs temperature

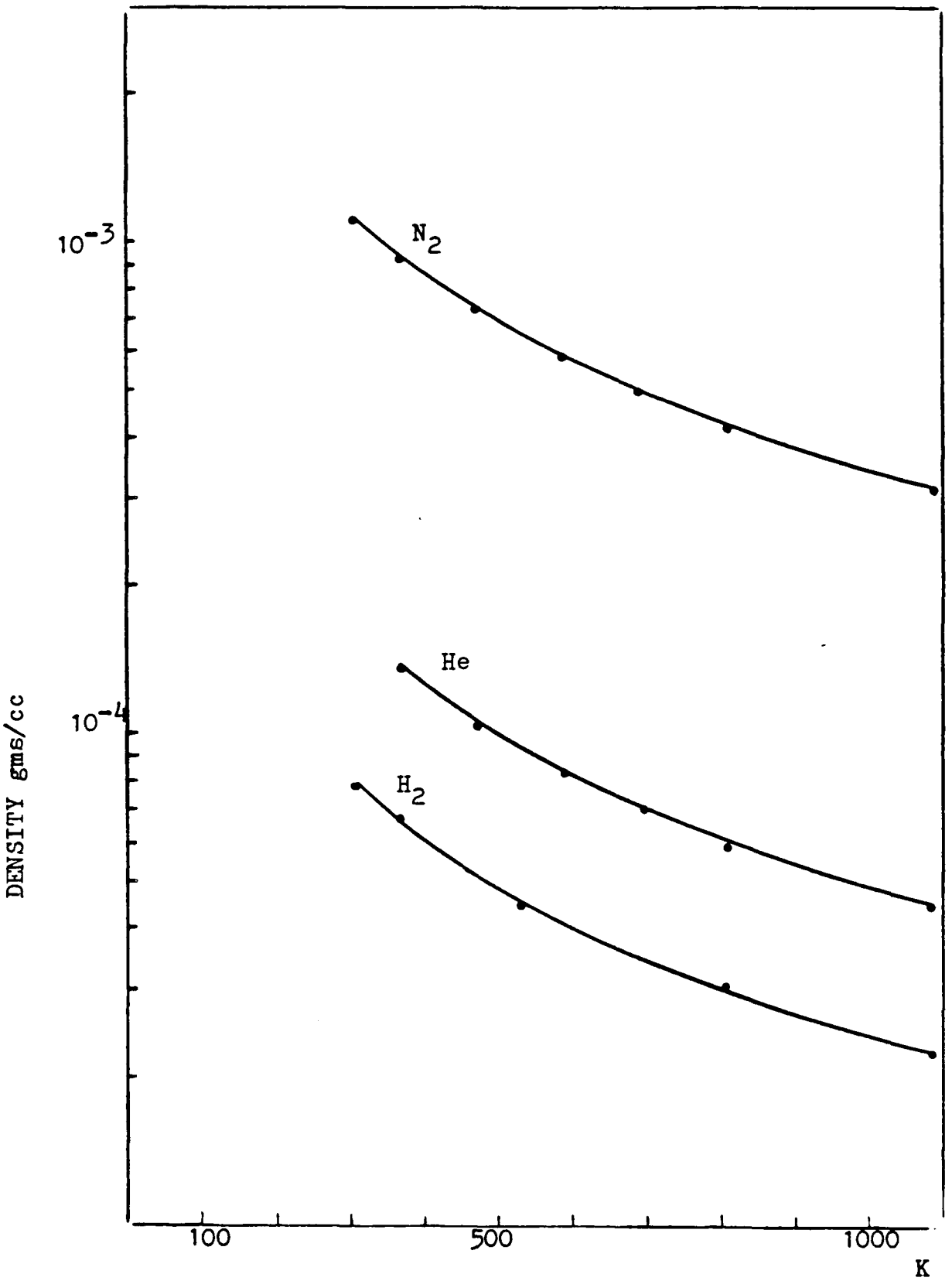

FIGURE 33: Density vs temperature

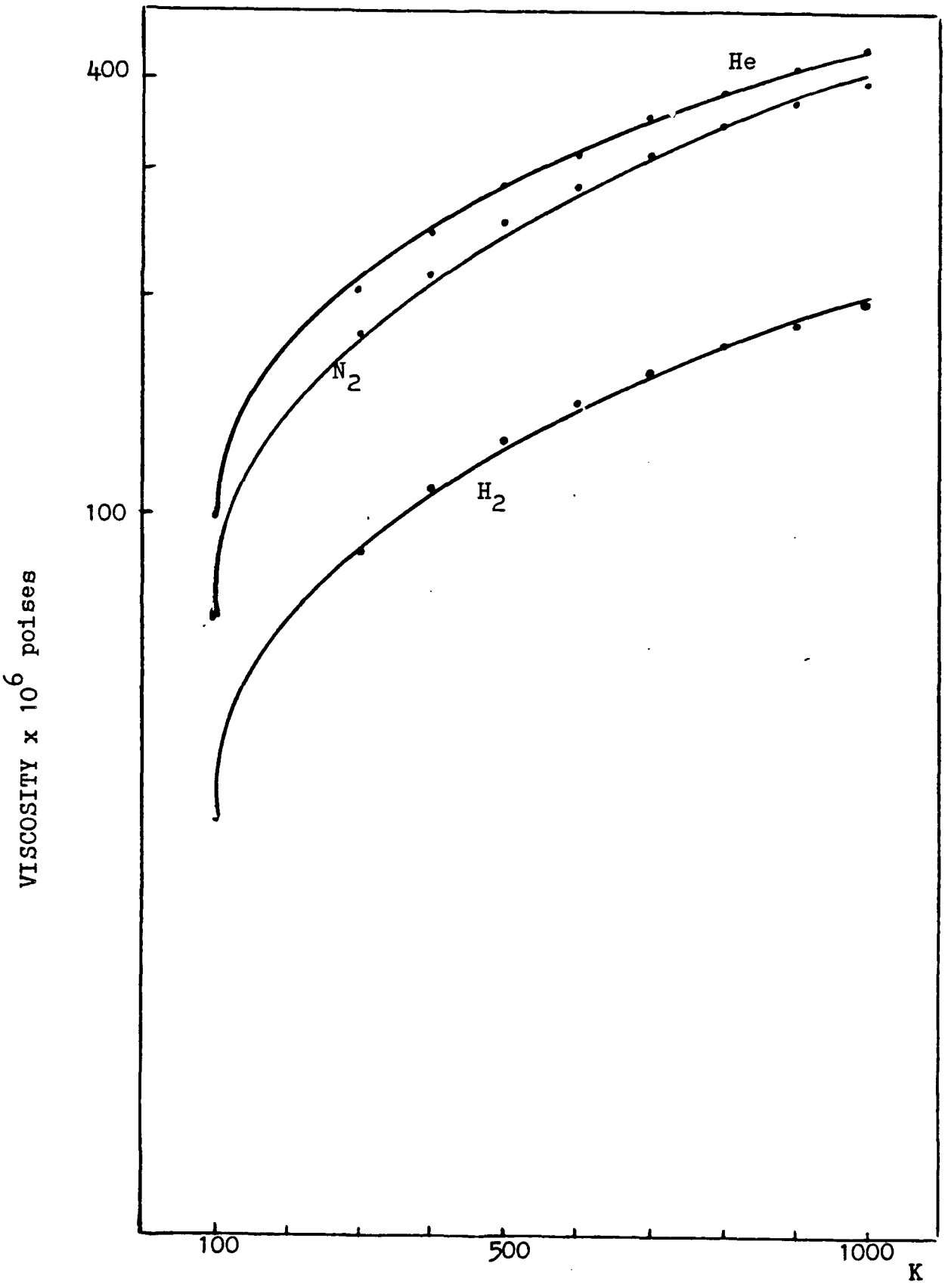

FIGURE 34: Viscosity vs temperature

reactions and thereby the growth process.

II SOURCE CHEMICALS

Although for the reasons already elaborated we chose to conduct our program using TMG, TEI and arsine , there is no fundamental reason why any of the other available source reactants would not give equally good epi-layers of GaInAs lattice matched to InP. However, the reaction chemistry would change significantly depending upon the reaction system chosen and therefore a need for proper design and operation to optimize process performance. Generally lower growth temperature perfcrmance with the TEI and TEG combination would be possible resulting in better quality layers. However the TMG and TMI combination would allow for thickness uniformities over relatively larger areas. Thus the optimum alkyl combination to be chosen would depend upon the specific criteria that needs to be optimized.

For the group V reactant arsine has been the conventional choice due to its reasonable cost and availability. Recently, a new group V sources Tertiary butyl arsine has been successfully used for the growth of GaAs at lower growth temperatures then arsine (33). Use of such sources for lowering the growth temperature of GaInAs could provide significant advantages.

III SUSCEPTOR TEMPERATURE

Clearly the susceptor temperature is the most important process parameter. Not only does it directly determine the rate and extents of the homogeneous gas phase reactions but also the

average number of broken bonds in the indium phosphide substrate as well as the growing GaInAs epi-film. Certainly the growth process should be operated at low temperatures but this cannot be arbitrarily set. A temperature setting that fails to provide the necessary activation energy for the generation of the mono alkyls will not only result in lower growth but increase the possibility of incorporating carbon into the grown film. Too high a susceptor temperature setting could enhance the rate of reactions R4d, R5c and R6c thereby compromising the single crystal structure of the grown film. The susceptor temperature for a given system design thus essentially determines the compositional uniformity and layer morphology. Operation at the optimum susceptor temperature is imperative for obtaining lattice-matched layers over large areas.

IV SYSTEM PRESSURE

The system operating pressure essentially sets the mean free path of reactant molecules and product radicals. Since this factor influences the extent of homogeneous gas phase reactions R1c and d, R2d, R3d and R4c and d, its influence on the availability of the group III monoalkyls for participation in reaction R7 would be of most significance. This can effect not only growth rates but also the grown layer composition.

The system pressure at fixed partial pressures of the input reactants determines the residence time of the reactants in the growth reactor. This can directly impact the extent of unimolecular decompositions in all the reactions R1 - R7.

V SOURCE REACTANT FLOWS

The partial pressures of the input reactants is a critical control parameter due to the wide range of reactions involved in the integrated growth process. The need for relatively higher partial pressures of the group III hydride is dictated by the equilibrium vapor pressures of the GaInAs elements at the growh temperatures employed. Since the indium-arsenic bond is weaker then the gallium-arsenic bond it determines the necessary overpressures for preventing the decomposition of the growing layer. Figure 35 shows the partial pressure of As_2, As_4, In and InAs gaseous species along the liquidus in the InAs system (34). It can be seen that for temperatures around 650 C roughly ten times more As_2 species are present then indium, however the input group V element arsine which would provide the As_2 species via reaction R6c is also consumed in the alternate reactions R1, R2, R3, R4 and R7. Therefore on the lower limit the ratio of group V hydride to group III alkyls has to be above a factor of 10 and for effective growth accounting for the kinetics and extents of all the reactions involved it is around 50 for our system.

The lower bound on the group III indium element according to Figure 35 is a partial pressure of arount 10^{-8} atm. at 650° C. However in order to have acceptable growth rates a supersaturation has to be established.

In our system this supersaturation is around $10^{-4} - 10^{-5}$ atm. for optimum specular layers. This comes about due to the fact that specular layers over large areas would only be possible if reaction R7 is not the rate limiting step. For if it is than the

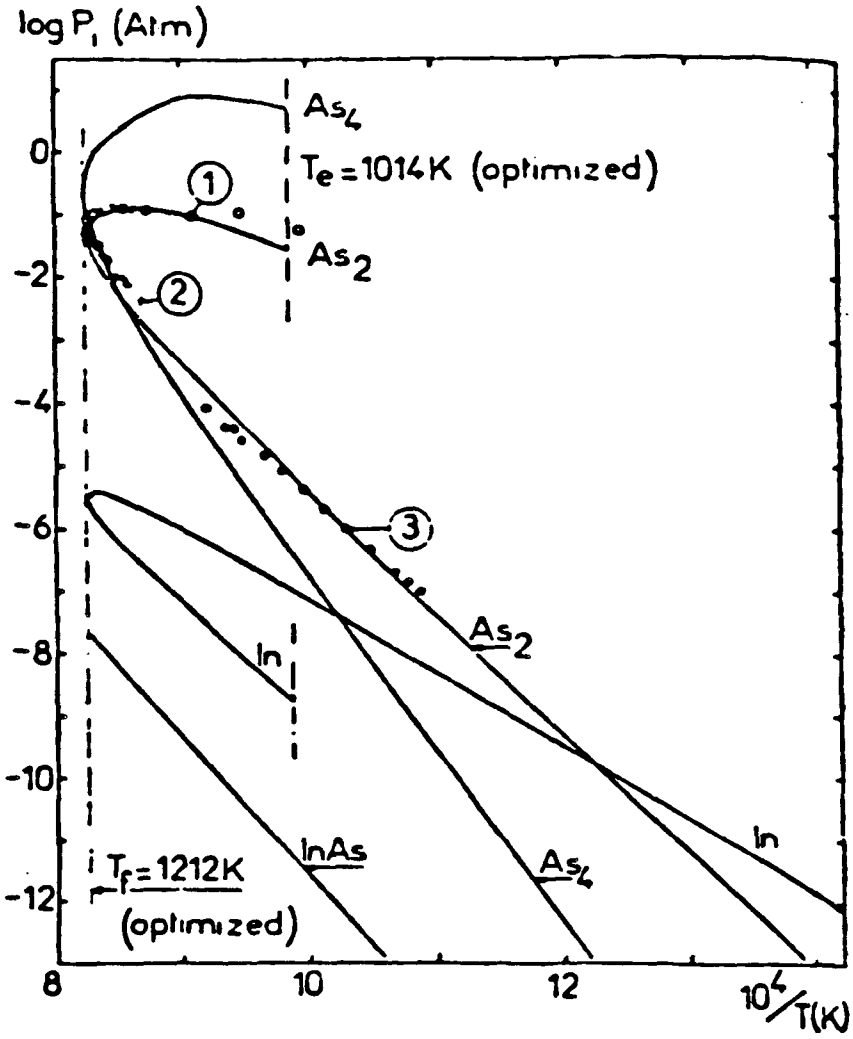

FIGURE 35: Optimized partial pressures of As_2, As_4, In and InAs gaseous species along the liquidus in the In-As system. (34).

tendency for the excess nutrient radicals to proceed down alternate pathways R4a and d, R5c and R6c would be enhanced. This would then result in element inclusions in the grown layer and ultimately polycrystalline structures. Since reaction R7 is not a thermally activated reaction, its kinetics can primarily be enhanced by increasing the concentration of the nutrient radicals. Since arsine is already in excess this would imply providing sufficient monoalkyl group III reactants. The correct partial pressures and relative ratios of the gallium and indium alkyls would depend upon the actual combination used for source reactants and system design.

IMPLICATIONS FOR SCALE UP

OMVPE of GaInAs involves the use of a cold wall vapor deposition system. We believe that the key requirements for such a system capable of reproducibly growing large area epi-layers include:

- The system must be stable and reliable and not impose unacceptable variations in growth rates and composition.
- The system must be reproducible and easy to control.
- The system must not impose unacceptable engineering and redesign for growing other quarternary and binary compounds.

The criteria of stability demands that the influence of the fluid flow phenomenon in the reactor should be invariant with time especially at the substrate surface where the vapor-solid transformation is realised. Reliability on the other hand requires that it should be possible to make predictable changes

in the growth process by manipulating the process parameters that have been identified previously. Both these criteria we believe can be accomplished by the following features:

A vertical reactor design that utilizes a rotating susceptor within a water cooled reaction vessel. The rotation speed of the susceptor would primarily influence the thickness of the hot diffusion layer and thus adds another degree of freedom as a control parameter. By fixing all other process parameters, an increase in the susceptor RPM would decrease the boundary layer thickness and thereby allow for engineering the reactions R1 - R7.

In order to eliminate the effect of jetting accompanied by the introduction of reactant into the reaction vessel a properly designed baffle to create a hold up time should be used. Our experience with a simple stainless steel mesh in our systemm has clearly allowed for the elimination of such a jetting effect thereby adding to the overall uniformity of the growth process.

The second criteria of reproducibility and ease of control requires that when the system is operated in a repetitive mode, it should be able to reproduce the results. Based on the alkyl dimer formation that occurs between the gallium and the indium compounds via R1 and the subsequent formation of the adduct in the presence of arsine via R2 and R3 it is importnt that these three reactions be controllable. Providing for adequate mixing firstly of the group III alkyls in the gas flow lines followed by the addition of arsine into this premixed flow should allow

for this reproducibility.

The growth of other binary and quaternary III-V compounds might require the use of alkyls with widely varying vapor pressures. Since these can differ by sometimes a factor of 2 or 3, it is thus important that the mass flow controllers used be capable of providing the needed accuracy over a rather broad range. Generally this cannot be achieved by the same controller and thereby requires the use of a controller designed for a specific range. Thus, it is important that the mass flow controllers within the gas distribution system are capable of being convieniently removed and reinstalled.

REFERENCES

1. M. Kawachi, A. Kawan and T. Miyashita, Electron. lett., 13, (1977) 442-443.
2. J. Conradi, F. P. Kapron and J. C. Dyment, IEEE Trans. Elec. Dev., ED-25, 2 (1978) 180-193.
3. T. Miya, Y. Terunuma, T. Hosaka and T. Miyashita, Electron. lett., 15, (1979) 106-108.
4. R.D. Maurer, E. J. Schiel, S. Kronenberg and R. A. Lux, Appl. Opt., 12, 9 (1973) 2024-2026.
5. D. Botez and G. Herskowitz, Proc. IEEE, June (1980) 68.
6. R.F. Leheny, A. A. Ballman, J. C. Dewinter, R. E. Nahory and M. A. Pollack, J. of Electronic Matls. 9, 3 (1980) 561-567.
7. D.L. Rode, Phys. Status Solidi., A32 (1975) 425.
8. M.B. Small, J. M. Blum and R. M. Potenski, Appl. Phys. Letters, 30, (1977) 42.
9. G.B. Stringfellow, Ann. Rev. Mater. Sci., 88, (1978) 73.
10. H. Heinecke, E. Veuhoff, N. Putz, M. Heyen and P. Balk, J. of Electronic Matls., 13, 5 (1984) 815.
11. M.R. Leys and H. Veenvliet, J. Crystal Growth, 55, (1981) 145.
12. D.H. Reep and S. K. Ghandhi, J. Electrochem Soc., 130, (1983) 675.
13. H. Krautle, H. Roehle, A. Escobosa and H. Beneking, J. Electronic Matls., 12, (1983) 675.
14. M. Koppitz, O. Vestavik, W. Pletschen, A. Mircea, M. Heyen and W. Richter, J. Crystal Growth, 68, (1984) 136.
15. R.H. Moss, J. Crystal Growth, 68, (1984) 78.

16. H.M. Manasevit and W.I. Simpson, J. Electrochem. Soc., 120, (1973) 135.

17. J.S. Whiteley, Phd Dissertation, Rensselaer Polytechnic Institute, Troy , New York, (1983).

18. G.E. Coates, M.L.H. Green, P. Powell and K. Wade, "Principles of Organometallic Chemistry", Chapman and Hall, London, (1970) 38-40.

19. J.P. Maher and D.F. Evans, Proc. Chem. Soc., (1961) 208.

20. S.P. Denbaars, B.Y. Maa, P.D. Dapkus, A.D. Danner and H.C. Lee, J. Crystal Growth, 77, (1986) 188-193.

21. M. Mashita, S. Horiguchi, M. Shimazu, K. Kamon, M. Mihara and M. Ishii, J. Crystal Growth, 77, (1986) 194-199.

22. M. Yoshida and H. Watanabe, J. Electrochem Soc., 132, 3 (1985) 677-679.

23. D.J. Meyer and T.J. Anderson, RADC-TR 85-224 Interim Report Dec. 1985.

24. J.E. Butler, N. Bottka, R.S. Sillmon and D.K. Gaskill, J. Crystal Growth, 77, (1986) 163-171.

25. M. Tirtowidjojo and R. Pollard, J. Crystal Growth, 77, (1986) 200-209.

26. G.B. Stringfellow, J. Crystal Growth, 68, (1984) 111.

27. D.H. Reep and S.K. Ghandhi, J. Electrochem. Soc., 130 (1983) 675.

28. J.P. Hirtz, M. Razeghi, M. Bonnet and J.P. Duchemin, GaInAsP alloy Semiconductors, ed. T.P. Pearsell, (1982) John Wiley & Sons Ltd.

29. S.K. Shastry, Phd dissertation (1982) Rensselaer Polytechnic Institute Troy, New York, (1982).

30. M.G. Jacko and S.J.W. Price, Canad. J. of Chem., 41, (1963) 1560-1567.

31. M.G. Jacko and S.J.W Price, Canadi. J. of Chem., 42, (1964) 1198.

32. H. Schlichting, Boundary Layer Theory, 7th Edition , (1979) McGraw Hill.

33. G.B. Stringfellow, Proceedings Third Biennial OMVPE Workshop Sept 21 (1987) Brewster Mass.

34. M. Tamir, A. Gabriel, C. Chatillon and I. Ansara, J.Crystal Growth, 69, (1984) 421-441.

35. J. P. Agnello and S.K. Ghandhi, J. Crystal Grrowth, 73, (1985) 453-459.

APPENDIX A

A MASS SPECTROMETRIC STUDY OF THE REACTION OF TRIETHYLINDIUM WITH ARSINE GAS

Paul D. Agnello

Sorab K. Ghandhi

Electrical, Computer, and Systems Engineering Department

Rensselaer Polytechnic Institute

Troy, New York 12180

Submitted to the Electrochemical Society

Point of Contact:

S.K. Ghandhi - (518) 276-6085

SK/87.1

June 11, 1987

ABSTRACT

A study of the premature room temperature gas-phase reactions involved in the growth of GaInAs using Et_3In, Me_3Ga and AsH_3 was undertaken, using a specially designed mass spectrometer sampling system on a conventional, low pressure OMVPE reactor. It was shown that the reaction of the Et_3In- AsH_3 mixture could be described by reversible bimolecular reaction kinetics within the limits of experimental error, and evidence for an adduct is presented. The equilibrium constant for this system was determined as 30 torr; the rates of forward and reverse reaction were 5 $(torr\text{-}sec)^{-1}$ and 0.15 sec^{-1} respectively. The implications of the reaction of this organometallic source with arsine on the growth mechanism is discussed in this paper.

INTRODUCTION

The growth of high quality GaInAs films is of considerable interest because of the usefulness of this material in fiber optic communications and in high speed devices. Here, the ternary alloy $Ga_{0.47}In_{0.53}As$ is lattice matched to InP, and is a useful material for sources and detectors in the 1.0 to 1.6 μm wavelength region [1], where silica fibers exhibit minimum loss. In addition, high electron mobility and high peak velocity at low electric fields [2, 3] make this material attractive for ultra fast digital applications.

Organometallic vapor phase epitaxy (OMVPE) is an important growth technique for these applications because extremely thin layers with abrupt composition and doping changes are readily achievable [4]. Further, this method lends itself to large scale commercial applications [5]. However, the growth of indium containing compounds by OMVPE is complicated by a room temperature, parasitic reaction between the indium-bearing species and the column V hydride, resulting in depletion of this reactant. Previous work with triethylindium (Et_3In) has shown [6, 7] that this reaction results in the formation of low vapor pressure reaction products, which produce wall deposits, accompanied by the general deterioration of crystal quality. These problems increase with increasing indium content in the grown materials, especially for $Ga_{1-x}In_xAs$ with $x > 0.25$ [8]. However, device quality material has been grown with $x = 0.53$, by suitable attention to reactor details [9]. Some workers have used trimethylindium (Me_3In), a high vapor pressure solid, as an alternate indium source [10] in order to reduce these problems. Nonetheless, Et_3In is preferred by others [11] for its ease of handling, and some of the best reported material has been grown from this source [12].

The work described here was undertaken to study the premature reactions involved in the growth of GaInAs using Et_3In, Me_3Ga and arsine (AsH_3) gas, and to obtain kinetic data which can be incorporated in a growth model. Previous studies of other organometallic sources by IR spectroscopy [13, 14], UV atomic absorption spectrometry

[15, 16] and mass spectrometry [17, 18] have been productive, but not always meaningful or useful due to the details of the sampling techniques and the ultimate sensitivity of the spectroscopic method used. None of these works have examined reaction kinetics. We have chosen to study the gas phase reactions using a mass spectrometer because of the excellent sensitivity of this technique. Moreover, we have designed a fast sampling system which enables us to study the kinetics of the gas phase reactions in a practical reactor configuration, without significantly altering the growth conditions and with high spatial resolution.

Early studies [19, 20] have attempted to determine kinetic data for the Et_3In-AsH_3 reaction from the composition of $Ga_{1-x}In_xAs$ layers grown under different reactor conditions. They have assumed that a complex is formed by the reaction:

$$Et_3In(g) + AsH_3(g) \rightarrow \text{Complex}(s) \qquad (1)$$

and have solved for the layer composition as a function of reactant partial pressures, describing the effect of this reaction by a single phenomenological parameter that depends strongly on the flow geometries and reactor conditions for which it was determined. This approach is highly machine-specific, and does not identify the underlying mechanism. In these studies, values obtained for this parameter differ by an order of magnitude, so that it is not possible to use the result to model the growth in a different reactor. In contrast, the utility of our approach is that kinetic data can be obtained which is applicable to any reactor geometry because it is representative of the basic underlying mechanism. To our knowledge, this represents the first direct study of the reactions between Et_3In and AsH_3.

EXPERIMENTAL

A differentially pumped mass spectrometer sampling system has been installed on a conventional low pressure OMVPE GaInAs epitaxial reactor for studying the room tem-

perature Lewis acid-base interactions in the reactant gases under typical growth conditions. The reaction chamber consists of a 50 mm I.D. quartz tube. A small diameter silica capillary (150 μm I.D., 250 μm O.D. and 300 mm long) is used as a probe. This capillary is introduced into the system from the gas inlet end by means of a flexible stainless steel bellows, which allows its position to be changed within the reaction chamber. The exit end of the capillary impinges on an orifice, 100 μm in diameter, in a skimmer chamber which is held at 5×10^{-3} torr by means of a roughing pump with a molecular sieve trap.

A micromanipulator system is used to optimize the position of the capillary with respect to the orifice, which connects directly to the ionization chamber of a UTI model 100C mass spectrometer. This spectrometer is enclosed in a bakeable stainless steel vacuum chamber, evacuated by a 150 ℓ/sec turbo molecular pump. An ultimate pressure of under 10^{-8} torr is achievable in this manner. The mass spectrometer is equipped with both an electron multiplier and a Faraday cup, and can scan over a range from 1 AMU through 300 AMU in 75 μsecs. The rated sensitivity of the unit is 10^{-14} torr Nitrogen, and the ionization energy is 70 eV. A schematic diagram of the measurement system is shown in Fig. 1.

The differentially pumped sampling system was designed for a transit time of less than 0.2 seconds, so that sampled gases are subjected to a minimum of interactions while in transit. In an ideal sampling system, no interactions should occur between the point of gas sampling and the detector. This would require a line of sight sampling system, which must also allow for the pressure to drop from the reactor pressure (near atmospheric) to the spectrometer operating pressures of about 10^{-6} torr. Such a system is, by its very nature, large and obtrusive, and would significantly alter conditions in the epitaxial reactor from those encountered during actual growth. For this reason, we designed our system with a small diameter capillary to sample the gases and used a differ-

entially pumped scheme to minimize the transit time. The flow through the capillary is viscous, so gas -gas interactions do take place. These interactions are the same as those occurring in the reactor, but over a shorter period of time.

Abrupt plugging of the capillary presented a problem from time to time; in fact, it had to be replaced on occasion during the course of this work. Other workers [21] have used a plug of quartz wool to avoid this problem. Unfortunately, this greatly increases the transit time in the sampling system, as well as the surface area of the sampling path. Consequently, we considered it inappropriate for our work.

We have considered the possibility that surface catalyzed reactions in the capillary may have a significant effect on interpretation of our results, especially in the light of prior work [22, 23]. We note, however, that past experiments involved [22] long intervals of time compared to the transit time in our system, or concentrations well in excess of those used for conventional epitaxial growth [23]. Moreover, our work will show that the extent of reaction changes significantly as a function of probe position in the reaction chamber even though the probe length is unaltered. Thus we do not expect that surface catalysis plays a significant role in the adduct formation reaction.

During the growth of GaInAs, we have noted the formation of an extremely thin, light brown, optically transparent film of polymeric material on a tube liner in front of the susceptor. It is possible that the inside surface of the capillary becomes similarly coated during the sampling process.

Once the gases exit the capillary, about 90% are pumped away in the skimmer chamber. The remainder pass through the orifice into the mass spectrometer chamber where the pressure is low enough so that further interactions are unlikely. The possibility of clustering due to adiabatic expansion of gases through the orifice was investigated by varying the skimmer chamber pressure for a constant set of reactor conditions. If the apparent alkyl-hydride reaction was actually caused by the formation of clusters due to

the adiabatic expansion of gases passing through the orifice, then variations in the skimmer chamber pressure should affect a change in the extent of reaction. No change was found, indicating that clustering is not a problem in this system. Furthermore, observed variations in the extent of the Et_3In-AsH_3 reaction as a function of probe position cannot be attributed to any sampling system artifact because the sampling system is unchanged.

Typical GaInAs growth parameters we have used in our OMVPE reactor are as follows: a total gas flow of 6 slm hydrogen at 152 torr with partial pressures of 0.01 torr each of Me_3Ga and Et_3In and 0.75 torr of arsine gas, and a growth temperature of 600-650°C. We have found that excellent material, as evidenced by mirror-like surfaces, a compositional uniformity of ± 0.01 over 2.5 cm $\times$ 2.5 cm layers, and an electron mobility above 10,000 cm^2/V-sec at room temperature, can be grown under these conditions. Furthermore, the tube liner experienced no weight gain after a run, indicating that the wall deposits were negligible, and that indium depletion is not a serious problem.

In this study, worst case growth conditions were investigated. A total flow of 3 slm of hydrogen was used with as much as 0.13 torr of Et_3In and up to 3.04 torr AsH_3 in some experiments. The lower total flow and higher reactant partial pressures increase the extent of the reaction and improve the signal to noise ratio in the mass spectrometer, thus enabling more accurate observations to be made over a wide range of arsine pressures.

OMVPE growth is typically carried out in a cold wall reactor so that we can expect a highly non-uniform temperature profile. Consequently, we have made measurements of gas temperature in our system under typical growth conditions. Our results show that the temperature remains constant, and close to room temperature, until within 0.5 cm upstream of the susceptor surface. This result is similar to that calculated and measured for comparable susceptor geometries and methods of heating [24, 25]. As a result, the

measurements reported here have been made with a cold susceptor. Nonetheless, some experiments were made with a r.f. heated susceptor to ensure that results were independent of its temperature.

RESULTS AND DISCUSSION

The reactions of alkyls with hydrides are uniquely different from alkyl-alkyl reactions, which are sometimes used for the growth of semiconducting compounds. Alkyl-hydride reactions often involve a smaller heat of formation than alkyl-alkyl reactions (typical values are 6 kcal/mole as compared to 20 kcal/mole), so that this quantity is difficult to measure by conventional methods. Moreover, the reaction products are usually metastable, and result in polymers by an alkyl elimination process. One objective of our study was to determine the equilibrium constants and the reaction rate constants for the Et_3In-AsH_3 reaction, which is important for the growth of GaInAs, and to use these data to make some meaningful conclusions about the reaction mechanism. These data can be used in a growth model which incorporates pre- reaction effects, and is thus suitable for predicting layer growth over large diameter slices.

The fragmentation patterns of the reactant species were first determined individually. Figure 2 shows the pattern for Et_3In, with the background signals subtracted for clarity. Here, the signal amplitudes were found to be linear, down to 10% of the Et_3In pressures used in this study. The $MeIn^+$, Me_2In^+ and $EtMeIn^+$ signals seen here are a result of the fragmentation process in the ionization chamber. (The fragmentation pattern for AsH_3 is not shown since it has been published [21, 26] elsewhere.) In our study, a fragment of the organometallic compound with a strong signal was monitored as a function of time, as the AsH_3 was introduced into the reactor. Changes in its magnitude can be attributed in part to a reaction between the organometallic species and the arsine, and in part to a dilution of the gases in the reactor upon the addition of the arsine. The effect of dilution was accounted for in all of the data presented in this paper.

Two complications arise in the interpretation of mass spectrometric data. First, the observed turn on and turn off transients for the organometallic species are a strong function of adsorption and desorption phenomena in the reactor and in the mass spectrometer, and depend greatly on the past history of the experiment. This is especially true for ethyl compounds such as Et_3In and Et_3Ga. By way of example, Fig. 3 shows a series of plots of the Et_2In^+ fragment, taken in a clean system (reactor and capillary) for a constant input partial pressure of Et_3In. Note that the immediate drop in the signal, once the AsH_3 is introduced, is modified by adsorption phenomena from run to run, but that the steady state extent of reaction is the same in all cases. In order to determine the reaction rate, it was necessary to determine the steady state extent of the reaction at various distances down the reactor. This was related to the time the reactants have spent together, and the rate constants determined in this manner.

A second complication arises from the nature of the detection scheme. In order to study the reaction of the various organometallic compounds we must monitor a daughter fragment which produces a large signal to ensure sufficient sensitivity. The largest daughter fragment is usually the di-alkyl metal for column III organometallic compounds. If the product formed by the reaction of the organometallic compound with arsine <u>also</u> fragments to the same di-alkyl metal, then its signal would not represent the amount of unreacted compound, so that the extent of reaction would be underestimated.

In the case of the Et_3In-AsH_3 reaction, the diethlyindium (Et_2In^+) fragment was found to drop to approximately zero under conditions of large AsH_3 excess, indicating that the reaction product does not fragment to Et_2In^+. We conclude that the Et_2In^+ signal represents the Et_3In remaining in the reactor.

We are now able to plot the organometallic compound Et_3In remaining in the reactor in steady state as a function of the distance from the entrance region of the reactor. From the average gas velocity, this distance may be converted into time. Figure 4

shows the Et_3In remaining in the reactor in steady state, as measured by comparing the Et_2In^+ fragment before and after the addition of AsH_3, as a function of arsine pressure and with distance from the inlet as a parameter.

This data leads us to several conclusions. First, the data taken at 6.5 and 9.5 cm from the reactor inlet are nearly identical; however, the Et_3In has not been fully consumed for AsH_3 pressures up to 10 times the Et_3In pressure. From this we conclude that an equilibrium has been attained between the reactants and the products by the time they have travelled 6.5 cm down the reactor, i.e., within 0.5 seconds upon mixing. Second, we note that the amount of Et_3In involved in the reaction is always less than or equal to the amount of arsine present, even at low pressures of AsH_3 where there is an excess of Et_3In. This strongly indicates that the reaction product forms as a l:n ratio of Et_3In to AsH_3, where n = 1, 2, 3....

Two observations lead us to conclude that the product is a 1:1 adduct of Et_3In and AsH_3. First, weak yet measurable signals were noted at 275 and 261 AMU when AsH_3 and Et_3In were mixed, as seen in Fig. 5. These signals change with probe position and cannot be attributed to any aspect of the sampling system. The signal at 275 AMU is probably the adduct (which has a mass of 280 AMU), with some deficit hydrogen atoms. The peak at 261 AMU is probably a daughter fragment of the adduct minus a hydrocarbon group and a few hydrogen atoms. (The ionization process can readily explain such losses.) Second, the AsH^+ and AsH_3^+ signals were found to increase about 5% when Et_3In was added to AsH_3. This implies the creation of a larger molecule that also has both AsH^+ and AsH_3^+ as fragments. Taken together, these represent strong evidence that the product is the 1:1 adduct of Et_3In and AsH_3.

An important additional observation made during these runs was that wall deposits were very slight and of uniform optical density along the entire 40 cm length of the reactor tube. This indicates that the adduct has a high vapor pressure, for the growth con-

ditions we have used in our work.

We assume that the reaction is of the form:

$$Et_3In(g) + AsH_3(g) \rightleftharpoons \text{Adduct}(g) \tag{2}$$

We have taken this reaction to be reversible as mentioned earlier because the extent of reaction did not seem to change when the probe was moved from 6.5 to 9.0 cm from the inlet, as shown in Fig. 4. For this reaction, the measured equilibrium amount of Et_3In consumed versus P_{AsH_3} can be simulated closely if we assume an equilibrium constant of 30 $torr^{-1}$. Based on this value the calculated equilibrium is represented by the heavy curve in the figure.

Figure 6 is a plot of the Et_3In remaining in steady state as a function of distance travelled down the reactor, for different arsine pressures. Note that these curves appear to originate from some point less than zero on the distance axis. This is because the gases are together for a short period of time in the mixing region, and before entry into the reactor. We estimate this time to be approximately 0.05 sec.

The Integral Method [27] can be used to determine the kinetic data, if we assume a mechanism for the Et_3In-AsH_3 reaction. In the interests of simplicity we will assume that Eq. 2 represents an elementary, reversible, bimolecular reaction whose reaction rate is given by:

$$\frac{d(P_{Et_3In})}{dt} = -k_2(P_{Et_3In})(P_{AsH_3}) + k_{-1}(P_{Adduct}) \tag{3}$$

where k_2 is the rate of forward bimolecular reaction, and k_{-1} is the rate of reverse monomolecular reaction. Substituting $A=P_{Et_3In}$, $B=P_{AsH_3}$, $x=P_{Adduct}$ and A_o, B_o as the initial reactant concentrations of A, B respectively gives:

$$\frac{dx}{dt} = \frac{d(P_{Adduct})}{dt} = -\frac{d(P_{Et_3In})}{dt} \tag{4}$$

$$\frac{dx}{dt} = k_2(A_0 - x)(B_o - x) - k_{-1}x \tag{5}$$

This can be rearranged as:

$$k_2 t = \int_0^{x_1} \frac{dx}{x^2 - (A_o + B_o + \frac{1}{K_{eq}})x + A_o B_o} \tag{6}$$

where $K_{eq} = k_2/k_{-1}$. Integrating, and taking the real value gives:

$$k_2 t = \left[\frac{1}{A_o - B_o + \frac{1}{K_{eq}}} ln\left[\left(\frac{x - A_o - \frac{1}{K_{eq}}}{x - B_o}\right)\left(\frac{B_o}{A_o + \frac{1}{K_{eq}}}\right)\right]\right] \tag{7}$$

$$k_2 t \triangleq C$$

This function is calculated at different times, for different input partial ressures, from the data of Fig. 6. Correcting for the mixing time of 0.05 secs., all curves were straight lines going on the origin. The slopes of these lines in each case gave the value of k_2 for a specific AsH_3 partial pressure.

Figure 7 shows the value of k_2 as a function of P_{AsH_3} values used in our experiments. Here, we note that the average value increases with reduced arsine pressure but so does the scatter. One possible explanation for this behavior is that the actual Et_3In-AsH_3 reaction is considerably more complex than the elementary, reversible, bimolecular reaction assumed for this analysis. We note, however, that the measurement equipment (digital mass flow controllers and UTI mass spectrometer) have significant instrument error at low flow rates and low measurement levels. Thus, data taken at low values of P_{AsH_3} is of questionable accuracy; it therefore serves no useful purpose to propose a more complex mechanism for this reaction, based on this data. With this in mind, we

adopt the k_2 value which is constant at the higher arsine pressures as the correct one for this reaction. The constant value of k_2, consistent over the entire range, is $k_2 = 5.0 \pm 1.0$ (torr - sec)$^{-1}$; as indicated by the dotted lines in the figure. Using this value, the value for k_{-1} is calculated as 0.17 sec^{-1}.

At this point, it should be mentioned that attempts were made to fit the data to an elementary irreversible bimolecular reaction, an elementary reversible bimolecular reaction with a fraction of the product taken as an inert solid, and a reversible bimolecular reaction with a constant vapor pressure of product in equilibrium with the solid. All of these forms provided a poorer fit to the data, further supporting our assumption of an elementary bimolecular reversible reaction.

From the previously determined equilibrium and reaction rate constants, we can now calculate the extent of reaction under any growth conditions. Equation (7) can be rearranged as:

$$x = \left[\frac{A_o - B_o + \frac{1}{K_{eq}}}{2}\left(\frac{1+f}{1-f}\right) + \frac{A_o + B_o + \frac{1}{K_{eq}}}{2}\right] \tag{8}$$

where f is given by:

$$f = exp\left[k_2 t\left(A_o - B_o + \frac{1}{K_{eq}}\right) + ln\left(\frac{A_o + \frac{1}{K_{eq}}}{B_o}\right)\right] \tag{9}$$

For typical growth conditions, a plot of adduct concentration versus distance down the reactor is shown in Fig. 8 for the same set of inlet flows but for different reactor pressures. A comparison of these curves demonstrates that the adduct reaction is almost complete in both situations. In experiments with the growth of GaInAs in our system, we have noted that operation at atmospheric pressure results in the formation of massive deposits ahead of the susceptor, and poor quality material. At 0.2 atm, however, the front of the reaction chamber is almost totally free of these products, resulting in high quality GaInAs layers. We conclude that the reduction of transit time by a factor

of 5, by operation at low pressure, primarily reduces the formation of polymers by alkyl elimination, so that growth proceeds from the adduct.

GENERAL COMMENTS

Our measurements emphasize that, for the Et_3In-AsH_3 reaction, growth occurs by the dissociation of an adduct in the thermal boundary layer. The rate of formation of this adduct, its vapor pressure, and its degree of dissociation at the growth temperature are all factors which must be considered in the growth process. Finally, alkyl elmination, leading to polymer formation, presents an adverse possibility which must be minimized for the growth of high quality material. For the Et_3In-AsH_3 reaction, K_{eq}=30 $torr^{-1}$, which corresponds to a heat of formation of 6.0 kcal/mole. Thus growth at 650°C involves almost complete dissociation of this product. This is in contrast to growth from the Me_3In-Me_3P adduct, where the heat of formation is 17 kcal/mole [28].

It is likely that the Me_3In-AsH_3 reaction proceeds at a faster rate and to a similar extent as the Et_3In-AsH_3 reaction. However, the resulting adduct would probably have a higher vapor pressure due to the smaller alkyl groups; in addition, the rate of polymer formation would have to be lower in order to achieve satisfactory growth at atmospheric pressure. Certainly, further work is required to establish if this is indeed the case.

CONCLUSION

We have used a specially designed mass spectrometer sampling system, in conjunction with a conventional low pressure OMVPE reactor to study, for the first time, the kinetics of the room temperature reaction of Et_3In-AsH_3. The reaction achieved equilibrium and was therefore considered to be reversible. The equilibrium constants for the Et_3In-AsH_3 reaction was 30 $torr^{-1}$. This reaction went to completion within 0.6 seconds of exposure to the higher pressures of arsine used in the study. Strong evidence was presented that the Et_3In-AsH_3 reaction product is a 1:1 adduct. In addition, mass spectrometer peaks near the expected mass of the adduct were observed, and further support

our arguments for adduct formation.

Using the Integral Method of analysis, and assuming that the Et_3In-AsH_3 system can be described by an elementary bimolecular reversible reaction, resulted in a good fit and the forward reaction rate constant was determined as 5 ± 1 $(torr\text{-}sec)^{-1}$. The equilibrium and forward reaction rate constants were used to calculate the extent of the reaction during typical atmospheric and reduced pressure growth conditions.

ACKNOWLEDGEMENT

The authors would like to thank J. Barthel for technical assistance, P. Magilligan for manuscript preparation, and M. Sherwin for computer reduction of the data. Technical discussions with Prof. J. Hudson, Dr. K. Jones and Mr. P. Chinoy were most helpful, and are greatly appreciated. This work was supported by Contract No. XL-5-05018-2 from the Solar Energy Research Institute, Golden, CO and by Contract No. F19628-84-C-0066 from the Air Force, through DEVCOM, Inc. Additional funds were provided by Agreement No. 970- ERER-ER-87 from the New York State Energy Research and Development Authority (NYSERDA). This support is hereby acknowledged.

REFERENCES

1. Y. Matsubhima and K. Sakai, GaInAsP Alloy Semiconductors, Ed. T.P. Pearsall (Wiley, 1982), pp. 413-436.
2. Y. Takeda, A. Sasaki, Y. Imamura and T. Takagi, J. Appl. Phys., 47, (1976) 5405.
3. T.H. Windhorn, L.W. Cook, and G.E. Stillman, IEEE Electron Device Lett., EDL-3, (1982) 18.
4. M. Razeghi, J.P. Hirtz, U.O. Ziemelis, C. Delalande, B. Etienne and M. Voos, Appl. Phys. Lett., 43, (1983) 585.
5. J.L. Tandon and Y.C.M. Yeh, J. Electrochem. Soc., 132, (1985) 662.
6. H.M. Manasevit and W.I. Simpson, J. Electrochem. Soc., 120 (1973) 135.
7. B.J. Baliga and S.K. Ghandhi, J. Electrochem. Soc., 121 (1974) 1642.
8. M.J. Ludowise, C.B. Cooper and R.R. Saxena, J. Elec. Matls., 10, (1981) 1051.
9. J.S. Whiteley and S.K. Ghandhi, Thin Solid Films, 104 (1983) 145.
10. A. Mircea, R. Azoulay, L. Dugrand, R. Mellet, K. Rao and M. Sacilotti, J. Electron. Mater., 13 (1984) 603.
11. M. Razeghi, M.A. Poisson, J.P. Larivain and J.P. Duchemin, J. Electron. Mater., 12 (1983) 371.
12. R. Saxena, V. Sardi, J. Oberstar, L. Hodge, M. Keever, G. Trott, K.L. Chen, and R. Moon, J. Crys. Growth, 77 (1986) 591.
13. M. Leys and H. Veenvliet, J. Crys. Growth, 55 (1981) 145.
14. J. Nishizawa and T. Kurabayashi, J. Electrochem. Soc., 130 (1983) 413.
15. J. Haigh and S. O'Brien, J. Crys. Growth, 67 (1984) 75.
16. J. Haigh and S. O'Brien, J. Crys. Growth, 68 (1984) 550.
17. M. Czerniak and B. Easton, J. Crys. Growth, 68, (1984) 128.
18. D. Squire, C.S. Dulcey and M.C. Lin, J. Vac. Sci. Technol., B3 (1985) 1513.
19. S. Whiteley and S.K. Ghandhi, J. Electrochem. Soc., 130 (1983) 1191.

20. K.L. Hess, D.L. Kasemset and P.D. Dapkus, J. Elect. Matls., 13, (1984) 779.

21. M. Yoshida, H. Watanabe and F. Uesugi, J. Electrochem. Soc., 132 (1985) 677.

22. C.H. Cheng, K.A. Jones and K.M. Motyl, J. Electron. Mater., 13 (1984) 703.

23. R. Didchenko, J.E. Alix and R.H. Toeniskoctter, J. Inorg. Nucl. Chem., 14 (1960) 35.

24. L.J. Giling, J. Electrochem. Soc., 129 (1982) 634.

25. M. Koppitz, O. Vestavik, W. Pletschen, A. Mircea, M. Heyen, and W. Richter, J. Crys. Growth, 68 (1984) 6.

26. H. Haspeklo, U. Konig, M. Heyen and H. Jurgensen, J. Crys. Growth, 77 (1986) 79.

27. P.W. Atkins, Physical Chemistry, W.H. Freeman & Co., San Francisco (1982).

28. G.E. Coates and R.W. Whitcombe, J. Chem. Soc., 3351 (1956).

FIGURES

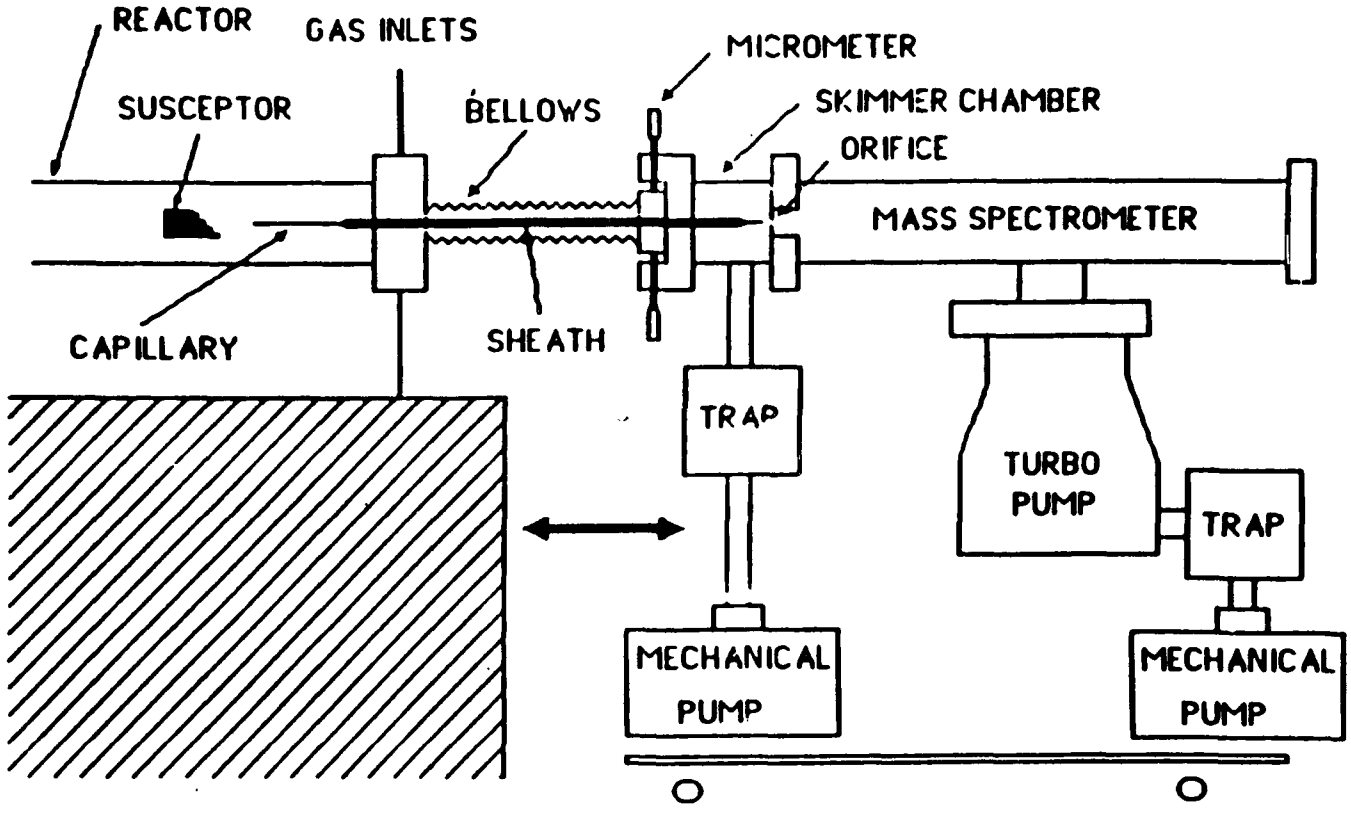
REACTOR
GAS INLETS
MICROMETER
SUSCEPTOR
BELLOWS
SKIMMER CHAMBER
ORIFICE
MASS SPECTROMETER
CAPILLARY
SHEATH
TRAP
TURBO PUMP
TRAP
MECHANICAL PUMP
MECHANICAL PUMP

FIGURE 1.

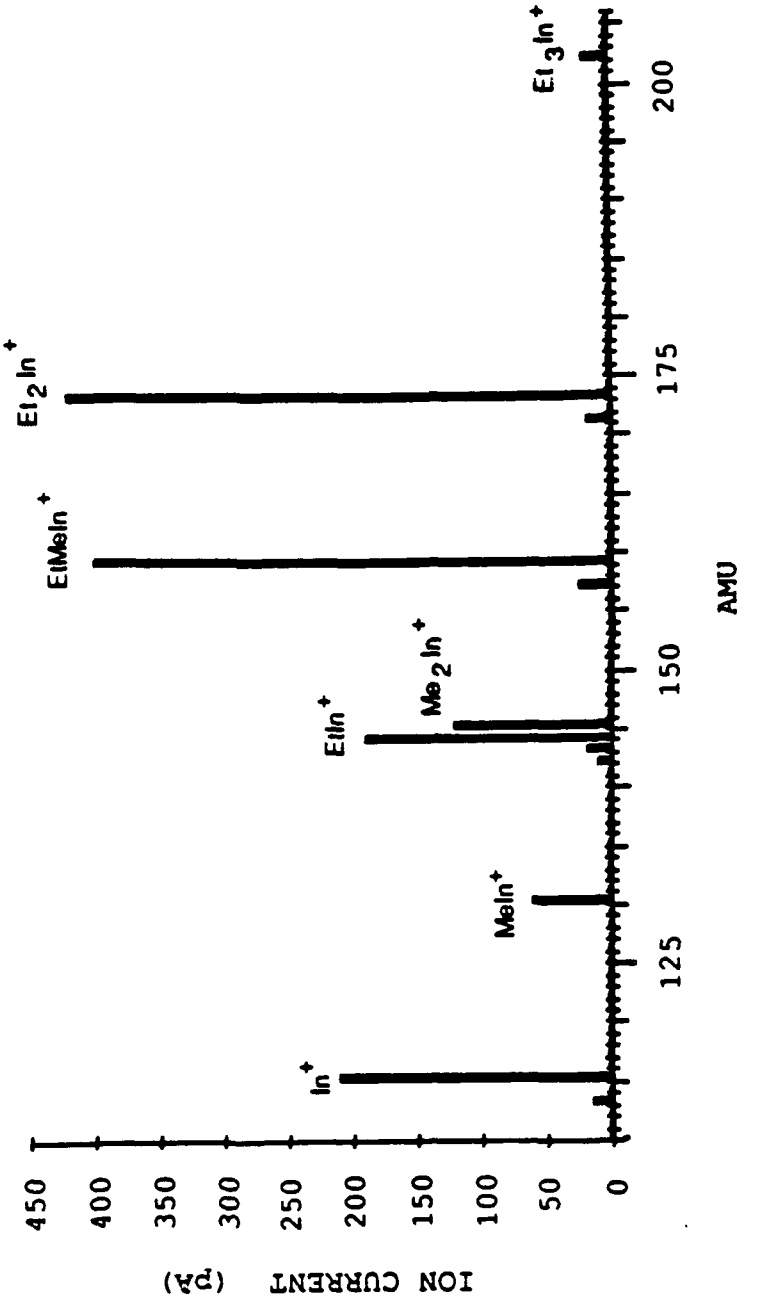
ION CURRENT (pA)
450
400
350
300
250
200
150
100
50
0
125
150
175
200
AMU
In+
MeIn+
EtIn+
Me2In+
EtMeIn+
Et2In+
Et3In+

FIGURE 2.

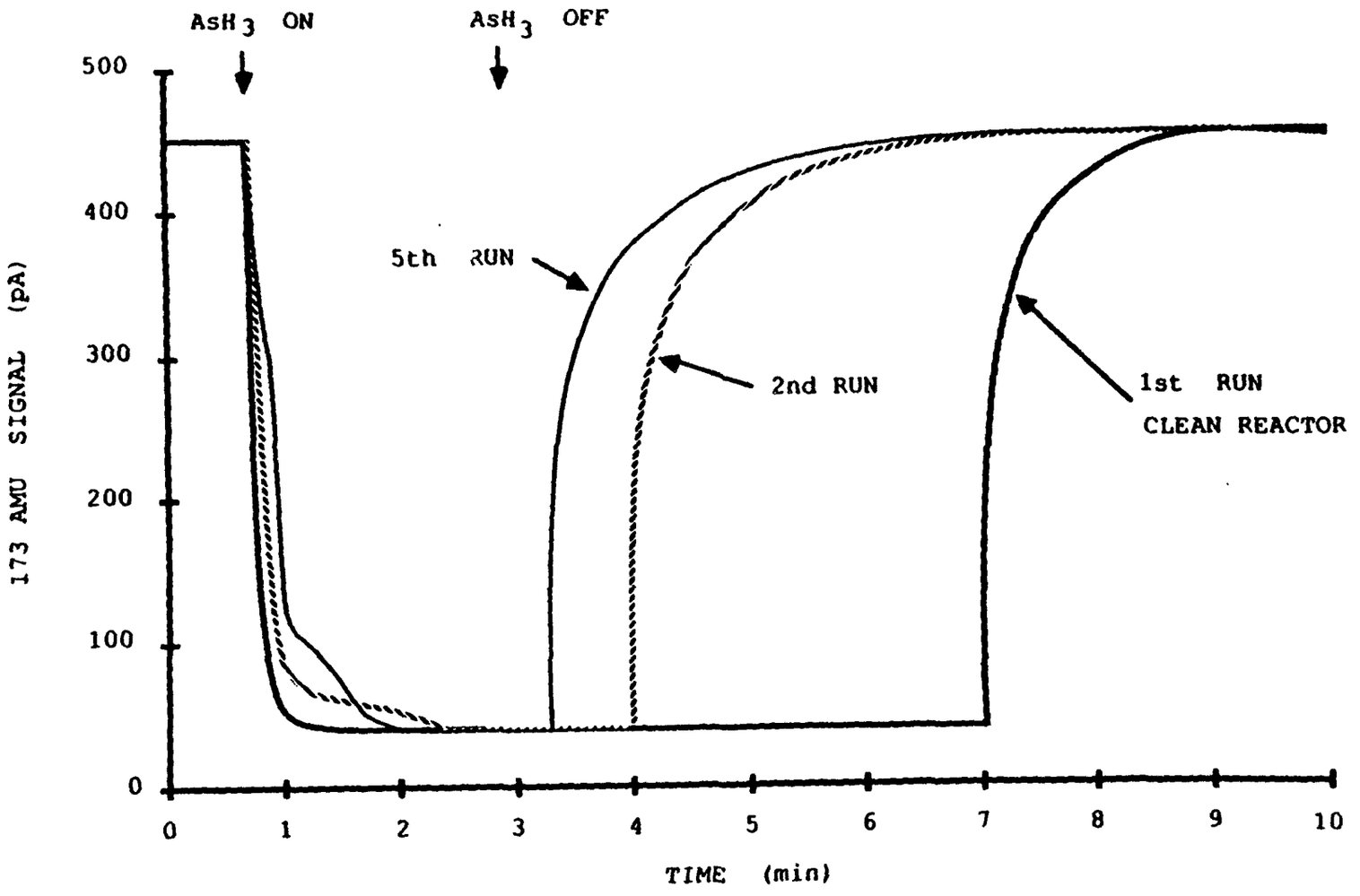
AsH3 ON
AsH3 OFF
500
400
300
200
100
0
173 AMU SIGNAL (pA)
5th RUN
2nd RUN
1st RUN
CLEAN REACTOR
0
1
2
3
4
5
6
7
8
9
10
TIME (min)

FIGURE 3.

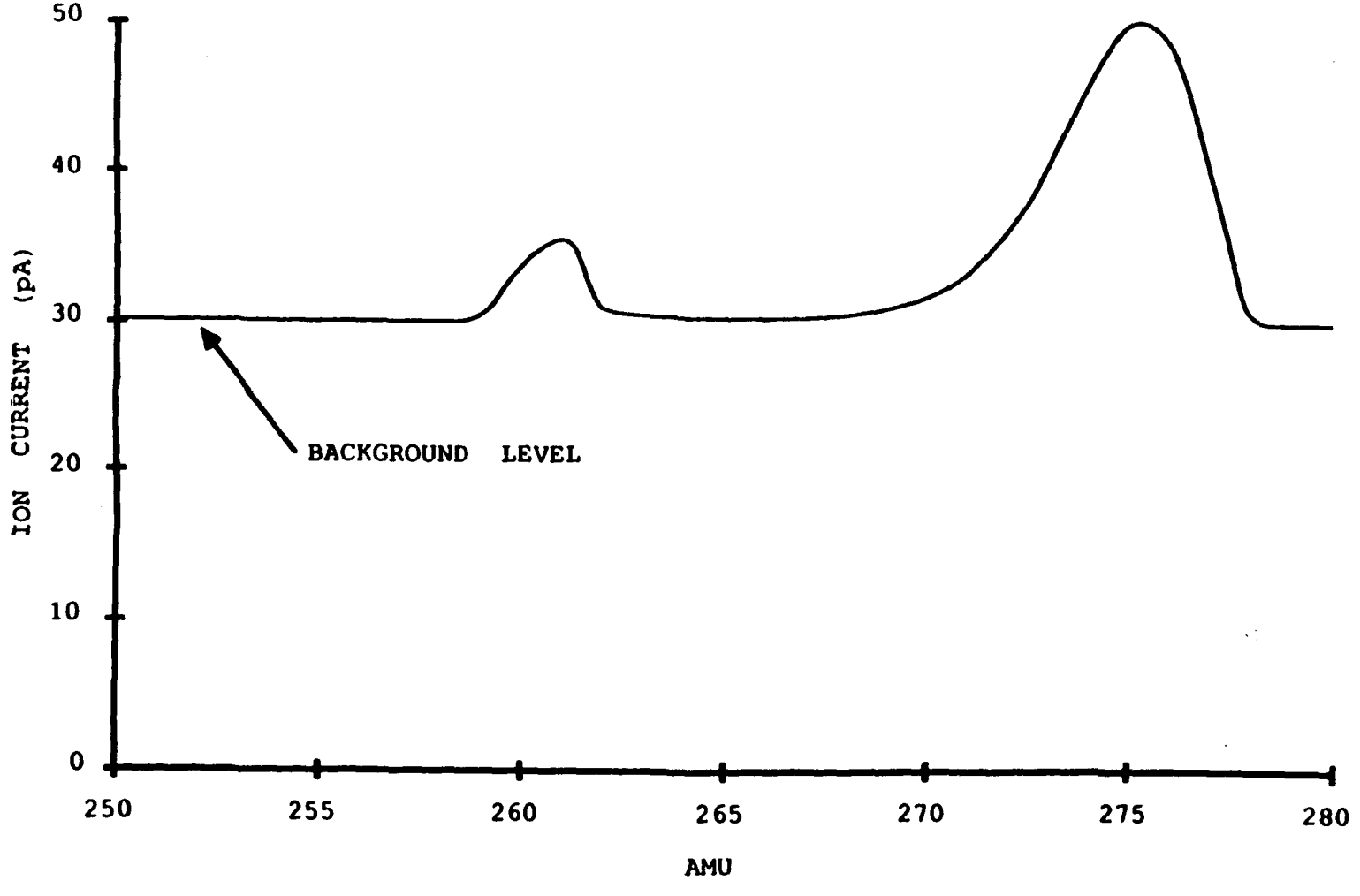
50
40
30
20
10
0
ION CURRENT (pA)
BACKGROUND LEVEL
250
255
260
265
270
275
280
AMU

FIGURE 4.

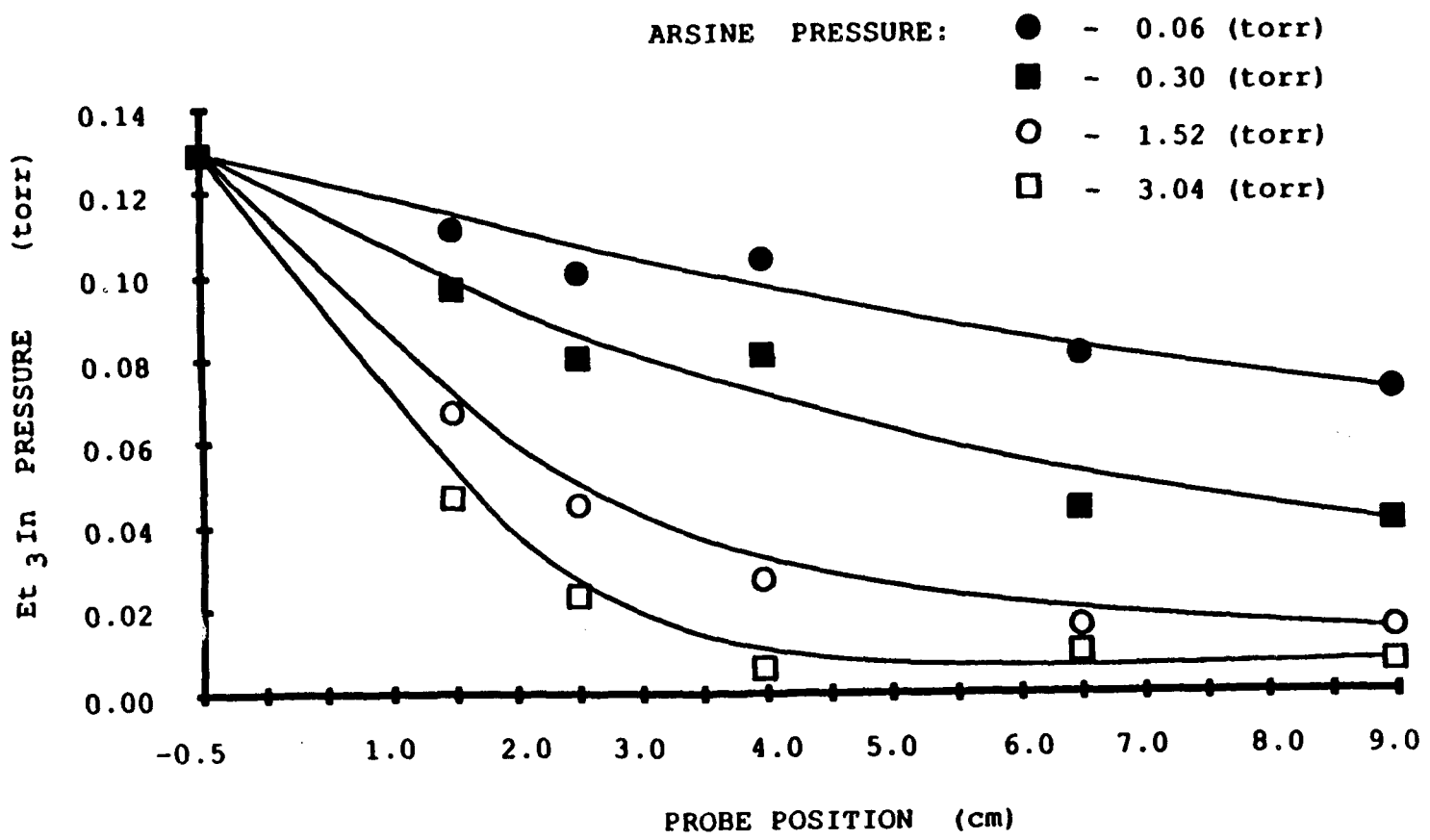
ARSINE PRESSURE:
● - 0.06 (torr)
■ - 0.30 (torr)
○ - 1.52 (torr)
□ - 3.04 (torr)
0.14
0.12
0.10
0.08
0.06
0.04
0.02
0.00
Et 3 In PRESSURE (torr)
-0.5
1.0
2.0
3.0
4.0
5.0
6.0
7.0
8.0
9.0
PROBE POSITION (cm)

FIGURE 5.

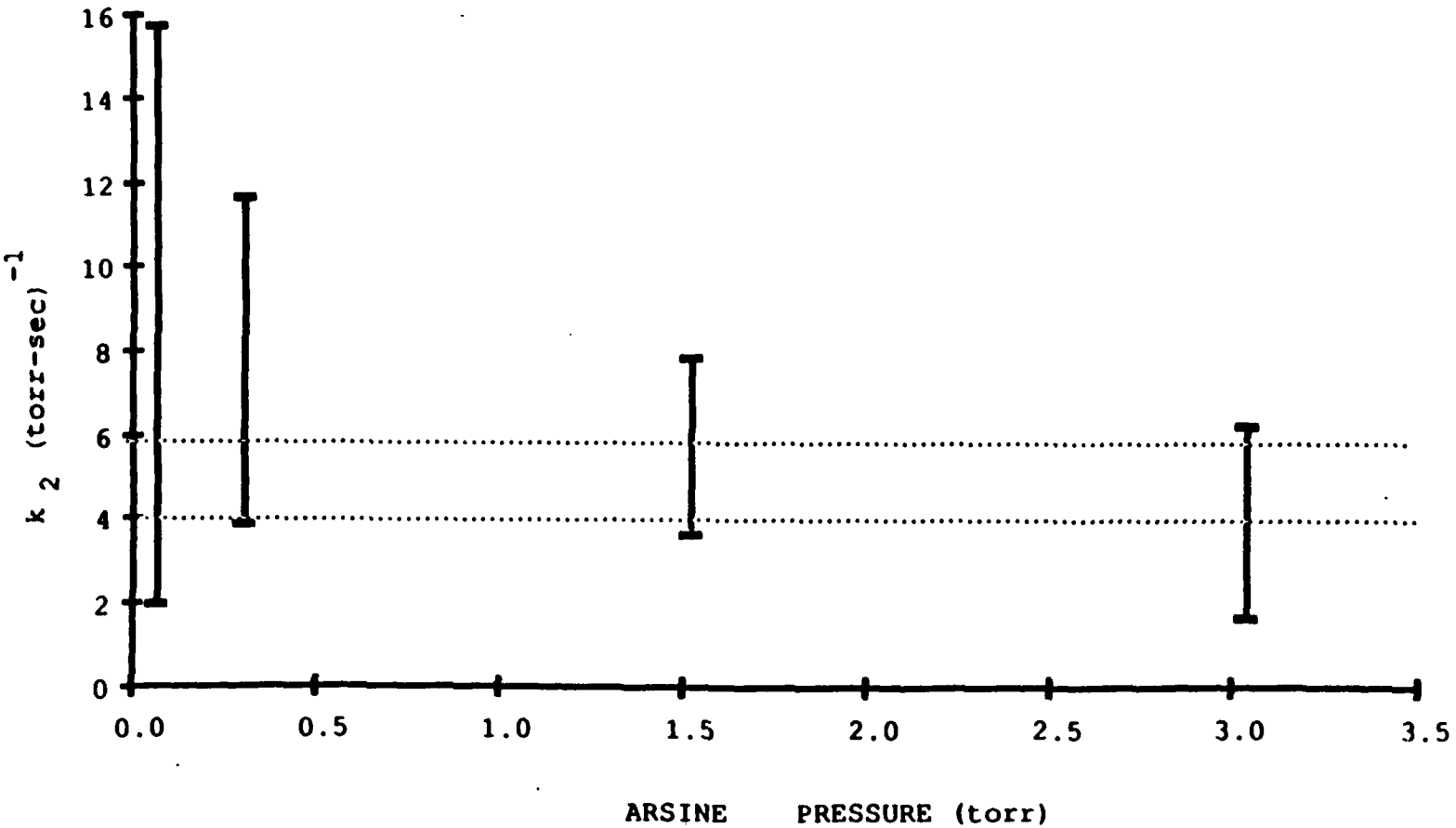
16
14
12
10
8
6
4
2
0
k_2 (torr-sec)$^{-1}$
0.0
0.5
1.0
1.5
2.0
2.5
3.0
3.5
ARSINE PRESSURE (torr)

FIGURE 6.

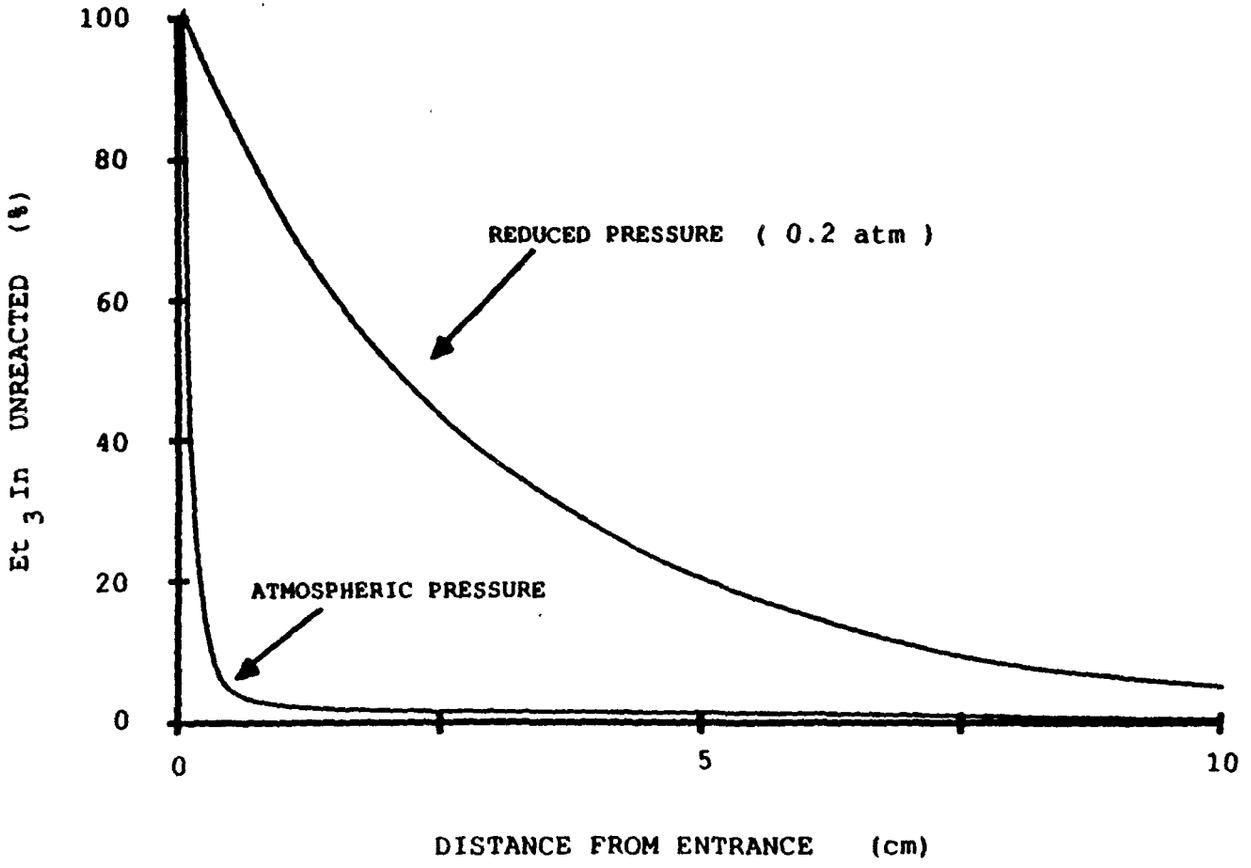
100
80
60
40
20
0
Et 3 In UNREACTED (%)
REDUCED PRESSURE (0.2 atm)
ATMOSPHERIC PRESSURE
0
5
10
DISTANCE FROM ENTRANCE (cm)

FIGURE 7.

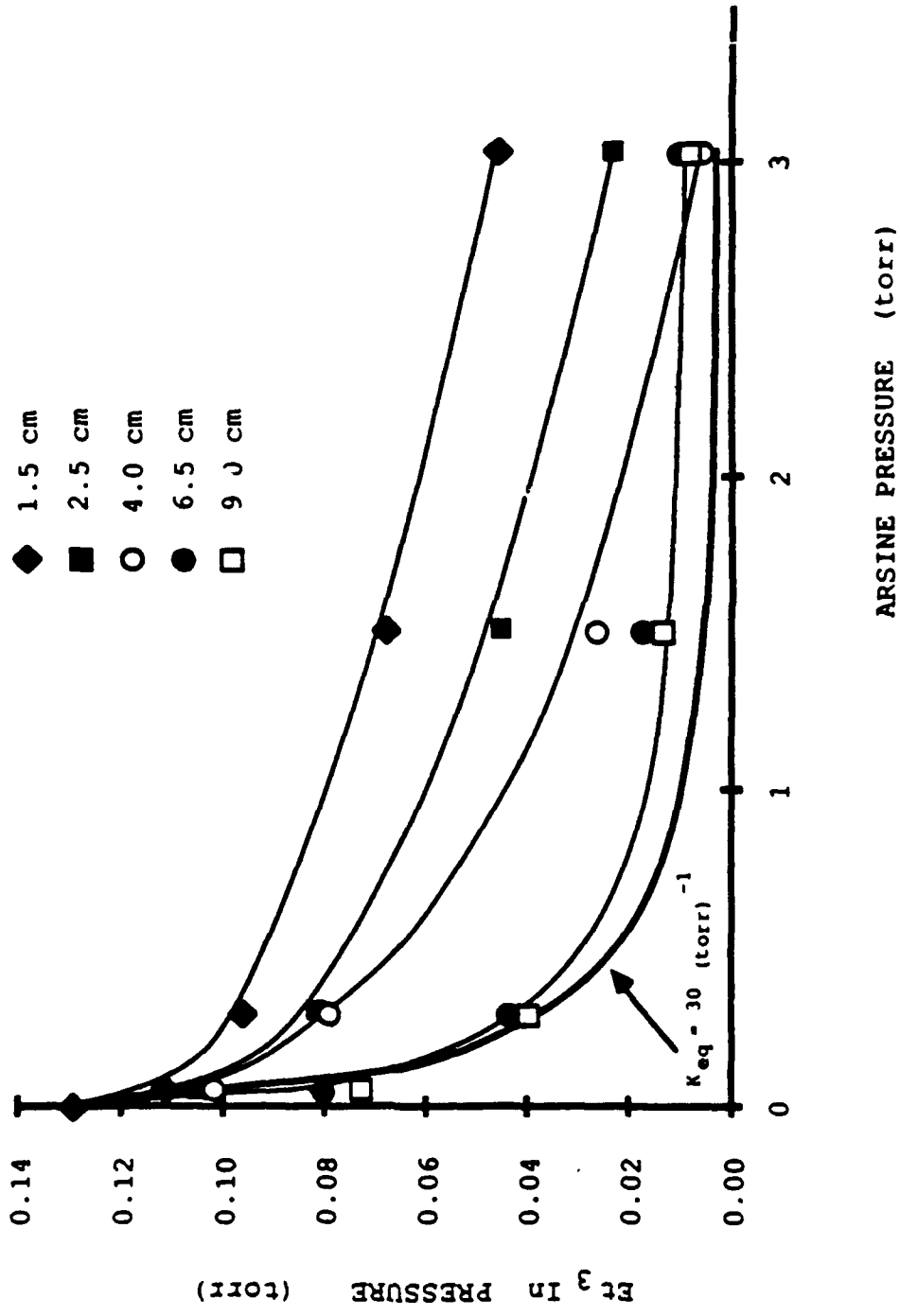
1.5 cm
2.5 cm
4.0 cm
6.5 cm
9 J cm
$K_{eq} = 30$ (torr)$^{-1}$
Et_3In PRESSURE (torr)
0.14
0.12
0.10
0.08
0.06
0.04
0.02
0.00
0
1
2
3
ARSINE PRESSURE (torr)

FIGURE 8.

APPENDIX B

A NOTE ON THE REACTION OF TRIMETHYLGALLIUM WITH ARSINE GAS

Paul D. Agnello

Sorab K. Ghandhi

Electrical, Computer, and Systems Engineering Department

Rensselaer Polytechnic Institute

Troy, New York 12180

Submitted to the Electrochemical Society

Point of Contact:

S.K. Ghandhi - (518) 276-6085

SK/87.23

July 17, 1987

ABSTRACT

The reaction of trimethylgallium (Me_3Ga) with arsine (AsH_3) was studied as part of an ongoing program of research in the growth mechanisms for compound semiconductors by organometallic vapor phase epitaxy. A differentially pumped mass spectrometer, with a sampling time of 0.2 seconds, was used in this study. The Me_3Ga-AsH_3 reaction was found to occur very rapidly at room temperature (under 0.2 secs); lower bounds for the equilibrium constant and the rate of forward reaction have been determined from these measurements.

INTRODUCTION

The work described here was undertaken as part of an ongoing study of the premature reactions involved in the growth of GaInAs using triethylindium (Et_3In), Me_3Ga and AsH_3 gas. A mass spectrometer was used because of its excellent sensitivity. Moreover, we have designed a differentially pumped, fast sampling system with a moveable probe, to study the kinetics of the gas phase reactions in a practical reactor configuration, without significantly altering the growth conditions and with high spatial resolution. This system has been installed on a conventional low pressure OMVPE GaInAs epitaxial reactor. Details of the system have been described elsewhere [1].

In our study, worst case growth conditions were investigated. A total flow of 3 slm of hydrogen at 152 torr was used with up to 0.02 torr of Me_3Ga, and up to 3.04 torr AsH_3 in some experiments.

RESULTS AND DISCUSSION

In our experiments, we noted that the observed turn on and turn off transients for the fragmentation signals from the organometallics species were a strong function of adsorption and desorption phenomena in the reactor and in the mass spectrometer, and depended on the past history of the experiment. This was especially true for the ethyl compounds Et_3In and Et_3Ga, but was not found to be a problem with Me_3Ga, and highly repeatable transients were observed.

A complication in the interpretation of mass spectrometric data arises from the nature of the detection scheme, which requires the monitoring of a daughter fragment. If the product formed by the reaction of the organometallic compound with arsine also fragments to the same daughter fragment, then its signal does not represent the amount of unreacted compound, so that the extent of reaction is underestimated.

For the Me_3Ga-AsH_3 reaction, the dimethylgallium ion (Me_2Ga^+) was monitored. This signal never drops completely to zero, regardless of probe position and/or AsH_3

overpressure. Moreover, from Table I, we note that the fragmentation pattern of the Me_3Ga-AsH_3 reaction shows a small increase in the signals associated with Ga^+ (69 AMU) and its isotope at 71 AMU. Otherwise, there is little difference in the proportions of other fragmentation products, despite the fact that the total signal dropped by about 20% upon the addition of AsH_3, because of the formation of reaction products. As a result it is not possible to conclude that the Me_2Ga^+ fragment during this reaction represents the Me_3Ga remaining in the reactor. However, it sets an upper bound to this quantity.

Figure 1 shows the Me_2Ga^+ remaining in the reactor in steady state as a function of P_{AsH_3}, with the probe positioned at 1.25 to 9.0 cm from the entrance region. This data was essentially independent of distance, indicating that the kinetics of this reaction are too fast to be observed with our sampling arrangement, and that equilibrium has been achieved. Assuming an elementary, reversible bimolecular reaction of the type observed for the Et_3In-AsH_3 case, we calculate a lower bound of 0.15 $torr^{-1}$ for the equilibrium constant, K_{eq}.

The Me_3Ga-AsH_3 reaction was found to reach its equilibrium state in a time that was less than the sampling time of our system (0.2 sec.). A lower bound for this parameter k_2, the rate of forward reaction, was calculated as 1.0 $(torr\ sec)^{-1}$, on the assumption that the rate equation was of the same form as an elementary, reversible, bimolecular reaction, and the fact that equilibrium was achieved within 5 cm from the inlet. We expect that the actual value of both K_{eq} and k_2 are much larger than these lower bounds.

GENERAL COMMENTS

Our measurements indicate that a significant portion of the organometallic source is delivered to the vicinity of the slice as an adduct, subsequently dissociating in the thermal boundary layer. The suitability of such a source for organometallic epitaxy is re-

lated to the degree of dissociation at growth temperatures and the vapor pressure of the adduct, rather than to the extent and rate of its pre-reaction. For example, it is generally assumed that the growth of GaAs from the reaction of Me_3Ga and AsH_3 presents no problem because there is no pre-reaction. Our work has shown that there is considerable pre-reaction. However, the reaction product has a high vapor pressure and does not eliminate methyl groups to eventually form polymers, so that it is easily transported to the susceptor and participates in the growth process.

The column V hydrides, AsH_3 and PH_3 are weaker Lewis bases than their corresponding alkyls because the hydrogens are less electron releasing than the alkyl groups. Thus, the adduct bonds are weaker and are difficult to measure by calorimetric or gas phase dissociation techniques. In addition, the adducts formed with column V hydrides do not seem to be very stable, because the hydrogens are Lewis acids and may cause alkyl elimination, subsequently leading to polymer formation [2].

By measuring the equilibrium of the adduct formation reaction between Et_3In and AsH_3 in our mass spectrometer sampling system we have been able to determine its very small (about 6 kcals/mole) bond energy [1]. As mentioned previously the Me_3Ga-AsH_3 reaction has not been as straightforward, so that the adduct bond energy could not be determined.

Studies of adduct formation between column III and column V alkyls have shown that adduct bond strength is reduced in the order Al →Ga →In [3]. In addition, column III methyl alkyls form stronger adduct bonds to column V alkyls than do the column III ethyl alkyls [4]. However, reversals may occur in acceptor strengths for a series of acceptors with a change in the reference Lewis base [5]. Thus we cannot conclusively state that the Me_3Ga-AsH_3 bond will be stronger than the Et_3In- AsH_3 bond. A technique more suitable to the measurement of the small heat of formation of the Me_3Ga-AsH_3 bond, such as the use of n.m.r. chemical shift [4], may be required to eventually resolve

this issue.

CONCLUSION

The Me_3Ga reaction with arsine was faster than could be measured by our present apparatus. However, it is reasonable to assume that the Me_3Ga- AsH_3 mixture reacted by the same mechanism as the Et_3In-AsH_3 mixture. Based on this assumption, lower bounds for the equilibrium constant and for the rate of forward reaction were set at 0.15 $torr^{-1}$ and 1.0 $(torr\text{-}\ sec)^{-1}$ respectively.

ACKNOWLEDGEMENT

The authors would like to thank J. Barthel for technical assistance, P. Magilligan for manuscript preparation, and M. Sherwin for computer reduction of the data. Technical discussions with Prof. J. Hudson, Dr. K. Jones and Mr. P. Chinoy were most helpful, and are greatly appreciated. This work was supported by Contract No. XL-5-05018-2 from the Solar Energy Research Institute, Golden, CO and by Contract No. F19628-84-C-0066 from the Air Force, through DEVCOM, Inc. Additional funds were provided by Agreement No. 970- ERER-ER-87 from the New York State Energy Research and Development Authority. This support is hereby acknowledged.

REFERENCES

1. P.D. Agnello and S.K. Ghandhi, J. Electrochem. Soc., submitted.
2. D.J. Schlyer and M.A. Ring, J. Organometal. Chem., 114, (1976) 9.
3. G.E. Coates and R.A. Whitcombe, J. Chem. Soc., (1956), 3351.
4. A. Leib, M.T. Emerson, and J.P. Oliver, Inorgan. Chem., 4, (1965) 1825.
5. R.S. Drago and B.B. Wayland, J. Am. Chem. Soc., 87, (1965) 3571.

FIGURE

Figure 1. Steady state dimethylgallium ion signal as a function of arsine pressure. (0.02 torr Me_3Ga, 152 torr H_2, 6 slm total flow.)

TABLE

1. Fragmentation pattern of Me_3Ga and of Me_3Ga-AsH_3.

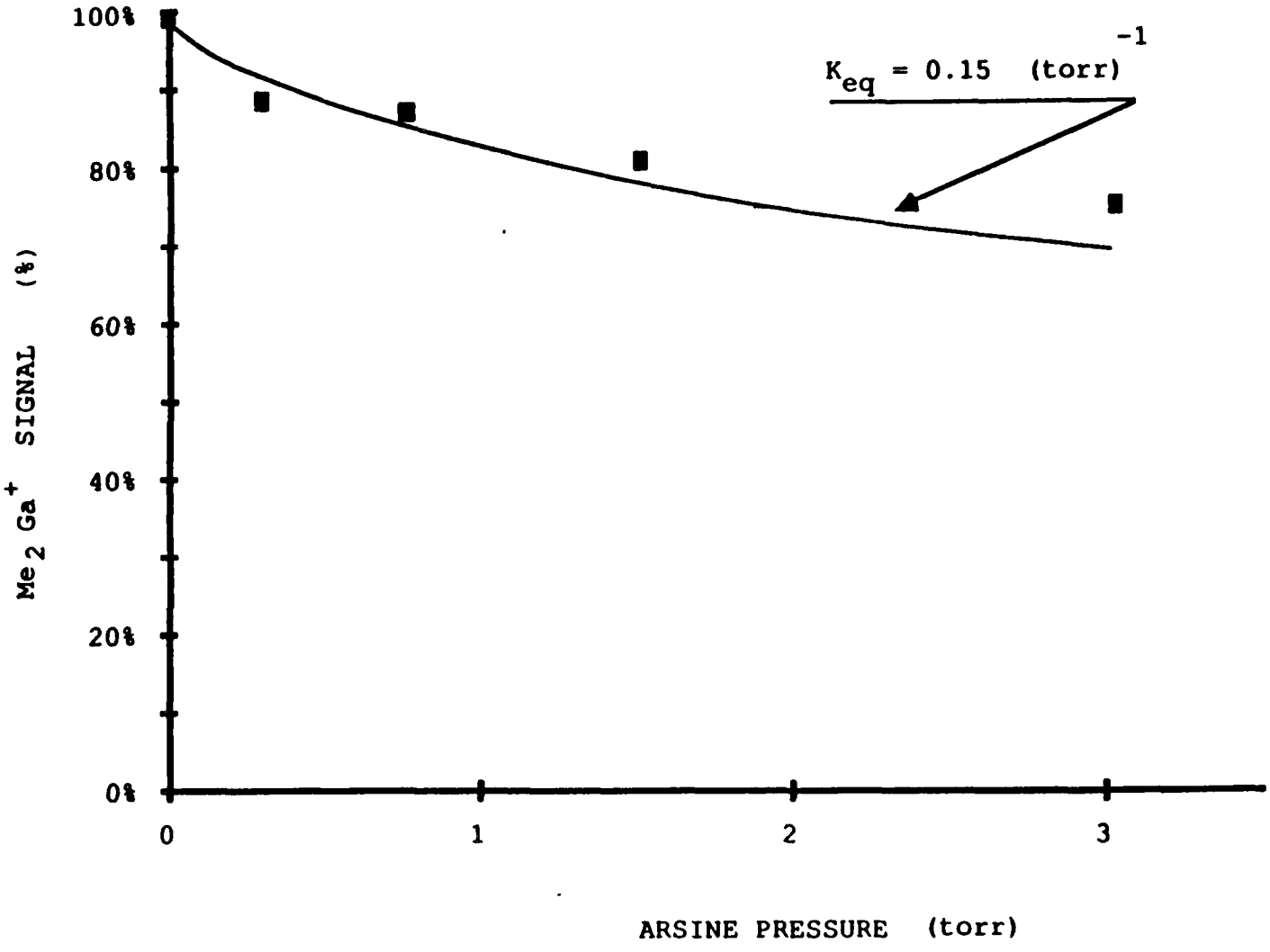
100%
80%
60%
40%
20%
0%
$Me_2 Ga^+$ SIGNAL (%)
K_{eq} = 0.15 (torr)$^{-1}$
0
1
2
3
ARSINE PRESSURE (torr)

FIGURE 1.

FRAGMENT	MASS AMU	Me_3Ga		Me_3Ga-AsH_3	
		ION SIGNAL (x 10^{-10} A)	NORMALIZED ION SIGNAL	ION SIGNAL (x 10^{-10} A)	NORMALIZED ION SIGNAL
Ga^+	69 71	2.425 1.463	0.64 0.39	2.225 1.375	0.70 0.43
$MeGa^+$	84 86	0.625 0.375	0.16 0.10	0.550 0.300	0.17 0.09
Me_2Ga	99 101	3.800 2.425	1.00 0.64	3.200 2.075	1.00 0.65
Me_3Ga	114 116	0.5 0.1	0.13 0.03	0.5 0.1	0.16 0.03

TABLE 1.

MISSION
of
Rome Air Development Center

RADC plans and executes research, development, test and selected acquisition programs in support of Command, Control, Communications and Intelligence (C^3I) activities. Technical and engineering support within areas of competence is provided to ESD Program Offices (POs) and other ESD elements to perform effective acquisition of C^3I systems. The areas of technical competence include communications, command and control, battle management information processing, surveillance sensors, intelligence data collection and handling, solid state sciences, electromagnetics, and propagation, and electronic reliability/maintainability and compatibility.